

Dissertation

Characterization of short polypropylene glycol monoalkylethers and design of enzymatic reaction media

Pierre Bauduin
University of Regensburg



At the Natural Sciences Faculty IV

Chemistry & Pharmacy

Mai 2005

Ph.D. Supervisor: Prof. Dr. Werner Kunz

Adjudicators: Prof. Dr. Werner Kunz

Prof. Dr. Barry W. Ninham

Prof. Dr. Claudia Steinem

Chair: Prof. Dr. Georg Schmeer

Preface

This thesis aims at the characterization of propyleneglycol monoalkylethers. It comprises different studies ranging from phase diagram determination to enzymatic activity. For this reason this thesis was written so that each chapter can be read independently. Separate bibliographies are given at the end of each chapter. Each chapter layout follows the usual convention: Abstract, Introduction, Results and Discussion and Conclusion. The different studies led to publications which are already published, accepted or submitted, summarized in the following Table. Co-authors on the Ph.D. work in Regensburg are listed. A complete list of publications and a list of poster presentations, which were presented at international congresses, are also given at the end.

Chapter	Publication
2	Bauduin, P.; Wattebled, L.; Schroedle, S.; Touraud, D.; Kunz, W. Temperature dependence of industrial propylene glycol alkyl ether/water mixtures. <i>Journal of Molecular Liquids</i> 2004 115(1), 23-28.
3	Bauduin, P.; Wattebled, L.; Touraud, D.; Kunz, W. Hofmeister ion effects on the phase diagrams of water-propylene glycol propyl ethers. <i>Zeitschrift fuer Physikalische Chemie</i> (Muenchen, Germany) 2004 218(6), 631-641.
4	Bauduin, P.; Renoncourt, A.; Kopf, A.; Touraud, D.; Kunz, W. Unified concept of solubilization in water by hydrotropes and co-solvents. <i>Langmuir</i> (Submitted) 2005 .
5	Bauduin, P.; Basse, A.; Touraud, D.; Kunz, W. Effect of short non-ionic amphiphiles derived from ethylene and propylene glycol alkyl ethers on the CMC of SDS. <i>Colloids and Surfaces A</i> (Accepted) 2004 .
6	Bauduin, P.; Touraud, D., Kunz, W. Design of low-toxic anionic temperature sensitive microemulsions using short propyleneglycol alkylethers as co-surfactants. <i>Langmuir</i> (Submitted) 2005 .
7	Bauduin, P.; Nohmie, F.; Touraud, D.; Neueder, R.; Kunz, W.; Ninham, B.W. Hofmeister Specific-Ion Effects on Enzyme Activity and buffer pH: Horseradish Peroxidase in citrate buffer. <i>Journal of Molecular Liquids</i> (Accepted) 2005 .
7	Bauduin, P.; Renoncourt, A.; Touraud, D.; Kunz, W.; Ninham, B. W. Hofmeister effect on enzymatic catalysis and colloidal structures. <i>Current Opinion in Colloid and Interface Science</i> 2004 9(1,2), 43-47.
8	Bauduin, P.; Touraud, D.; Kunz, W.; Ninham, B.W. The influence of structure and composition of a reverse SDS microemulsion on enzymatic activities. <i>Journal of Colloid Interface Science</i> (Submitted) 2005 .

Acknowledgements

The present work took place between October 2002 and May 2005 at the Department of Physical Chemistry for Natural Sciences at the University of Regensburg under the leadership of Prof. Dr. Werner Kunz.

First and foremost, I would like to thank Prof. Dr. Werner Kunz not only for giving me the opportunity to do my Ph.D. in his lab but also for his unstinting support in countless ways both privately and professionally.

I would also like to thank Prof. Dr. Barry W. Ninham with whom I had the privilege to work during his stay in Regensburg. His kindness and his innovative way of seeing Science were of great help for me.

Thanks to Prof. Dr. Jean-Marie Aubry for accepting me in his lab in May 2004, within the framework of an exchange between his laboratory in Lille and the laboratory of Regensburg, and for the always fruitful scientific discussions we had during this time and before that.

I would like to thank all my research group-colleagues, for whom a single page of thanks would not suffice, for their kindness and technical support down these years. Special thanks to Didier Touraud for his constant support and his unique and unconventional way of approaching the Science.

More personally, I would like to thank: Andreas G. who became a true friend during these last three years and tried to teach me the nice bavarian dialect (I'm afraid he did not succeed well but anyway...), Sigrid whose friendship and constant cheerfulness contributed to my well-being in the lab ¹, Alina, Astrid, Cristina, Andreas K., Chamsoudine, Nicolas and John for their friendship.

Of course I would like to thank my family not only for putting me on earth, but also for coming to my assistance whenever I needed it. Without them I would never have become what I am today.

Last but not least I want to particularly offer my heartfelt thanks to Audrey Renoncourt for her unvaluable support in the lab and in the every-day life.

¹Sigrid: thank you so much for importing these delicious Dutch honey waffles in Bavaria and for bringing them into our lives!

Acknowledgements

Contents

Preface	i
Acknowledgements	iii
Introduction	7
1 Overview of “glycol ethers” and of their industrial applications	9
1.1 Glycol ethers	9
1.2 Health effects	11
1.3 Structures and properties of propylene glycol alkyl ethers (C_nPO_m)	14
1.3.1 Structures	14
1.3.2 Synthesis and isomer compositions	14
1.3.3 Physical properties and comparisons to other solvents	15
1.4 Propylene glycol alkyl ethers (C_nPO_m): efficient and low toxic industrial solvents	17
1.4.1 Deinking of cables	17
1.4.2 Degreasing of metal plates	21
Bibliography	29
I Properties and characterization of C_nPO_m/water mixtures	31
2 Temperature dependence of propylene glycol alkyl ether/water mixtures	33
2.1 Introduction	33
2.2 Materials and Methods	34
2.2.1 Materials	34
2.2.2 Phase diagram determination	35
2.2.3 Surface tension measurements	36
2.3 Results and Discussion	36
2.3.1 Phase diagrams	36
2.3.2 C_3PO_1 /water system	38
2.3.3 n-propyl C_nPO_m / water phase diagrams	39
2.3.4 C_3PO_m /water phase diagrams	40
2.3.5 C_4PO_m /water phase diagrams	40

2.3.6	Comparison of the LCST values between the C_nEO_m s and the C_nPO_m s	41
2.4	Conclusion	42
Bibliography		43
3	Hofmeister effects on propylene glycol propyl ethers	47
3.1	Introduction	47
3.2	Experimental	50
3.2.1	Materials	50
3.2.2	Cloud point determination	50
3.3	Results	51
3.4	Discussion	54
3.5	Conclusion	57
Bibliography		59
4	Unified concept of solubilization in water by hydrotropes and co-solvents	63
4.1	Introduction	63
4.2	Experimental	65
4.2.1	Materials	65
4.2.2	Solubilization experiments	66
4.3	Modelling	66
4.4	Results and Discussion	66
4.4.1	Solubilization curves: comparison between hydrotrope, co-solvent and surfactant	66
4.4.2	Aqueous solubilization in the water rich part: the hydrotropic behavior	69
4.4.3	The ordering of the hydrotropes	71
4.4.4	The extent of the hydrophobic part in hydrotrope molecules: a determining factor in the hydrotropic efficiency	72
4.5	Conclusion	75
Bibliography		77
II Co-surfactant properties of C_nPO_ms		81
5	Effect of propyleneglycol monoalkylether on the CMC of SDS	83
5.1	Introduction	83
5.2	Materials and Methods	84
5.3	Results and Discussion	86
5.4	Conclusion	93
Bibliography		95

6	Propyleneglycol monoalkylethers as co-surfactants in the design of microemulsions	97
6.1	Introduction	97
6.2	Experimental Section	99
6.2.1	Materials	99
6.2.2	Phase diagrams determination	99
6.2.3	Phase transition determination by increasing temperature . .	100
6.3	Results and Discussion	101
6.3.1	C_nPO_m as co-surfactant in the formation of microemulsions .	101
6.3.2	Temperature dependence of C_nPO_m /SDS based systems . . .	103
6.3.3	Design of an anionic monophasic temperature sensitive microemulsion using C_4PO_3 as co-surfactant	108
6.4	Conclusion	111
	Bibliography	113
III	Enzymatic activity	119
7	Hofmeister Specific-Ion Effects on Enzyme Activity and Buffer pH	121
7.1	Introduction	121
7.2	Materials and Methods	122
7.2.1	Materials	122
7.2.2	Determination of the ABTS kinetic constants	123
7.3	Results	123
7.3.1	pH variation of a 0.025M citrate buffer with salt concentration	123
7.3.2	K_{mABTS} and $V_{maxABTS}$ as a function of pH	125
7.3.3	K_{mABTS} and $V_{maxABTS}$ as a function of salt concentration . .	125
7.4	Discussion	126
7.4.1	Can we trust our pH values?	126
7.4.2	The catalytic constants K_{mABTS} and $V_{maxABTS}$	128
7.4.3	The catalytic efficiency ($V_{maxABTS} / K_{mABTS}$)	128
7.5	Conclusion	131
7.6	Appendix	131
	Bibliography	135
8	Enzymatic activity in reverse SDS microemulsions	137
8.1	Introduction	137
8.2	Materials and Methods	140
8.2.1	Materials	140
8.2.2	Conductivity Experiments	140
8.2.3	Preparation of the Reaction Mixtures	140
8.2.4	Determination of Enzyme Activity	140

Contents

8.3	Results	142
8.3.1	Phase diagrams of microemulsions	142
8.3.2	Conductivity Measurements	142
8.3.3	Preliminary Enzymatic Tests	146
8.3.4	Dependence of the enzymatic activity on the alcohol carbon number for various buffer contents	147
8.4	Discussion	148
8.4.1	Phase Diagrams	148
8.4.2	Conductivity measurements	150
8.4.3	Preliminary Enzymatic Tests	151
8.4.4	Microemulsions: the dependence of the enzymatic activity on the number of carbon atoms in the alcohols at different water contents	152
8.5	Conclusion	157
Bibliography		161
Conclusion		171
List of Figures		173
List of Tables		179
List of Publications		181
List of Poster Presentations in Congress		183

Introduction

The toxicological and environment matters associated with the massive use of chlorinated solvents as well as ethers derivated from ethylene glycol in degreasing process and cleaning formulations involved a regulatory review. Therefore, the industry was obliged to decrease their use and to search for new compounds. The use of ethers derivated from propylene glycol (also called Dowanols P-series or C_nPO_m), much more environmentally-friendly, presented an apparently very efficient solution². That is why these compounds occur frequently in everyday life products. Nevertheless, our knowledge about their physico-chemical properties still remains incomplete. The main aim of this thesis was to study the properties and the behavior of propylene glycol alkylethers (C_nPO_ms). They are more than simple solvents insofar as they exhibit additional properties.

This thesis is split up into three parts. A preliminary introductory chapter concerning glycol ether solvents, which include C_nPO_ms , is given first. This discusses the general background, structures, standard properties and applications. The toxicity of ethylene and propylene glycol ethers (C_nEO_ms and C_nPO_ms) is also mentioned and compared. Deinking and degreasing tests are discussed to illustrate the efficiency of C_nPO_ms as industrial solvents.

Then in the first part the properties of C_nPO_ms in aqueous mixtures were studied. The binary phase diagrams C_nPO_m /water versus temperature were determined precisely by automated turbidity measurements. The salt effects on the phase transition observed in these binary phase diagrams were also assessed. Information extracted on the system itself and some general considerations concerning salt specificity (Hofmeister series) are then highlighted. Ion effects, and more specifically specific ion effects, are an extensive focus in this thesis. The ability of certain C_nPO_ms to solubilize hydrophobic compounds in water³ was also investigated. By comparing the C_nPO_m solubilization curves to that of more usual hydrotropes and co-solvents, a consistent picture can be extracted on the hydrotrope/co-solvent solubilization processes. The hydrophobic part in hydrotrope or co-solvent molecules was shown to influence the aqueous solubilization strongly.

In the second part, the behavior of C_nPO_ms as co-surfactant, i.e. when used in addition to a surfactant, was investigated. At first this was done in dilute surfactant systems by studying the critical micellar concentration (CMC) decrease of sodium dodecyl sulfate through co-surfactant addition, i.e. some C_nPO_ms , n-alcohols and ethyleneglycol monoalkylethers. This method permitted an evaluation of the co-surfactant behavior of each of the compounds studied and thus to classify them. The topology of the corresponding water/SDS/co-surfactant ternary phase diagrams was compared with these results. Then with awareness of the temperature dependence of C_nPO_m /water systems, the design of temperature sensitive anionic microemulsions was elaborated by addition of dodecane as oil phase to the latter ternary system and by using C_nPO_ms as co-surfactant.

²To illustrate this point it is worth remarking that there are more than 10,000 patents dealing with propylene glycol alkylethers for diverse applications and in different fields.

³This phenomenon is sometimes called "hydrotropy".

Such microemulsions, used as reaction media facilitate separation and purification steps of the reaction product. As reaction media for enzymatic reactions, microemulsions have several advantages: (1) the confined aqueous droplets presented by water-in-oil microemulsions is reminiscent of the confined water presented “in vivo” in living species e.g. in plants or animals. The study of enzymatic activity in microemulsions might therefore bring information on the local physico-chemical conditions in biological systems. (2) The water and oil phases in microemulsions being intimately mixed allow the design of new bio-reactions. In this context enzymatic reactions were investigated in the third part. A model enzymatic reaction based on *horseradish peroxidase* (HRP) was chosen and at first studied in buffer solutions. Salt effects on both buffer pH and enzymatic activities were investigated. Then enzymatic activities in microemulsions were measured. Correlations between enzymatic activity and microemulsion microstructures were drawn.

1 Overview of “glycol ethers” and of their industrial applications

Abstract

Used substantially since the 1970s, glycol ethers are remarkable solvents. They have multiple industrial uses and are present in a broad line of goods usually employed by the consumer (paints, varnishes, household goods). The majority of glycol ethers currently marketed were tested for their toxic properties (genotoxicity, carcinogenicity, effect on the reproduction and the development). The establishment of the genotoxicity of two solvents derived from ethylene glycol led to the progressive phase-out of the whole line of the ethylene glycol based solvents from the market and from the formulations in domestic products. Industrialists gradually replaced glycol ethers of the ethylenic series by glycol ethers of the propylenic series, these being much less toxic.

Glycol ether(s) having (1) an established toxicity on the reproduction are ethylene glycol methyl ethers (C_1EO_m) and ethyl ethers (C_2EO_m , with $m < 3$) and their acetates (C_1EO_mAc and C_2EO_mAc) and propylene glycol methyl ether (C_1PO_1), and (2) a potential carcinogenicity is ethylene glycol butyl ether (C_4EO_1).

To illustrate the good solvent property of C_nPO_m s, some deinking and degreasing tests were undertaken. C_nPO_m s do not have the disadvantages that present short ketones and petroleum distillates, i.e. toxicity, which are usually used for these applications. For this reason C_nPO_m s could be thus proposed as an alternative to the use of toxic solvents.

1.1 Glycol ethers

“Glycol ethers” is a common denomination for a group of industrial oxygenated solvents. More than 40 different industrial solvents are concerned by this denomination. They can be classified in two groups: the ethyleneglycol and propyleneglycol alkylethers¹ (see Fig. 1.1). Several other non-systematic terminologies are actually often used, to name a few: ethylene and propylene oxide-based glycol ethers; C_nEO_m (C_iEO_j , C_iE_j) and C_nPO_m (C_iPO_j , C_iP_j); E and P series according to the nomenclature used by the Dow Chemical Co.[1] ... For practical reasons, the

¹Note that the U.S. Environmental Protection Agency (EPA) has determined that propylene glycol ethers are not included within the category “glycol ethers” because of toxicological considerations (see section 1.2). This is an exception to the practice and in most other countries the term “glycol ethers” includes both ethylene and propylene glycol alkylethers.

1 Overview of “glycol ethers” and of their industrial applications

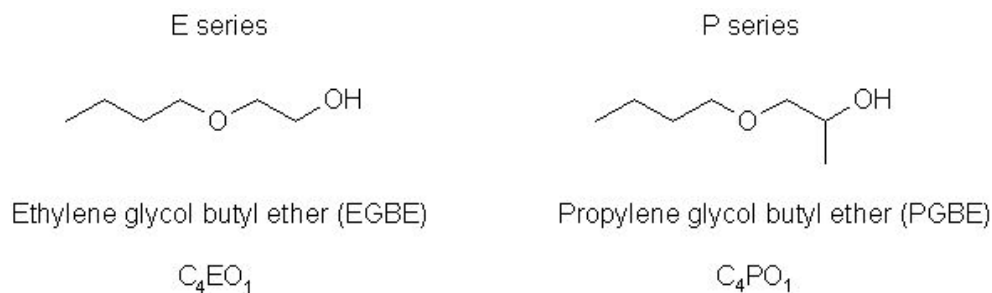


Figure 1.1: Formula of glycol ethers from the ethylene and propylene glycol series (E and P series).

terminology “ C_nEO_m and C_nPO_m ” will be used in this thesis to refer to ethylene and propylene glycol alkyl ethers.

Glycol ether solvents are widely used in industry, e.g., as chemical intermediates or as process solvents, and in formulated products, e.g., in: coatings, inks, cleaners, brake fluids, deicers and cosmetics [1]. The glycol ether concentration in these products is very dependent on the type of application. It ranges from 1% to 100%. The use of pure glycol ethers is rare. A particular case is that of ethyleneglycol ethyl acetate (C_2EO_1Ac) as cleaning solvent in serigraphy. In 2000 the total consumption of glycol ethers for all uses in Europe was around 400,000 tons. Over 80% of these are spread over a few industrial sectors such as: coatings, inks and in cleaning products. They were first introduced as commercial products in the late 1920s. At a time when n-butyl acetate was the primary solvent for use in coatings, the introduction of the glycol ether solvents was a major step forward for the coatings industry. Even today when the coatings formulator has a wide range of solvents to work with, glycol ether solvents still fill a unique role in coatings formulations.

Until 1980 ethyleneglycol solvents were the main marketed glycol ethers, probably because of the easier availability of ethylene oxide, required for their synthesis (see Section 1.3), by comparison with propylene oxide. The publication of several experimental studies that prove the toxicity of some glycol ethers derived from ethylene oxide has led to the replacement of ethylene glycol ethers by propyleneglycol ethers, these being much less toxic (see Section 1.2). In 1997, 75% of the production of glycol ethers belonged to the propyleneglycol ether series.

The main interest in glycol ethers derives from the fact that they are both hydrophilic and lipophilic. Consequently their main applications are based on their ability to co-solubilize water and hydrophobic compounds. An example of one of the most important applications of glycol ethers is the solubilization of resins in water in the formulation of aqueous paints. It is mostly for this reason that the properties of aqueous mixtures of propylene glycol ethers will be extensively studied in the present work (see Part I).

Because of their excellent performance properties (evaporation rate, solvent or co-solvent ability, mild odor, good coupling ability, good solvent release in paints) a complete line of glycol ether solvents of various molecular weights has been de-

veloped. There are currently nine domestic manufacturers of ethylene oxide-based glycol ether solvents (Eastman Chemical Products Inc., Lyondell Co., Union Carbide Co. Inc., Dow Chemical Co., Shell Chemical Co., Olin Chemical Corp., Texaco Chemical Co., ICI Corp. and PPG Industries Inc.). These products are supplied under a number of different trade names (see Table 1.1). The most commonly encountered names are Dowanol, Cellosolve and Arcosolv.

It is the combination of desirable properties that causes these products to be widely used in industry, especially in the coating industry. While there are some other types of solvents with evaporation rates in the same range as the glycol ethers (see Table 1.3), none of these products have the same combination of attractive properties for use in coatings.

Trade name	Company
Cellosolve solvent	Union Carbide
Carbitol solvent	Union Carbide
Ektasolve solvent	Eastman
Dowanol solvent	Dow
Oxitol solvent	Shell
Dioxitol solvent	Shell
Polysol solvent	Olin
Arcosolve	Lyondell
Jeffersol solvent	Texaco

Table 1.1: Trade names for glycol ether solvents.

1.2 Health effects

Ethylene glycol ethers have of late received some media attention and are now included on some government lists of hazardous substances. This is because the smallest molecular weight ethylene glycol ethers² were found to cause adverse male and female reproductive effects and birth defects in rodent studies[2, 3, 4]. In Europe and in the United States the governments have declared that those particular ethylene glycol ethers “were not used in consumer products for the past 20 years” [5]. In Table 1.2 some historical facts from the discovery of ethylene glycol ether toxicity to the beginning of their phase-out from formulated products and from industrial processes are summarized.

All glycol ethers have a high potential for pulmonary, oral and dermal absorption. Ethylene glycol ether exposure can result in depression of the central nervous system, resulting in headaches, bone marrow damage, drowsiness, weakness, slurred speech, tremor, and blurred vision. Most ethylene glycol ethers can damage red cells or

²ethylene glycol methyl ethers (C_1EO_m) and ethyl ethers (C_2EO_m , with $m < 3$) and their acetates (C_1EO_mAc and C_2EO_mAc)

1 Overview of “glycol ethers” and of their industrial applications

Date	Event
January 1981	Santa Clara Center for Occupational Safety and Health publishes a technical report documenting that glycol ethers cause reproductive disorders in animals, citing a NIOSH (National Institute of Occupational Safety and Health) Study.
May 1982	California Department of Health Services (Hazard Evaluation System and Information Services) issues health warning to California workers on glycol ether solvents, finding that “glycol ethers have damaged the reproductive systems of test animals, raising the possibility that they may cause similar effects in humans.”
May 1982	Semiconductor Industry Association (SIA) issues alert to semiconductor executives regarding glycol ether health effects, particularly reproductive effects.
September 1983	Chemical Manufacturers Association issues Research Status Report on glycol ethers, documenting extensive reproductive toxicity in animal studies.
January 1989	SIA signs a \$3.5 million research grant with researchers at U-C Davis to conduct industry-wide health study. 15 companies agree to participate in a study of 18,000 workers. The results have not been released. IBM does not participate, preferring to conduct its own study.
December 1992	SIA study results reveal that women working in silicon wafer manufacturing rooms who handled photo resist chemicals such as glycol ethers, suffered higher rates of miscarriage than women in the industry who worked in non-fabrication room locations. This study re-confirmed results of IBM and DEC studies. Health and safety advocates and environmental groups launch the Campaign to End the Miscarriage of Justice, calling on the industry to adopt aggressive goals and time tables for the phase-out of glycol ethers and other reproductive toxins.
1994	Industry begins phase-out of ethylene-based glycol ethers.

Table 1.2: From the discovery of ethylene glycol ether toxicity to the beginning of their phase-out from formulated products and from industrial processes.

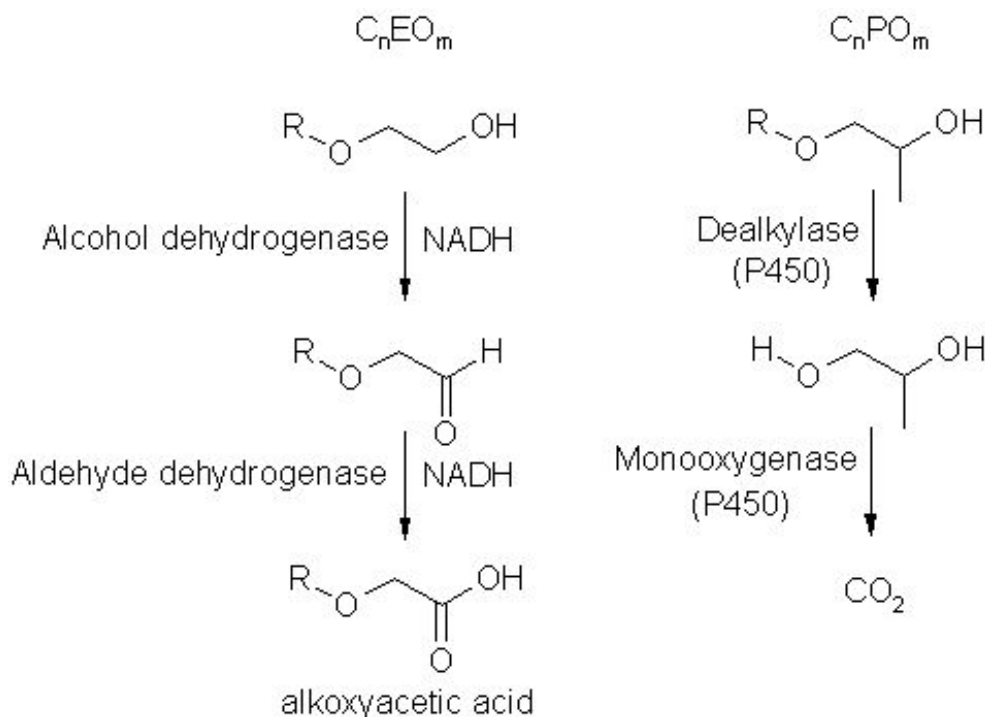


Figure 1.2: Metabolisms of ethylene and propylene glycol ethers (C_nEO_m and C_nPO_m).

damage the bone marrow, where blood cells are formed, and cause anemia. Some of the ethylene glycol ethers were also found to have genotoxic effects *in vitro* (C_4EO_1 , C_2EO_1 and C_1EO_1) or *in vivo* (C_1EO_1 , C_1EO_2). The ethylene glycol monobutyl ether (C_4EO_1) was found to present carcinogenic effects by animals. It is important to note that C_4EO_1 (see Fig. 1.1) is one of the most widely used solvent in cleaning products (see [6]) and is regarded as the most toxic glycol ether [4].

The metabolism of ethylene glycol ethers is mainly done via the enzymes alcohol dehydrogenase and aldehyde dehydrogenase (Fig. 1.2) [7]. This leads to the production of aldehydes and alkoxyacetic acids having alkyl chains corresponding to those of the metabolized glycol ethers. The hematotoxic and genotoxic effects of ethylene glycol ethers are ascribed to the production of these toxic metabolites. Aldehydes and alkoxyacetic acids are able to penetrate the nucleus of cells and then to alter the genome structure. By increasing the number of ethylene glycol units, i.e. m in C_nEO_m , the production of alkoxyacetic acid, and consequently the toxicity, was observed to decrease. We remark that the products used by the consumers which can contain glycol ethers, except paints, are household products (C_4EO_1 , C_4EO_2) and cosmetics (C_4EO_1 , C_4EO_2 and C_1PO_1 mainly in hair dyeing formulations and C_2EO_2 in body creams).

In contrast, propylene glycol ethers are not included on most lists of hazardous chemicals. In the U.S., the Environmental Protection Agency (EPA) has issued numerous lists of hazardous chemicals to be regulated in emissions to air and wa-

ter and control of hazardous waste. Although the EPA’s glycol ether definitions are broad, they have always included only ethylene glycol ethers. Propylene glycol ethers have never fallen within the definitions. The toxicity data available do not mention any genotoxic or hematotoxic effects, except for the propyleneglycol methyl ether (C_1PO_1) for which the metabolism is known to be similar to the one of ethylene glycol ethers [3, 4]. The propylene glycol ethers metabolism is done by the cytochrome P450, which has dealkylase and monooxygenase activities (Fig. 1.2). This leads to the formation of propylene glycol and then to CO_2 which is eliminated by the lungs. For information the LD50, i.e. the Lethal Dose 50% in g/Kg (rat ingestion)³, of some propyleneglycol derivatives are given in Table 1.4, p. 20, and compared to those of classical solvents. Because of the concern about the toxicity of the ethylene oxide-based products, the number of propylene oxide-based products available has increased a lot the past 10 years. Our interest will now focus on them.

1.3 Structures and properties of propylene glycol alkyl ethers (C_nPO_m)

1.3.1 Structures

The different molecules concerned by the definitions of glycol ethers are summarized in Fig. 1.3. The usual definition includes as glycol ethers only mono- and di-ethers of ethylene glycol, diethylene glycol, and triethylene glycol. Note that the U.S. government definition includes only the ethylene glycol series and not the propylene glycol series, whereas in Europe the definition of glycol ethers includes both series. Ethoxylated surfactants used in soaps and detergents, which have long carbon chains (C_nEO_m , $n > 7$), have never been considered to be traditional glycol ethers. Ethoxylated surfactants do not share the physical or chemical toxicological properties of “glycol ethers”. The “glycol ethers” we shall study are propylene glycol monoalkylethers (C_nPO_m , with $n = 1, 3, 4$ and $m = 1-3$, see Tables 1.3 and 2.1 for their chemical names.)

1.3.2 Synthesis and isomer compositions

Glycol ethers are obtained, usually under basic catalysis, by reaction of ethylene or propylene oxide with an alcohol. A monoalkylether (methyl, ethyl, propyl, butyl or hexyl) is then obtained. In Fig. 1.4, the synthesis of C_3PO_1 and C_3PO_2 are given as examples. The addition of one mole of propylene oxide to one mole of alcohol leads to the formation of C_3PO_1 which consists of a mixture of two chemical isomers, one primary and one secondary alcohol. Under basic catalysis, the formation of the secondary alcohol is favoured and represent around 90% of the reaction product,

³The Lethal Dose 50% gives a first measure of “direct” toxicity, but not the genotoxicity, of a chemical product.

1.3 Structures and properties of propylene glycol alkyl ethers (C_nPO_m)

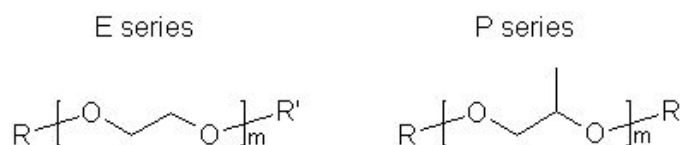


Figure 1.3: Formula of glycol ethers of the ethylene and propylene glycol series (E and P series), where: $m = 1, 2$, or 3 ; R = alkyl alkyl chain C_7 or less or R = phenyl or alkyl substituted phenyl; $R' = H$ or alkyl chain C_7 or less; or OR' consisting of carboxylic acid ester, sulfate, phosphate, nitrate, or sulfonate.

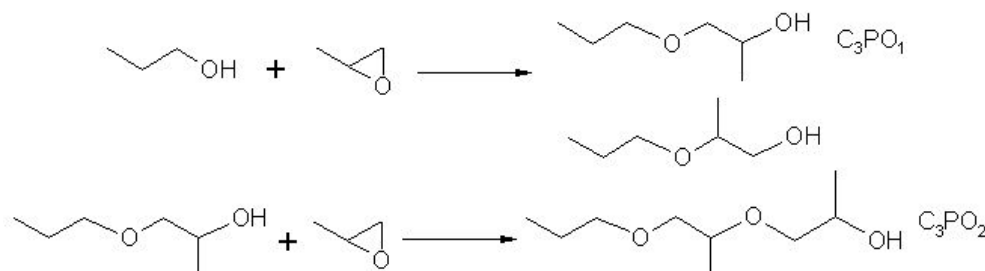


Figure 1.4: Synthesis of C_3PO_1 and C_3PO_2 .

the rest corresponding to the primary alcohol. The addition of a second mole of propylene oxide leads to the formation of C_3PO_2 which is consequently composed of eight different chemical isomers. In Fig. 1.4 only the major C_3PO_2 isomer is given. The chemical isomers composition of C_3PO_2 (industrial solvent obtained from the Dow Company) has recently been determined with gas chromatography/mass spectroscopy analysis, see Fig. 1.5 [8]. This analysis shows that the purity of commercial C_3PO_2 is rather good in so far as only C_3PO_2 isomers are present⁴. It can be assumed that all compounds having two propyleneglycol units, i.e. C_nPO_2 , present the same repartition in the different chemical isomers. In contrast the synthesis of ethylene glycol monoalkylether is done by reaction of ethylene oxide with an alcohol without formation of different chemical isomers.

1.3.3 Physical properties and comparisons to other solvents

The classical physical properties such as: boiling point, density, refractive index, Hansen parameters ... of C_nPO_m s are already known [1], some of them are given in Table 1.3. It can be seen that the boiling points of most of the studied C_nPO_m s lie between 100 and 250°C. These solvents can thus be distilled at atmospheric pressure or under vacuum, enabling their easy recovery and purification. Except for C_1PO_1 which was found to be genotoxic (see Section 1.2), the C_nPO_m s studied show flash point higher than those of classical solvents, also given in Table 1.3.

⁴The presence of C_4PO_2 isomers (0.26%) is probably not due to the chemical reaction itself but rather due to some remaining traces of C_4PO_2 present in the cuve in which C_3PO_2 was stored.

1 Overview of “glycol ethers” and of their industrial applications

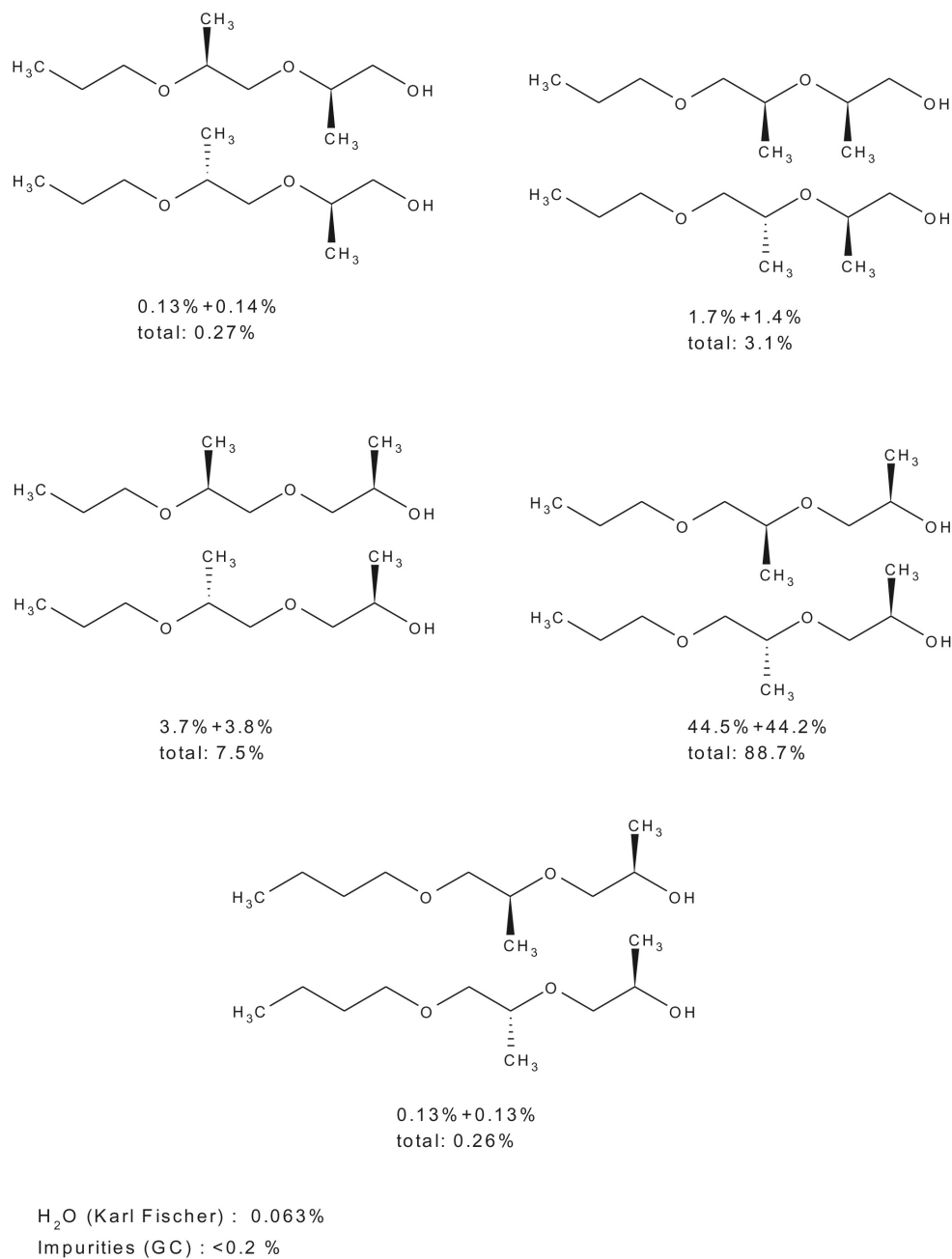


Figure 1.5: Composition of an industrial C_3PO_2 determined with gas chromatography/mass spectroscopy analysis. The mass % of each isomers was determined by the pic area obtained from gas chromatography (column Stabiwax-DA).

1.4 Propylene glycol alkyl ethers (C_nPO_m): efficient and low toxic industrial solvents

This is important because C_nPO_m solvents are then much safer to handle, because they are less flammable and explosive than the classical solvents. This is not true for the chlorinated solvents: dichloromethane and T-1,1,1 (1,1,1-trichloroethane), which are not flammable but show acute toxicity. Moreover C_nPO_m solvents are often used in aqueous media. It is known that the flash points of monophasic mixtures of water and of a flammable solvent are much higher than those of the pure flammable solvents especially for mixtures having high water contents. The aqueous solubilities of C_nPO_m s are discussed in Chapter 2.

Hansen parameters or solubility parameters are the most convenient and commonly used parameters for the characterization of solvents [9]. Hansen parameters have found their greatest use in coating industry to aid in the selection of solvents. In Fig. 1.6, δ_P vs. δ_H plot is given and shows the location of various common solvents and of some C_nPO_m s. Such a representation permits one to clearly characterize the solvent properties of C_nPO_m s in comparison to other classical solvents. As expected the C_nPO_m s appear to be intermediate between the glycols/alcohols and the ethers.

1.4 Propylene glycol alkyl ethers (C_nPO_m): efficient and low toxic industrial solvents

In order to highlight the good solvent property of the C_nPO_m s studied some deinking and degreasing tests were carried out. For these applications the solvents have to present some characteristics such as good efficiency, low toxicity, low flammability. In deinking and degreasing processes e.g. in the mechanics and the electronics industries, solvents such as short ketones (acetone, methylethylketone MEK) and industrial solvents composed of petroleum distillate (isoparaffin)⁵ are generally used due to their high efficiencies and low costs. Nevertheless they present a certain number of disadvantages as: high flammability (very low flash point, see Table 1.3) and toxicity. C_nPO_m s do not have these disadvantages and could be proposed as an alternative to the use of short ketones and petroleum distillates. Tests were then designed to evaluate the efficiency of C_nPO_m s as deinking and degreasing solvents. These studies were done in collaboration with industrial partners whose constant aim is the finding of new non-toxic and environmentally-friendly solvents.

1.4.1 Deinking of cables

The aim of this work is to find an appropriate solvent to remove ink from industrial cables furnished by an industrial partner. There is substantial economical and environmental incentive to remove ink (deink) from heavily printed plastic pieces so that

⁵Petroleum distillates are mixtures of short hydrocarbons, as alkanes and alkenes, and sometimes contain benzenic derivatives that show acute toxicities. Short alkanes, such as hexane, are neurotoxic.

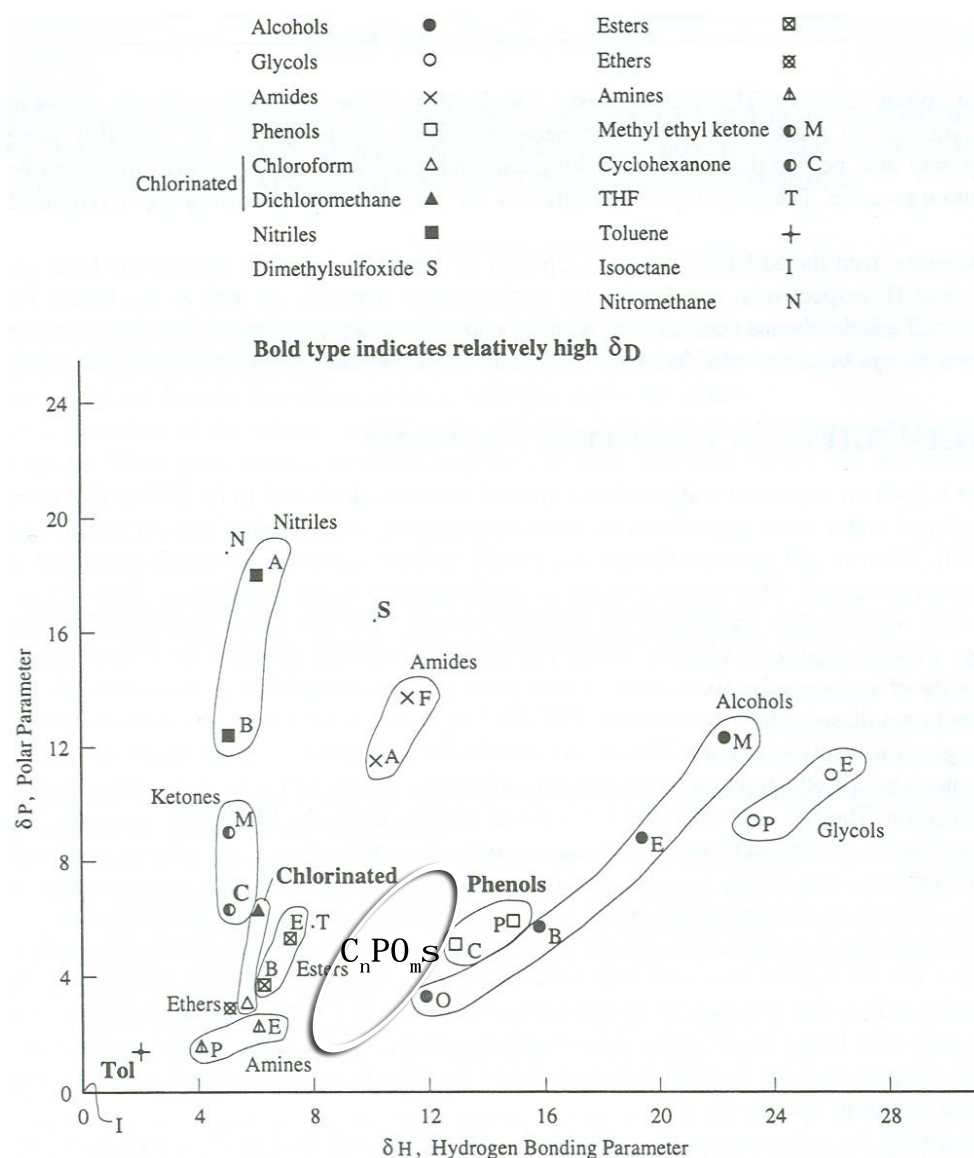


Figure 1.6: δ_P vs. δ_H plot showing the location of various common solvents and of some C_nPO_m s. The glycols are ethylene glycol (E) and propylene glycol (P). The alcohols include methanol (M), ethanol (E), 1-butanol (B) and 1-octanol (O). The amides include dimethylformamide (F) and dimethyl acetamide (D). The nitriles are acetonitrile (A) and butyronitrile (B). The esters are ethyl acetate (E) and n-butyl acetate (B). The amines are ethyl amine (E) and propyl amine (P). The phenols are phenol (P) and m-cresol (C). The ethers are symbolized by diethyl ether.

Product name	Flash point(°C)	Evaporation rate($\eta_{\text{ButAcet}=1}$)	Boiling point (°C)	Hansen Parameters (J/cm^3)		
				δ_D	δ_P	δ_H
C_1PO_1	31 [†]	0.62	120	15.6	7.2	13.6
C_1PO_2	75	0.035	190	15.5	4.0	11.5
C_1PO_3	121	0.0026	243	15.1	3.5	11.5
C_3PO_1	48 [†]	0.21	149	15.1	5.7	11.7
C_3PO_2	88	0.014	213	15.0	3.0	9.6
C_3PO_3	130	0.0009	261	15.0	2.6	8.6
C_4PO_1	63	0.093	171	14.9	4.9	10.7
C_4PO_2	100	0.006	230	14.8	2.5	8.7
C_4PO_3	126	0.0004	271	14.8	1.7	7.9
<hr/>						
CH_3PO_1Ac	42 [†]	0.33	146	16.1	6.1	6.6
$CH_3PO_2CH_3$	65	0.13	175	14.9	2.1	3.8
C_4EO_1	61	0.09		16.0	5.1	2.3
Acetone	18 [‡]	7.7	56	15.5	10.4	7.0
MEK	-9 [‡]	3.8	79.6			
Ether	-40 [‡]	37.5	35			
Ethanol	13 [†]	1.7	78.3	15.8	8.8	19.4
Propan-1-ol	15 [†]	1.1	97.5			
Isopropanol	12 [†]	2.5	82			
Butan-1-ol	29-35 [†]	0.5	118			
Limonen	72 [†]	<1				
Dichloromethane	Not flammable	14.5	39.8	18.2	6.3	6.1
Propylencarbonate	>135	<0.005	239			
Ethyl acetate	-4	4.5	77			
Toluene	4 [‡]	2	120	18	1.4	2.0
<hr/>						
[†] Flammable						
[‡] Highly flammable						

Table 1.3: Flash point (°C), evaporation rate ($\eta_{\text{ButylAcetate}} = 1$) and LD50 (Lethal Dose 50% in g/Kg, rat ingestion) of some industrial solvents.

it can be reused to produce clear plastic pieces [10]. Two different types of cables were tested: a white one made of PVC (Polyvinyl chloride) and a yellow one made of PU (Polyurethane). A test was set up in order to compare the deinking power of different solvents. To evaluate the flammability and the toxicity of a solvent, we shall compare the flash points and the LD50 (Lethal Dose 50% for rats after oral dispensing).

The deinking test consists of soaking an absorbing paper sheet with the solvent studied and then counting the number of wipings of a printed part of the cable. The results are given in Table 1.4, in which the deinking power is displayed. The first number corresponds to the number of wipings which is sufficient to remove the most of the ink but some ink remains on the cable. The second one corresponds to the complete removal of the ink from the cable. In this case the lower the number is, the better the deinking power. A number of 1 means that one wiping is sufficient for a complete removing of the ink and a number above 18 corresponds to a very bad deinking power. The precision is evaluated to ± 1 and was sufficient to classify the solvents according to their deinking power.

Solvent	Deinking power		Flash point(°C)	LD50 (g/Kg)
	PVC	PU		
C ₁ PO ₁	≈15-18	3-5	31	7.2
C ₁ PO ₂	≈15-18	4-5	75	5.13
C ₁ PO ₃	>18	4-5	121	3.2
C ₃ PO ₁	>18	4-5	48	2.0-4.35
C ₃ PO ₂	>18	4-5	88	>2.00
C ₃ PO ₃	>18	8-10	130	
C ₄ PO ₁	>18	3-4	63	Irritant 3.3
C ₄ PO ₂	>18	5-6	100	3.7
C ₄ PO ₃	>18	12-14	126	2.6
CH ₃ PO ₁ Ac	2-3	1-2	42	Irritant 8.53
CH ₃ PO ₂ CH ₃	4-6	1-2	65	3.3
Acetone	1-3	1	18	Toxic 9.0
MEK	1-3	1	-9	Toxic 6.0
Ethanol	doesn't work	6-8	13	7.06
Isopropanol	doesn't work	8-10	12	5.84
Butan-1-ol		9-11	29-35	Harmful 0.79
Limonen	>18	4-6	72	Irritant
Propylenecarbonate	4-6	3-4	>135	28.0
Ethyl acetate	1	1	-4	5.62

Table 1.4: Deinking power obtained with polyvinyl chloride (PVC) and polyurethane (PU) cables (see text), Flash point (°C), evaporation rate ($n_{ButylAcetate} = 1$) and LD50 (Lethal Dose 50% in g/Kg, rat ingestion) of some industrial solvents.

It is clear from the results (Table 1.4) that the type of polymer the cable is made from is a critical factor in the choice of a deinking solvent. So the solvent has to be adapted to the type of treated cable (polymer). The deinking efficiency of a solvent depends on two main factors which are (1) the ability of the solvent to solubilize the ink and (2) the ability of the solvent to make the polymer to swell.

The best results for deinking power are obtained with short ketones (acetone, methylethylketone MEK). These are well known for their exceptional solvent property. This becomes a disadvantage for example in the case of PVC cable because of the solubilization of this polymer. Moreover the extreme flammability, toxicity and evaporation rate of short ketones make their use impossible in industrial deinking processes. These two short ketones have only been used in this study to provide a source of comparison. It is nevertheless possible to find a compromise with other less toxic solvents, the C_nPO_m s. The deinking powers of C_nPO_m s show a large disparity. The whole range of C_nPO_m s shows a better deinking power in the case of the PU cable, except for the higher lipophiles C_3PO_3 and C_4PO_3 . Only the $CH_3PO_2CH_3$ (methoxylated C_1PO_2) and CH_3PO_1Ac (acetylated C_1PO_1) compounds give good deinking power for the two types of cable (PVC, PU). The better solvent property of these two solvents, in comparison to the C_nPO_m s, is not surprising because these molecules are hydrogen bond acceptors only. Consequently they cannot form intermolecular hydrogen bonds, so reducing the cohesive energy between the solvent molecules (see Table 1.3 the δ_H Hansen parameters of $CH_3PO_2CH_3$, CH_3PO_1Ac and the others C_nPO_m s). Solubility of hydrophobic compounds, i.e. the ink or the polymer, in the solvent is usually higher in solvents having a low δ_H parameter [9].

The compounds $CH_3PO_2CH_3$, CH_3PO_1Ac and propylene carbonate stand out as the better solvents for deinking in this study, these three solvents display numerous advantages: low toxicity, low evaporation rate and good deinking power. The flash point of $CH_3PO_2CH_3$ and CH_3PO_1Ac are respectively 65 and 42°C. This means they are too close to the limit of flammability to be considered comfortably as non flammable. This problem could be solved if some small quantity of water was added. However the deinking power should be worse and a compromise has to be found. Propylene carbonate displays exceptional properties: good deinking efficiency, very high flash point, very low evaporation rate and very low toxicity in comparison to C_nPO_m s. Nevertheless propylene carbonate has the disadvantage that it is more expensive than C_nPO_m s and of course more so than the classical solvents. In conclusion the C_nPO_m s studied could be proposed for industrial deinking process with some restrictions or qualifications on the type of polymer matrix which is used.

1.4.2 Degreasing of metal plates

The aim of this study is to find a degreasing agent (solvent) for the treatment of copper and aluminium plates for mechanics and electronics industries. In these industries short ketones (acetone, MEK) and industrial solvent composed of petroleum distillate (isoparaffin) are also generally used for this purpose [11]. The use of such solvents leads to similar disadvantages as those cited in the deinking study

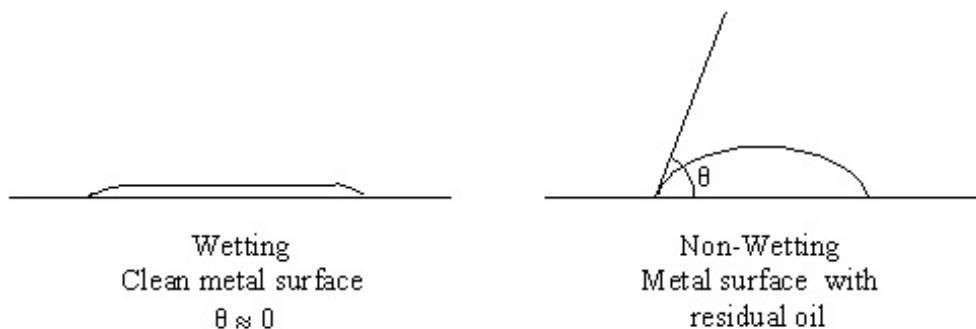


Figure 1.7: Wetting and non-wetting of a water droplet on plan surfaces, θ represents the contact angle of the water droplet.

(see Section 1.4.1).

For the formulation of degreasing agents many parameters have to be considered, so in most cases a systematic study has to be made. In the present study some parameters are kept constant, such as the type of plate and the oil to be removed:

- aluminium plates (standard aluminium of computer screen) and mineral oil *WISURA NFW* from the supplier *WISURA*
- copper plates (standard copper plates from the industrial partner) and the oil *Lubricor*, a triglyceride oil.

A valuable way to estimate the degreasing power of a solvent on a plane surface is to measure the contact angle of a water droplet on the surface [12, 13]. If the oil is removed from the plate the water spreads completely on the metal plate⁶. And if some oil remains on the plate the water droplet does not spread and a high contact angle is observed (see Fig. 1.7).

The degreasing test is designed to measure the contact angle after a standard degreasing process: at first the plates are cut into small pieces (2×1cm). In order to measure the contact angle, a small piece is consequently immersed in the solvent under test with magnetic stirring (200 RPM) for 5 min (see Fig. 1.8). The aluminium plates were already covered by the mineral oil whereas the copper plates were covered manually, as homogeneously as possible, with the triglyceride oil. The contact angles have been measured as a function of time because a kinetic factor associated with water droplet spreading appears [14].

Note that the repartition of the oil film on the plates can be nonhomogeneous. So the experimental error can be partially explained by this fact. That is why the measurements are done several times (at least 3 times) for each solvent tested. From these different measures, error bars were calculated and displayed in the graphs.

⁶Wetting by water appears only on clean hydrophilic surfaces, here metal, devoid of residual oil.

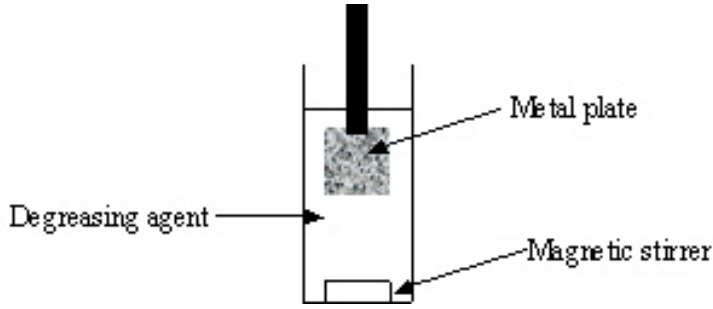


Figure 1.8: Cleaning of a metal plate (see text).

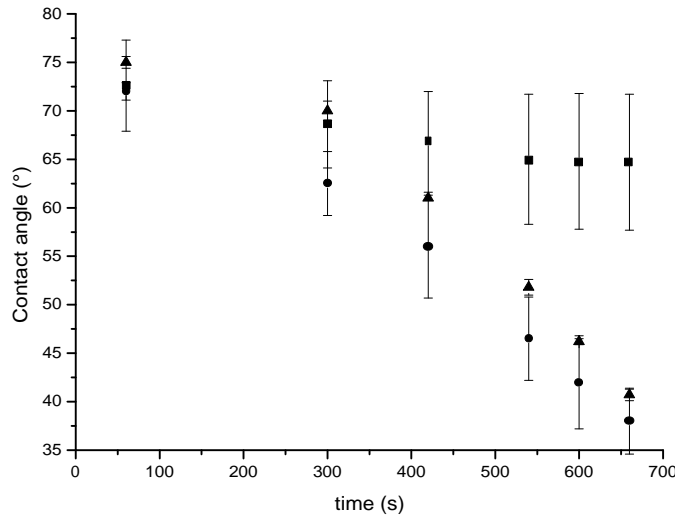


Figure 1.9: Contact angle θ of a water droplet on aluminium plates as a function of time: plate without treatment (■), clean plate (●) and plate after acetone treatment (▲).

Aluminium plates

First, contact angles were measured with (1) a plate without treatment, i.e. covered with mineral oil, and (2) with a clean plate, from which the oil was completely removed by acetone treatment with strong mechanical energy (see Fig. 1.9). With the clean plate the contact angle decreases strongly with time, i.e. the water droplet spreads rapidly, whereas with the plate covered with oil the contact angle remains high (no spreading). We shall then consider that the quicker the droplet spreads, the cleaner is the plate. After treatment of a plate with acetone according to our test (5 min, 200 RPM, see Fig. 1.9), the contact angles were also measured. The resulting curve is similar to that obtained with the “clean plate”. This means that the treatment realized with acetone, according to our test, is sufficient to remove most of the oil present on the plates.

This test was realized with different propylene glycol alkylethers: $\text{CH}_3\text{PO}_2\text{CH}_3$ (1), $\text{CH}_3\text{PO}_1\text{Ac}$ (4), C_3PO_1 (2), C_3PO_2 (3) and with a petroleum distillate (Isopar G) commonly used as a degreasing solvent (see Fig. 1.10). The resulting curves *contact angle vs. time* are compared with those obtained with the clean and greasy plates. C_3PO_1 and $\text{CH}_3\text{PO}_1\text{Ac}$ give nearly the same result as in the case of the clean plate, that means the degreasing power of these solvents is as good as that of acetone for this application. No oil remains on the plate after treatment. For $\text{CH}_3\text{PO}_2\text{CH}_3$ and C_3PO_2 no such clear conclusions can be drawn. The degreasing powers of these solvents are not as good as those preceeding. The classical degreasing agent: petroleum distillate Isopar G (Isoparaffin) gives results similar to those with a clean plate (see Fig. 1.10). Hence the degreasing powers of C_3PO_1 and $\text{CH}_3\text{PO}_1\text{Ac}$ with Isopar G are comparable.

In the electronics industry, the degreasing of metal pieces is most of the time done by immersing the pieces to be degreased in an ultrasound bath filled with solvent(s). For this reason similar measurements were redone with plates treated in such an ultrasound bath (during 5min) that contained the solvent studied. The same conclusions can be done as with the treatment with the magnetic stirrer.

Copper plates

At first a comparison is made between the measurements obtained (1) with a copper plate covered with the Lubricor oil and (2) with a perfectly clean copper plate obtained after a complete removal of the oil with acetone treatment and strong mechanical energy. The result can be seen in Fig. 1.11. As for the study on the aluminium plates, the contact angle, in the two cases presented show a rather different evolution with the time. In the case of the plate covered with the Lubricor oil the contact angle is essentially constant with the time. This means that the water droplet does not spread. In the case of the clean plate the contact angle is very high at the beginning of the measurement and decreases strongly and linearly with time until very low contact angles are attained.

Acetone, $\text{CH}_3\text{PO}_2\text{CH}_3$, C_3PO_1 and $\text{CH}_3\text{PO}_1\text{Ac}$ were tested following our degreasing procedure. The results are compared with those obtained for: (1) the plate covered with the Lubricor oil and (2) the clean plate, see Fig. 1.11. The results for the plate covered with the Lubricor oil and the clean plate are plotted on this figure. They represent the two extreme cases. The proposed solvents lie between these. The three proposed solvents and acetone give nearly the same behavior with respect to contact angle evolution with the time, in comparison to the curve obtained with a clean plate. This means that the degreasing power of these solvents is good. Apparently no oil remains on the plate after treatment. However it is not possible with this present measurement technique to compare the efficiency of these solvents with one another.

To summarize, the degreasing of hard surfaces with C_nPO_m s appears to be efficient with different oils and metal surfaces. Such measurements do not prove with certainty the complete remove of the oil but give nethertheless an important infor-

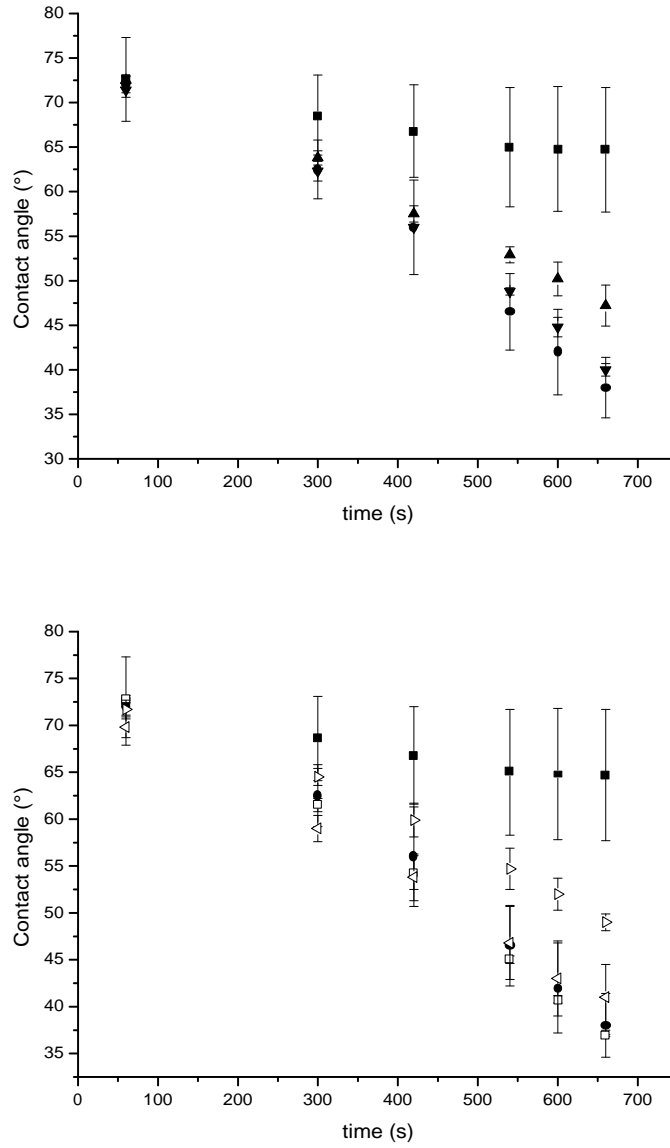


Figure 1.10: Contact angle θ of a water droplet on aluminium plates as a function of time: plate without treatment (■), clean plate (●), plates after treatment with: C_3PO_2 (▲), C_3PO_1 (▼), $CH_3PO_2CH_3$ (▷), CH_3PO_1Ac (◁) and with Isopar G (◻).

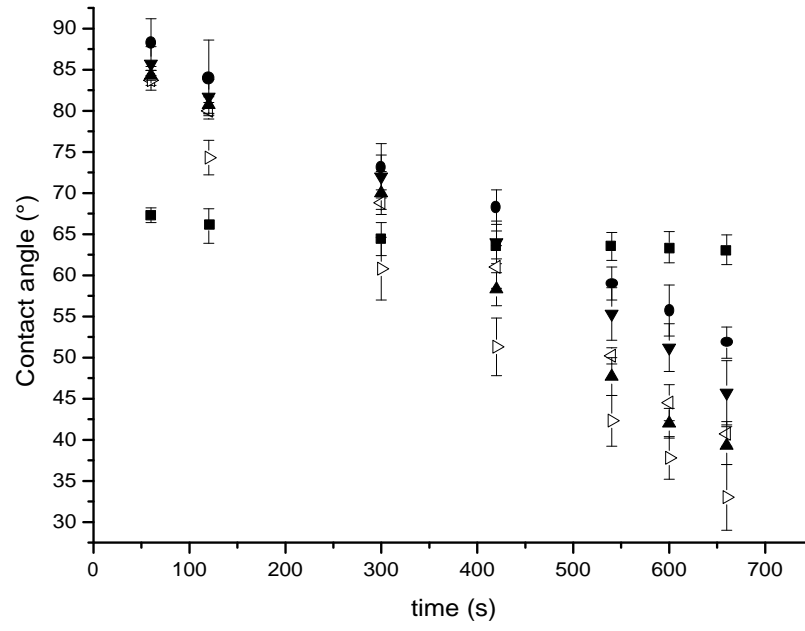


Figure 1.11: Contact angle θ of a water droplet on copper plates as a function of time: plate without treatment (■), clean plate (●), plates after treatment with: acetone (▲), C₃PO₁ (▼), CH₃PO₂CH₃ (▷) and with CH₃PO₁Ac (◁).

1.4 Propylene glycol alkyl ethers (C_nPO_m): efficient and low toxic industrial solvents

mation on the degreasing or non-degreasing property of a solvent. If the residual oil remaining on the plate has to be known exactly, some further analysis will be necessary. The use of C_nPO_m s for the degreasing of hard surfaces can be proposed as a valuable alternative to the use of toxic solvents as acetone or petroleum distillates usually used.

1 Overview of “glycol ethers” and of their industrial applications

Bibliography

- [1] <http://www.dow.com/glycoether/index.htm>.
- [2] S. Cordier, A. Bergeret, J. Goujard, M.C. Ha, and S. Ayme. Congenital malformation and maternal occupational exposure to glycol ethers. *Epidemiology*, 8:35, 1997.
- [3] B. Bingham, B. Cohrssen, and C. H. Powell. *Glycols and glycol ethers / synthetic polymers / organic sulfur compounds / organic phosphate*. *Patty's Toxicology*, volume 7. Wiley, 2001.
- [4] J. Etiemble. Les ethers de glycol, une toxicité variable selon les composés. *L'actualité chimique*, 145, 2003.
- [5] <http://www.pgep.org/>.
- [6] E. W. Flick. *Advanced Cleaning Product Formulations*. Noyes Publications, New York, 1999.
- [7] <http://www.inrs.fr>, glycol ethers.
- [8] Klaus Lunkenheimer, Simon Schroedle, and Werner. Kunz. Dowanol dpnb in water as an example of a solvo-surfactant system: Adsorption and foam properties. *Progress in Colloid and Polymer Science*, 126:14–20, 2004.
- [9] C. M. Hansen. *Hansen Solubility Parameters*. CRC Press, London, 2000.
- [10] H. Gecol, J. F. Scamehorn, S. D. Christian, B. P. Grady, and F. Riddell. Use of surfactant to remove water based inks from plastic films. *Colloids and Surfaces A*, 189:55, 2001.
- [11] E. B. Saubestre. *Detergency: Theory and test methods, Cleaning of metals*, chapter 19, pages 707–727. Marcel Dekker, New York, 1975.
- [12] Standard guide for testing cleaning performance of products intended for use on resilient flooring and washable walls. Technical report, ASTM D 4488-95, 2001.
- [13] <http://www.cleansolutions.org/analyticalmethods.html>.

Bibliography

- [14] T. P. Yin. Kinetics of spreading. *Journal of Physical Chemistry*, 73(2):2413, 1969.

Part I

Properties and characterization of C_nPO_m /water mixtures

2 Temperature dependence of propylene glycol alkyl ether/water mixtures

Abstract

The miscibility of propylene glycol ethers C_nPO_m with water is studied in the temperature range between 0 and 80°C. Several of these systems show a lower critical point of demixion, also called Lower Critical Solution Temperature (LCST), near room temperature. The shapes of the phase diagrams are discussed in detail and compared to those of the widely used but (geno)toxic ethylene glycol alkyl ether(C_nEO_m)/water mixtures. The addition of propylene glycol groups is found to decrease the aqueous solubility of a molecule whereas the addition of ethylene glycol groups is well known to increase it.

2.1 Introduction

Since the 1980s toxicological studies showed that the solvents derived from glycol ether and used in degreasing and cleaning process are hazardous to health and may present genotoxic activity [1], see Section 1.2 for more details. Consequently, there is a quest for new and less harmful low cost products with comparable physical and chemical properties. The ethers derived from propylene glycol, also called propylene glycol alkyl ether (C_nPO_m), seem to be an interesting alternative to ethylene glycol ethers (C_nEO_m) [2]. There is now a great number of patents dealing with them and their widespread industrial applications [2, 3]. They are amphiphilic compounds of low molecular weight and combine solvent (liquid state, volatility, low cost) properties with water surface tension lowering and co-surfactant properties¹. C_nPO_m s have some properties similar to the typical linear and short-chain ethylene glycol alkyl ethers, also called ethoxylated alcohols C_nEO_m ($i \leq 4$ and $j \leq 2$). The C_nEO_m have already been studied in detail in the presence of water and simple hydrocarbons [4, 5, 6]. These (geno)toxic molecules constitute the reference for our study of C_nPO_m s. The difference between the chemical structures of C_nPO_m and ethoxylated alcohols C_nEO_m lies in the fact that the latter possess an ethylene glycol group (EO) while C_nPO_m has a propylene glycol group (PO), which is known to increase the oil solubility of a molecule. Such a chemical group is present in the

¹The co-surfactant properties of C_nPO_m will be extensively studied in Part II of this thesis

well-known block copolymers, condensed with ethylene glycol groups $(\text{PO})_n(\text{EO})_m$, termed Pluronic®. These are widely used for the templating of mesoporous [7, 8] or as boosters to assist microemulsion formation [9]. The PO group can also be found in some surfactants where they are used as a spacer, between the hydrophilic head and the lipophilic tail thus permitting one to adjust the hydrophilic/lipophilic balance (HLB) and to optimize the solubilization of a given oil [10]. In comparison to the C_nEO_m , very little attention has been paid to the short C_nPO_m s in the literature, except in patents. As a result, the physico-chemical behavior of these molecules is not yet widely known. In a few papers special aspects of these molecules have been studied [11, 12, 13, 14, 15, 16]. For example, the C_nPO_m s have been found to participate in the formation of efficient microemulsions² for cleaning formulations or as chemical reaction media [10]. The effect of polyoxypropylene chains (PO_m) in nonionic amphiphiles (especially the studied C_nPO_m s) on their adsorption properties at the solution-air interface was also investigated [12, 13]. Note that Sokolowski [14] made an interesting comparison of C_nEO_m and C_nPO_m s in terms of their hydrophilic/hydrophobic balance. The short amphiphiles C_nEO_m have been recently studied by ultrasonic and dielectric spectroscopy [17, 18, 19]. It results that such molecules form microheterogeneous structures when mixed with water. These structures are related to mechanisms of dimerization by hydrogen bonding and also by hydrophobic interaction. Such spectroscopic measurements were not performed here due to the fact that the C_nPO_m are mixtures of isomers which make the interpretation of the spectra much more intricate. A detailed chemical analysis of a typical C_nPO_m representative, namely the dipropylene glycol mono propyl ether (C_3PO_2) is published elsewhere [20] and is reproduced in Fig. 1.5. The analysis shows that 4 chemical isomers are present, each of them consisting of 2 diastereomers which are themselves mixtures of 2 enantiomers. On the whole, 16 isomers are present. It can be assumed that the other C_nPO_m s with 2 PO groups (like C_4PO_2 , c.f. Table 2.1) present a similar isomer distribution. The C_nPO_m s containing 3 PO group are not yet analyzed for their isomer composition. In the present study the temperature dependence of some C_nPO_m /water mixtures is investigated. To this purpose phase diagrams are established and surface tension measurements are performed. The temperature dependence of C_3PO_1 aqueous mixtures was pointed out nearly 80 years ago [16] but has not been studied further in the open literature.

2.2 Materials and Methods

2.2.1 Materials

The propylene glycol alkyl ethers (C_nPO_m s) studied were all supplied by Dow Chemical except for the propylene glycol tert-butyl ether ($\text{iso-C}_4\text{PO}_1$). This was supplied by Lyondell Company. All of these C_nPO_m are used without further purification. The molecules differ in their chemical structures by the number of propylene glycol

²The formation of anionic microemulsions formed with C_nPO_m s will be investigate in Chapter 6

groups (PO), between 1 and 3, as well as in the alkyl chain which is an n-propyl or n-butyl group except for the iso-C₄PO₁ which is a tert-butyl group. The aqueous solubility data and purity grade of all the products are given in Table 2.1. Usual short n-alcohols are included to support the discussion of the phase diagram. The solubility data at 25°C were calculated from the phase diagrams of C_nPO_ms/water systems in Figs. 2.1 and 2.2. All of the products are mixtures of isomers and the purity is indicated in Table 2.1, which represents the total content of all these isomers present in the commercial products.

Chemical Name	Abbr.	Purity %	S _o at 25°C (mass %)	S _w at 25°C (mass %)
1-propoxy-methanol	C ₁ PO ₁	>99.5	∞	∞
di(propylene glycol) methyl ether	C ₁ PO ₂	>99	∞	∞
tri(propylene glycol) methyl ether	C ₁ PO ₃	>97.5	∞	∞
1-propoxy-2-propanol	C ₃ PO ₁	99	∞	∞
di(propylene glycol) propyl ether	C ₃ PO ₂	>98.5	17.1	20.6
tri(propylene glycol) propyl ether	C ₃ PO ₃	>97	14.4	14.9
propylene glycol butyl ether	C ₄ PO ₁	>99	5.3	14.9
di(propylene glycol) butyl ether	C ₄ PO ₂	>98.5	4.8	10.4
tri(propylene glycol) propyl ether	C ₄ PO ₃	>95	3.9	8.6
propylene glycol tert-butyl ether	iso-C ₄ PO ₁	>99	16.6	20.4
1-propanol	PrOH	>99	∞	∞
1-butanol	BuOH	>99.5	7.35 [†]	20.27 [†]
1-pentanol	PeOH	>99	2.20 [†]	7.46 [†]
tert-butanol	TBuOH	>99	∞	∞

[†]from refs. [21, 22, 23, 24]

Table 2.1: Chemical name, abbreviation, purity grade, solubility of organic compound in water at 25°C (mass %) (S_o) and water solubility in organic compound at 25°C (mass %) (S_w) of the studied propylene glycol alkyl ether (C_nPO_m) and of some classical n-alcohols.

2.2.2 Phase diagram determination

Water and C_nPO_ms are completely miscible below a certain temperature. This is called the cloud point here in analogy to polyethoxylated surfactants. Above the cloud point, the system is biphasic. The cloud points of the mixtures were determined by using an in house-constructed turbidity apparatus [25] which permits six samples to be measured at one time and provides a constant heating rate of 2°C/hour between 0 to 80°C. The temperature precision of the measures is estimated to be ±0.05°C.

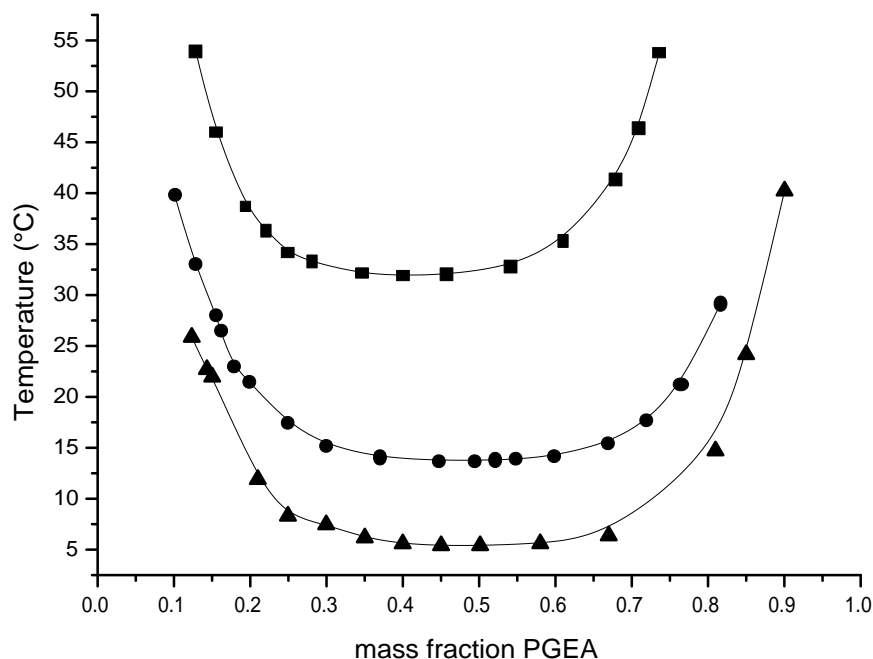


Figure 2.1: Cloud point versus the C_3PO_m mass fraction for: C_3PO_1 (▲), C_3PO_2 (●) and C_3PO_3 (■) /water systems.

2.2.3 Surface tension measurements

The surface tension of the C_3PO_1 /water system was determined with a tensiometer Krüss K10T using the ring method. The temperature was kept constant at $25 \pm 0.1^\circ\text{C}$.

2.3 Results and Discussion

2.3.1 Phase diagrams

All the methyl derivatives with 1 (C_1PO_1), 2 (C_1PO_2) or 3 PO groups (C_1PO_3) (see Table 2.1) are completely miscible with water at any temperature between 0 and 100°C . This high compatibility between the methyl derivatives and water is reflected by the high release of heat observed during mixing. The other C_nPO_m derivatives studied all show a partial demixing with water in this temperature range, see Figs. 2.1 and 2.2. As in the case of the short C_nEO_m , an increase in temperature results eventually with a broad biphasic region, where one water-rich phase is in equilibrium with one C_nPO_m -rich phase. No further phases could be detected.

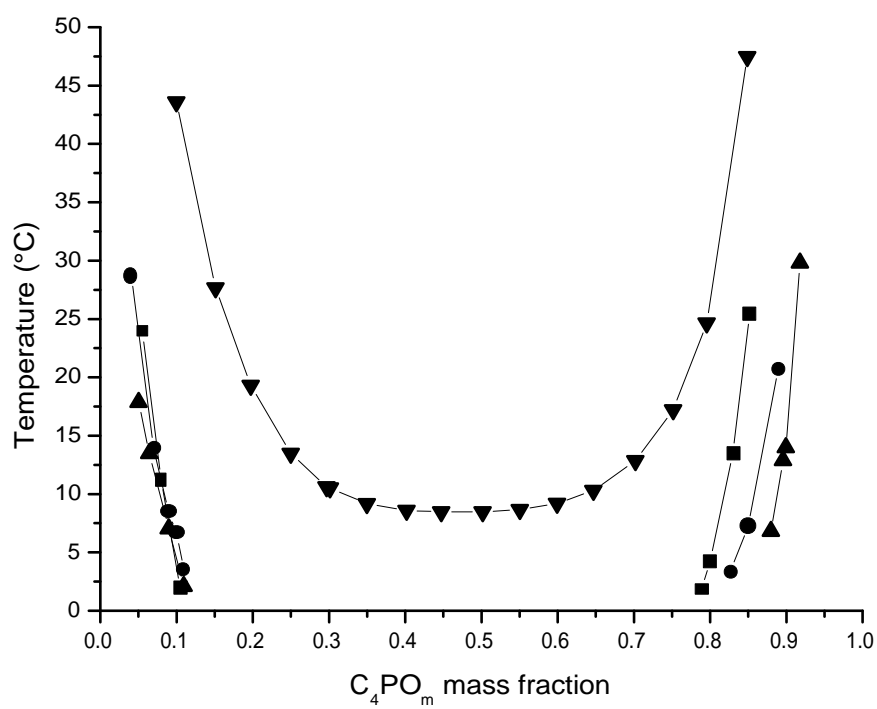


Figure 2.2: Cloud point versus the C_nPO_m mass fraction for: C_4PO_1 (▲), C_4PO_2 (●), C_4PO_3 (■) and iso- C_4PO_1 (▼) /water systems.

2.3.2 C₃PO₁/water system

The C₃PO₁/water phase diagram (see Fig 2.1) shows that the miscibility between water and C₃PO₁ is no longer total for temperatures above 31.9°C. This temperature is called the lower critical solution temperature (LCST) [6]. In comparison to 1-propanol, which is completely miscible with water until 100°C, the chemical structure of C₃PO₁ can be regarded as a 1-propanol molecule condensed with a PO group. The presence of a PO group in the C₃PO₁ molecule imparts the temperature dependence property to the C₃PO₁/Water system and decreases the hydrophilicity compared to 1-propanol. LCSTs near room temperature are usually found only for hydrogen-bonding compounds that have strong solvation interactions with water [6]. Increasing the temperature reduces this interaction and thus promotes phase separation. In the case of C_nPO_m as in the case of the classical ethylene glycols the strong interactions with water come from the hydrogen bond donor and acceptor properties of the hydroxyl function (-OH) and from the hydrogen bond acceptor property of the ether function (-O-). However, there is one difference. Whereas in short C_nEO_m/water mixtures ultrasonic spectroscopy studies suggested that C_nEO_m may form dimers [17, 18, 19], preliminary quasi-elastic light scattering (QELS) and small angle neutron scattering (SANS) experiments on C_nPO_m did not yield any hint at such an association in the water-rich regions [26]. Possibly the more bulky structure of the propylene glycol groups prevents such an association. Of course, in the C_nPO_m-rich phases the molecules must aggregate, but ordered structures like micelles or so are not found. The overall aspect of the phase diagram is similar to corresponding C_nEO_m/water mixtures, but the C_nPO_m/water mixtures have lower LCSTs. For example C₄EO₁ is an isomer of C₃PO₁ and its mixtures with water present a LCST at 49°C in comparison to 31.9°C for the C₃PO₁/water system. The effect of the PO group present in the C₃PO₁ molecule reduces the hydrophilic property in comparison to 1-propanol, while the ethylene glycol group present in the C₄EO₁ increases the hydrophilic property in comparison to 1-butanol. In the present system the maximum phase separation (cloud point) occurs over a wide range of C₃PO₁ mass fraction, between 0.12 and 0.75. To give an explanation for the location of the left limit (water-rich part of the phase diagram) the surface tension curve of the C₃PO₁/Water system was measured at 25°C (Fig 2.3). The surface tension decreases quite rapidly with increasing C₃PO₁ mass fraction, but not so sharply as in the case of classical surfactants and sharper than for the case of the corresponding n-alcohol (1-propanol) [27]. Beyond a C₃PO₁ mass fraction of about 0.2 the surface is widely saturated with C₃PO₁ and the surface tension remains nearly constant at higher C₃PO₁ concentrations. The water-C₃PO₁ interactions are strong enough at 25°C to ensure complete miscibility. At higher temperature the phase separations occur at C₃PO₁ mass fractions near to 0.12 meaning that bulk C₃PO₁ is no longer sufficiently hydrated by the water molecules. Note that for a composition of 0.12 mass percent of C₃PO₁ (the minimum C₃PO₁ concentration where C₃PO₁ is always soluble in water independently of the temperature) about 60 water molecules per C₃PO₁ molecule are present. So, once the surface is saturated with C₃PO₁ and less

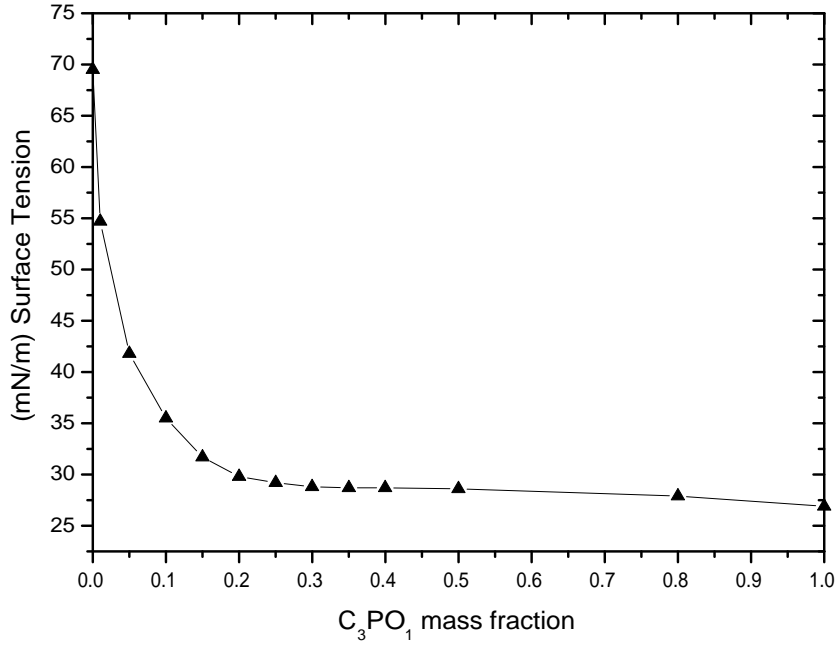


Figure 2.3: Surface tension σ (\blacktriangle , mN/m), measured at 25°C, versus C_3PO_1 mass fraction for the C_3PO_1 /water system.

than some tens of water molecules per C_3PO_1 molecule are present, demixing is energetically favoured at higher temperatures.

2.3.3 n-propyl C_nPO_m / water phase diagrams

For higher C_3PO_1 mass fraction (>0.12) the cloud point sharply decreases until the LCST ($T \approx 32^\circ\text{C}$, C_3PO_1 mass fraction ≈ 0.4). At the mass fraction corresponding to the LCST, the number of water molecules per C_3PO_1 molecule is between 9 and 10. At higher C_3PO_1 mass fractions the system is reversed and the water molecules become solvated by C_3PO_1 molecules. No phase separation occurs for C_3PO_1 mass fractions higher than about 0.75, which corresponds to 2 or 3 water molecules per C_3PO_1 molecule. Spectroscopic and SANS measurements suggest that in the case of an alcohol a hydroxyl group (-OH) can bind directly with 2 and 3 water molecules [28]. So even at higher temperatures the direct interactions between the C_3PO_1 alcohol groups and water remain sufficiently high to prevent demixion. But, unlike the mixtures at lower temperatures, no water aggregates can exist. They immediately go to the water-rich phase.

2.3.4 C₃PO_m/water phase diagrams

The number of PO group for C₃PO₁, C₃PO₂ and C₃PO₃ is respectively 1, 2 and 3. Fig. 2.1 shows that the shape of the phase diagrams of their mixtures with water are comparable. Note that for C₃PO₂/water and C₃PO₃/water mixtures a very slight turbidity can be observed at mass fractions around and slightly below 0.25 and at any temperature between 0 and 80°C. This phenomenon is probably the consequence of the demixing of very hydrophobic isomers or impurities, such as C₄PO₂, that are present in the commercial product in very small amounts. It seems that the topology of the phase diagrams for C₃PO₂ and C₃PO₃ is not so sensitive to the presence of these hydrophobic isomers. The LCST for C₃PO₁, C₃PO₂ and C₃PO₃ decreases with increasing numbers of PO group from 1 to 3, respectively: 31.9, 13.8, and 5.4°C and in the same series the biphasic region becomes larger. Contrary to the ethylene glycol group, which imparts hydrophilicity to a molecule, the circumstance of adding a PO group to a molecule decreases its hydrophilicity. The solubility of water in C_nPO_m decreases more sensitively than the solubility of C_nPO_m in water with increasing numbers of PO group. The LCSTs of all three propyl C_nPO_m/water mixtures are not far away from room temperature. Therefore these mixtures are convenient and low-toxic media in which to perform organic reactions in a homogeneous environment. The low temperature mixture has interesting solubilization properties for both lipophilic and hydrophilic compounds. Hence such systems provide an alternative to reactions in two-phase systems with phase transfer catalysts. By a simple heating process hydrophilic and lipophilic reaction products can then be separated. The boiling points of C_nPO_m (e.g. boiling point of C₃PO₁ = 149°C at ambient pressure, see Table 1.3) makes distillation processes relatively easy and thus both organic and hydrophilic products can be recovered in an easy way without further expensive purification steps. Of course, the reaction components may shift the LCSTs of the mixtures. How strong these shifts can be will be demonstrated in Chapter 3 for salts[29]. But the addition of further neutral components can counterbalance these shifts if they are a nuisance to the process.

2.3.5 C₄PO_m/water phase diagrams

Phase diagrams for the n-butyl derivatives (C₄PO₁, C₄PO₂ and C₄PO₃) with water are presented in Fig 2.2. Considering the n-butyl derivatives as the condensation of a molecule of 1-butanol (itself partially soluble with water, see Table 2.1) with PO group (itself decreasing hydrophilicity), the partial solubility of n-butyl derivatives is not surprising. Moreover, the biphasic region becomes larger when the number of PO group increases, especially in the C_nPO_m-rich part of the diagram, as we have already observed for the n-propyl derivatives. As regards the iso-C₄PO₁ (Fig. 2.2) a completely miscibility with water is observed for temperatures below 8.7°C (LCST). The difference of water solubility between C₄PO₁ and iso-C₄PO₁ (Table 2.1) follows the same trend as 1-butanol and tert-butanol (see also Table 2.1). The ramification of the butyl residue increases the water solubility, probably because the hydrophobic

surface of the ramified molecules is smaller than the surface of linear chain molecules. The iso-C₄PO₁/water mixture shows a demixion curve situated between those of the C₃PO₂ and C₃PO₃ water systems and in line with their respective LCSTs of 13.8 and 5.4°C. This means that the iso-C₄PO₁ has a hydrophilic affinity between the latter two compounds. In conclusion it can be stated that the hydrophilic property of such short amphiphiles and thus the phase behavior of these compounds in mixtures with water (cloud points) can be adjusted by a convenient choice of (1) the number of carbon atoms composing the alkyl chain n , (2) the ramification of the alkyl chain, and (3) the number of PO group m .

2.3.6 Comparison of the LCST values between the C_{*n*}EO_{*m*}s and the C_{*n*}PO_{*m*}s

The LCST values of the C_{*n*}PO_{*m*}s studied and of the corresponding isomers C_{*n*}EO_{*m*} are summarized in Table 2.2. In the case of C₃PO₁ the LCST values of its two pure isomers, primary and secondary alcohol, obtained by Cox et. al. [16] are included. Generally primary alcohols are less soluble in water than secondary alcohols, which is not the case of the two isomers of C₃PO₁. The propylene glycol ethers present lower LCST in comparison to their corresponding ethylene glycol ether isomers. Moreover it can be remarked that the LCST values of C₃PO₁ and C₅EO₂ are very close. This means that the hydrophilicity of these two molecules is comparable. Similar remarks apply to iso-C₄PO₁ and C₈EO₃ (LCST = 8°C [30]) and to C₃PO₃ and C₁₂EO₄ (LCST = 4°C [30]). Nevertheless C₈EO₃ and C₁₂EO₄ are true surfactants, i.e. micelle forming surfactants, and may not be considered as solvents.

propyleneglycol ether		ethyleneglycol ether	
C _{<i>n</i>} PO _{<i>m</i>}	LCST (°C)	C _{<i>n</i>} EO _{<i>m</i>}	LCST (°C) [†]
C ₃ PO ₁	31.9	C ₄ EO ₁	
C ₃ PO ₁ (primary alcohol)	42.8 [‡]	C ₄ EO ₁	49.0
C ₃ PO ₁ (secondary alcohol)	34.5 [‡]	C ₄ EO ₁	
C ₃ PO ₂	13.8	C ₅ EO ₂	34
C ₃ PO ₃	5.4	C ₆ EO ₃	44
iso-C ₄ PO ₁	8.7	C ₅ EO ₁	N.A.
[†] see ref. [30]			
[‡] see ref. [16]			

Table 2.2: LCST values of the studied C_{*n*}PO_{*m*}s and of their corresponding C_{*n*}EO_{*m*} isomers.

2.4 Conclusion

In this work we studied the temperature-dependent phase behaviour of mixtures of industrial C_nPO_m s with water. All these systems display at least partial miscibility and a larger solubility range at lower temperature. Moreover for the n-propyl and tert-butyl derivatives studied, a LCST is observed near room temperature. This type of phase behavior is typical for hydrogen bonding compounds that have strong interactions with water, due to the presence of hydroxyl and ether functions in the molecules. C_nPO_m molecules can be considered as the combination of short alcohols (propanol, butanol) with a certain number of propylene glycol groups (m from 1 to 3). We can conclude that adding a PO group to 1-propanol or tert-butanol induces strong temperature dependence in the phase diagrams of C_nPO_m /water mixtures between 0 to 100°C with interesting consequences for organic synthesis and extraction. In contrast to the usual (genotoxic) ethylene glycol groups, a PO group decreases the hydrophilic property of an alcohol but this effect is weak in comparison to the addition of a carbon atom to the n-alkyl chain of the n-alcohol. The following series of hydrophilicity is found: 1-propanol > C_3PO_1 > C_3PO_2 > iso- C_4PO_1 > C_3PO_3 > 1-butanol > C_4PO_1 > C_4PO_2 > C_4PO_3 > 1-pentanol. A surface tension study of the C_3PO_1 /Water system showed that the molecule is indeed surface active, but not so much as classical surfactants. No organized aggregates such as micelles are formed. Nevertheless the C_nPO_m s have excellent solvent properties. Precise phase diagrams are the first step to a better understanding of the solubilization process of these industrial compounds that are current in widespread use as degreasing and paint solvents or as coupling agents in formulation industries.

Bibliography

- [1] J. Etienneble. Les ethers de glycol, une toxicité variable selon les composés. *L'actualité chimique*, 145, 2003.
- [2] <http://www.pgep.org/>.
- [3] <http://www.dow.com/glycolether/index.htm>.
- [4] M. Kahlweit, E. Lessner, and R. Strey. Influence of the properties of the oil and the surfactant on the phase behavior of systems of the type water-oil-nonionic surfactant. *Journal of Physical Chemistry*, 87:5032–40, 1983.
- [5] M. Kahlweit, E. Lessner, and R. Strey. Phase behavior of ternary systems of the type water-oil-nonionic surfactant. *Colloid and Polymer Science*, 261:954–64, 1983.
- [6] Robert G.. Laughlin. *The Aqueous Phase Behavior of Surfactants*. Academic Press, London, UK, 1996.
- [7] Dongyuan Zhao, Jianglin Feng, Qisheng Huo, Nicholas Melosh, Glenn H. Fredrickson, Bradley F. Chmelka, and Galen D. Stucky. Triblock copolymer syntheses of mesoporous silica with periodic 50 to 300 angstrom pores. *Science (Washington, D. C.)*, 279:548–552, 1998.
- [8] Dongyuan Zhao, Qisheng Huo, Jianglin Feng, B. F. Chmelka, and Galen D. Stucky. Nonionic triblock and star diblock copolymer and oligomeric surfactant syntheses of highly ordered, hydrothermally stable, mesoporous silica structures. *Journal of the American Chemical Society*, 120:6024–6036, 1998.
- [9] B. Jakobs, T. Sottmann, R. Strey, J. Allgaier, L. Willner, and D. Richter. Amphiphilic block copolymers as efficiency boosters for microemulsions. *Langmuir*, 15:6707–6711, 1999.
- [10] M. Minana-Perez, A. Graciaa, J. Lachaise, and J.-L.. Salager. Solubilization of polar oils in microemulsion systems. *Progress in Colloid & Polymer Science*, 98:177–9, 1995.
- [11] John Klier, Christopher J. Tucker, Thomas H. Kalantar, and D. P. Green. Properties and applications of microemulsions. *Advanced Materials (Weinheim, Germany)*, 12:1751–1757, 2000.

- [12] R.M. Stephenson. *Journal of Chemical and Engineering Data*, 38:134–8, 1999.
- [13] K. Lunkenheimer, H.-R. Holzbauer, and R. Hirte. Novel results on adsorption properties of definite n-alkyl oxypropylene oligomers at the air/water interface. *Progress in Colloid & Polymer Science*, 97:116–20, 1994.
- [14] Adam. Sokolowski. Chemical structure and thermodynamics of amphiphile solutions. 2. effective length of alkyl chain in oligooxyalkylenated alcohols. *Colloids and Surfaces*, 56:239–49, 1991.
- [15] L. F. Komarova and Yu. N. Garber. Physical properties of dihydric alcohol ethers. *Zhurnal Organicheskoi Khimii*, 7:2507–9, 1971.
- [16] H. L. Cox, Wm. L. Nelson, and L. H. Cretcher. Reciprocal solubility of the normal propyl ethers of 1,2-propylene glycol and water. closed solubility curves. ii. *Journal of the American Chemical Society*, 49:1080–3, 1927.
- [17] U. Kaatze, K. Menzel, R. Pottel, and S. Schwerdtfeger. Microheterogeneity of 2-butoxyethanol/water mixtures at room temperature. an ultrasonic relaxation study. *Zeitschrift fuer Physikalische Chemie (Muenchen, Germany)*, 186:141–70, 1994.
- [18] U. Kaatze, M. Kettler, and R. Pottel. Dielectric relaxation spectrometry of mixtures of water with isopropoxy- and isobutoxyethanol. comparison to unbranched poly(ethylene glycol) monoalkyl ethers. *Journal of Physical Chemistry*, 100:2360–6, 1996.
- [19] K. Menzel, A. Rupprecht, and U.. Kaatze. Broad-band ultrasonic spectrometry of ciej/water mixtures. precritical behavior. *Journal of Physical Chemistry B*, 101:1255–1263, 1997.
- [20] Klaus Lunkenheimer, Simon Schroedle, and Werner. Kunz. Dowanol dpnb in water as an example of a solvo-surfactant system: Adsorption and foam properties. *Progress in Colloid and Polymer Science*, 126:14–20, 2004.
- [21] Atherton. Seidell. *Solubilities of Inorganic and Organic Compounds. 2nd Ed. revised and enlarged*. D. Van Nostrand Co. Inc., 1928.
- [22] H. Stephen and T. Stephen. *Solubilities of Inorganic and Organic Compounds, Vol. 1: Binary Systems, Part II*. 1963.
- [23] P. M. Ginnings and Rhoda. Baum. Aqueous solubilities of the isomeric pentanols. *Journal of the American Chemical Society*, 59:1111–13, 1937.
- [24] Ibert. Mellan. *Industrial Solvents Handbook. 2nd Ed*. Noyes Data Corporation, Park Ridge, N.J., 1977.

- [25] Simon Schroedle, Richard Buchner, and Werner. Kunz. Automated apparatus for the rapid determination of liquid-liquid and solid-liquid phase transitions. *Fluid Phase Equilibria*, 216:175–182, 2004.
- [26] <http://www.ill.fr/>, 2002, experimental report n°: 9-10-634.
- [27] Gonzalo Vazquez, Estrella Alvarez, and Jose M.. Navaza. Surface tension of alcohol water + water from 20 to 50 degc. *Journal of Chemical and Engineering Data*, 40:611–14, 1995.
- [28] D. T. Bowron and S. Diaz. Moreno. Structural correlations of water molecules in a concentrated alcohol solution. *Journal of Physics: Condensed Matter*, 15:121–127, 2003.
- [29] Pierre Bauduin, Laurent Wattebled, Didier Touraud, and Werner. Kunz. Hofmeister ion effects on the phase diagrams of water-propylene glycol propyl ethers. *Zeitschrift fuer Physikalische Chemie (Muenchen, Germany)*, 218:631–641, 2004.
- [30] Mario Corti, Claudio Minero, and Vittorio. Degiorgio. Cloud point transition in nonionic micellar solutions. *Journal of Physical Chemistry*, 88:309–17, 1984.

3 Hofmeister ion effects on the phase diagrams of water/propylene glycol propyl ethers

Abstract

The influence of different salts on the lower critical solution temperature (LCST) of mixtures of propylene glycol propyl ether (C_3PO_1) and of dipropylene glycol propyl ether (C_3PO_2) with water was determined experimentally. It was observed that the temperature shifts follow precisely the same Hofmeister series for anions that was originally found for salting-in and salting-out effects for protein solutions. A slight cation specificity in contrast to that for anions was found. The results are similar to the observations found for mixtures of water with non-ionic surfactants. In the case of (C_3PO_2) mixtures with water, temperature dependent phase diagrams in the presence of one salting-in ($NaSCN$) and one salting-out (Na_2SO_4) salt were measured at a fixed salt concentration in water of 0.041M. The results can be qualitatively understood by assuming a different hydrophobicity for both types of salts. They further hint at a strong degree of solute determined cooperative water structure.

3.1 Introduction

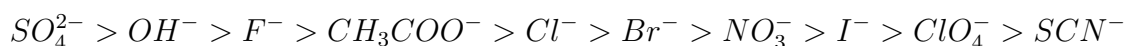
Ions play an essential role in numerous systems and processes, both in nature and technology. Much effort has been made over many decades to understand ionic effects both at the macroscopic, and at more and more microscopic levels, and to infer their consequences for the properties of matter. Barthel and co-workers carried out a tremendous amount of work to understand the properties of aqueous and especially non-aqueous electrolyte solutions [1]. They considered all kinds of bulk solutions properties, thermodynamic, kinetic, structural and dynamic ones. Further to the huge amount of new and highly precise data that they could obtain, Barthel's chemical model is generally held to be a physically sound and pragmatical approach to describe short-range ion-ion interactions and hence specific ion effects. As a result many macroscopic properties could be reproduced consistently in dilute solutions [1].

Specific ion effects are particularly important at interfaces, be they between solids and liquids, e.g. in mesoporous systems [2], between macromolecules and simple salt

solutions as in protein- buffer solutions [3, 4], between liquid and gas phases such as air and sea water [5] or between two immiscible liquid phases [6].

Franz Hofmeister, a pharmacologist, was the first to study such specific ion effects at interfaces in detail. Carried out in the second half of the 19th century, his work contains a wealth of information that has been widely ignored over the last 50 years, partially because all his papers were written in German. Two of his most relevant papers have been recently translated and republished into English [7].

Since the work of Hofmeister, salts or ions or, more specifically anions, have been classified as salting-in (structure-breaking) or salting-out (structure-making) according to their ability to increase or decrease the solubility of proteins in water. This classification is known as the Hofmeister series. For anions it is:



Here the most salting-out ion is on the extreme left, and the most salting-in ion is on the extreme right side. The chloride ion is often borderline and has nearly no influence on salting-in or out.

By and large the series turned out to be much the same for a great number of properties that involve interfaces. So something unique must be behind this behaviour¹. It is remarkable that up to now there is no real quantitative explanation for this series. Dispersion forces [8, 9, 10] have reasonably been invoked as a factor². More often, a specific change of ionic hydration at an interface due to ion-solvent induced dipole interactions [11] (or dispersion self energy changes) are assigned major responsibility for the effects. The difficulty is that these specific ion phenomena are the consequence of a very subtle interplay of several interactions, including steric, dielectric, and many body quantum mechanical effects.

In order to obtain a better insight into the Hofmeister series, precise and reliable experimental data are needed. They should be simple enough to be interpreted or modelled in an unambiguous way. In this sense, protein solubility is probably too complicated, because a protein does not have a well-defined surface, and specific chemical interactions between ions and some amino-acid groups always occur.

The surface tension of aqueous electrolyte solutions is probably the simplest property that reflects the Hofmeister series, and an attempt has been made recently to model it [12]. In the present work we focus on another simple property. That is the demixing temperature of an aqueous salt solution and an organic solvent. Such experiments have already been done for aqueous solutions in contact with typical non-ionic surfactants [13, 14, 15] and polymers [16, 17]. We mention also an old

¹In Chapter 7, anion specific effect will be studied on the pH of citrate buffer and on enzymatic activity.

²By Van der Waals-Lifshitz-dispersion forces we mean the totality of many body quantum mechanical electromagnetic fluctuation forces excluding electrostatics. These are either missing from standard primitive model theories of electrolytes and interfaces, or treated inconsistently in theories of particle interactions like that of DLVO. Ninham's and Yaminski's paper [10] proves that dispersion forces must contribute to specificity

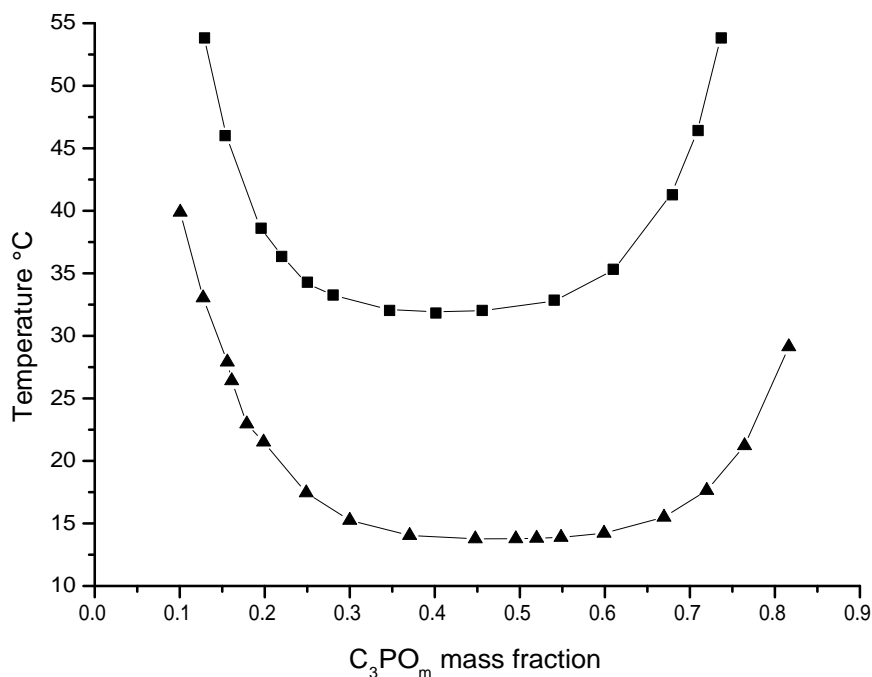


Figure 3.1: Phase diagrams of C_3PO_1 (■) and C_3PO_2 (▲) mixtures with pure water as a function of temperature.

study by McDevit and Long [18], who measured the solubility of benzene in aqueous solutions as a function of salt type and concentration. They also found a Hofmeister series.

The organic solvents we used in the present study are two propylene glycol propyl ethers with one (C_3PO_1) and two (C_3PO_2) propylene glycol groups, respectively. Their structure and their temperature dependent phase diagrams in mixtures with pure water are shown in Fig. 3.1.

There are several reasons to study these particular systems:

- Propylene glycol ethers (C_nPO_m) have lower critical solution temperatures (LCSTs) close to room temperature. Consequently, it is easy to study them experimentally. Furthermore, the transition from a complete miscibility to a biphasic liquid system close to room temperature offers interesting options for reaction and extraction processes, especially because C_nPO_m are not, or not very, toxic. Salts can be used to adjust precisely the desired demixing temperatures.
- Although the C_nPO_m /water systems have phase diagrams similar to those for water and short non-ionic surfactants, like short-chain polyethylene glycol ethers (C_nEO_m), C_nPO_m are more reminiscent of organic liquids than of sur-

factants. Thus no microstructuring in the form of micelles, liquid crystals or other mesophases is known for C_nPO_m mixtures with water. The reason is that only the terminal -OH group is hydrophilic, whereas the propylene oxide groups are not, in contrast to ethylene oxide groups [19, 20]. In this respect the C_nPO_m s can be compared to classical aliphatic alcohols. Nevertheless, the C_nPO_m are very slightly amphiphilic and they may form more or less undefined aggregates. A consequence is that their temperature dependent behaviour in mixtures with water resembles the behaviour of non-ionic surfactants and of organic liquids which strongly interact with water through hydrogen bonds such as tetrahydrofuran, nicotine, triethylamine etc. In analogy to water-surfactant mixtures we call here the lower critical points of demixing cloud points. But in contrast to typical surfactants the advantage of C_nPO_m s is that the influence of salts can be compared over a wide range of water-to- C_nPO_m ratios, because no well-defined structures or phase transitions occur below the cloud point.

- Unlike many surfactants C_nPO_m s are available in a highly pure state as regards the monodispersity of the number of propylene glycol groups. Only the presence of different isomers must be taken into account [21], see Fig. 1.5.

In the present study two types of experiments were performed: first the shift of the LCST as a function of salt concentrations was determined for both the C_3PO_1 /water and C_3PO_2 /water mixtures and for different salts. Then the cloud point shifts due to a certain amount of sodium sulfate and sodium thiocyanate ($c = 0.041M$, in water) were measured for different water/ C_3PO_2 ratios.

3.2 Experimental

3.2.1 Materials

All electrolytes were purchased from Fluka, Merck or Aldrich with a purity grade superior to 99% . C_3PO_1 (99%) and C_3PO_2 (98.5%) were supplied by Dow Chemical and also used without further purification. All chemicals were used without further purification.

3.2.2 Cloud point determination

The cloud points (CP) were determined with the help of a newly constructed apparatus that allows the precise determination of phase transitions as a function of temperature [21]. With this apparatus six mixtures can be simultaneously analyzed with a constant heating and cooling rate of $2^\circ C$ per hour. It was checked that heating and cooling yielded the same cloud points. The precision of the transition temperatures is about $\pm 0.05^\circ C$.

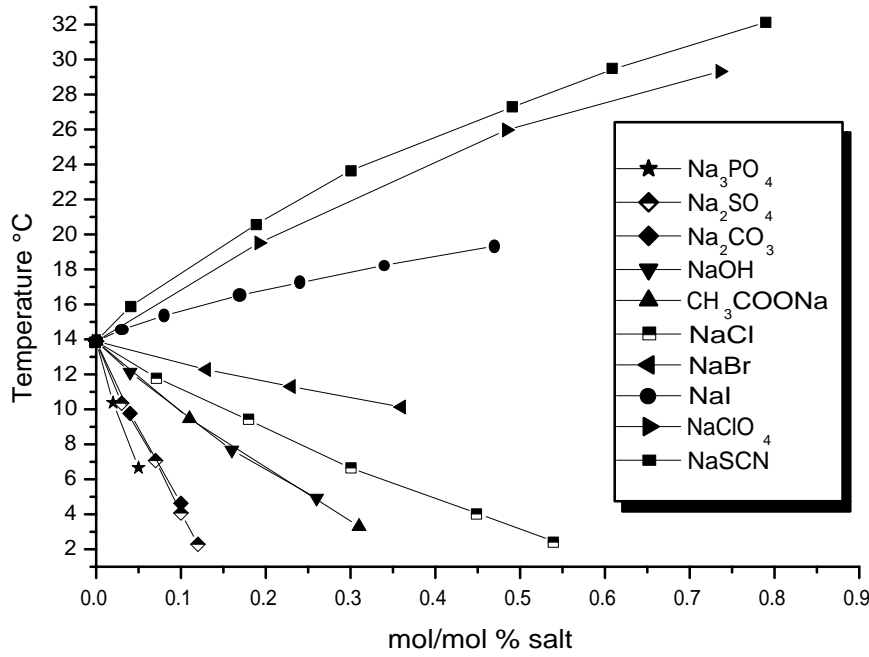


Figure 3.2: The shifts of the LCST of the C_3PO_2 /water mixture upon the addition of salts. Positive shifts indicate a salting-in effect of the ions whereas negative shifts can be interpreted as the manifestation of a salting-out effect. The sequence of the curves follows exactly the Hofmeister series for anions. The slope of the linear parts of all curves is described by Eqn. (3.1) and indicated in Table 3.1.

3.3 Results

The results for the C_3PO_2 -aqueous salt solution mixtures are shown in Fig. 3.2. As can be seen, the shift in the LCSTs are linear with salt concentration over a wide concentration range. Therefore the curves can be represented as:

$$LCST(c) = LCST(c = 0) + ac \quad (3.1)$$

for these concentrations. $LCST(c)$ is the minimum demixing temperature (in °C) of the mixture at a given salt concentration and $LCST(c = 0)$ is the corresponding temperature of the pure binary C_nPO_m -water mixture without salt. c is the number of mmol of salt per 1 mole of C_nPO_m -water mixture.

The a values obtained with the sodium salts are given in Table 3.1. Note that the LCST (i.e. the lowest cloud point) is found for a C_3PO_2 mass fraction of 0.55 and a C_3PO_1 mass fraction of 0.45, both corresponding to a molar ratio C_3PO_m /water of 1/8, c.f. Fig. 3.1. For all the 1:1 salts studied the different a values are all plotted

in Fig. 3.3 and summarized in Table 3.2.

	<i>a</i> coefficient(°C/mmoles of salt added in 1 mole of mixture)	
	C ₃ PO ₂ / water mixture (mass fraction = 0.55)	C ₃ PO ₁ / water mixture (mass fraction = 0.45)
Na ₃ PO ₄	-14.40	/
Na ₂ SO ₄	-9.62	-11.95
Na ₂ CO ₃	-9.32	/
NaOH	-3.55	/
NaAc	-3.49	/
NaCl	-2.07	-2.80
NaBr	-1.02	/
NaI	1.74	/
NaClO ₄	2.38	/
NaSCN	3.17	3.42

Table 3.1: *a* coefficients for different sodium salts according to Eqn. (3.1) in °C per mmoles of salt added to a mixture of C_nPO_m and water with a total liquid amount of 1 mole. The liquid mixtures have a molar ratio of 1/8 C_nPO_m/water. The accuracy of the *a* coefficient is better than 0.2 °C/mmoles.

According to Table 3.1 and to Fig. 3.3 the Hofmeister series for anions appears to be well followed whatever the nature of the cation. In contrast a very slight specificity is observed for cations, except for the very hydrophobic cations: NBU₄⁺ and Gu⁺ which show higher *a* values. Therefore no classification can be established for the cations. The *a* values range from highly negative numbers corresponding to a strong salting-out behaviour f.i. for sodium phosphate to pronounced salting-in effects for instance for sodium thiocyanate. Whatever the nature of the cation, except for NBU₄⁺ and Gu⁺, the borderline between a salting-in and a salting-out behaviour in the series is between bromide and iodide.

In the case of the C₃PO₁/water mixture the influence of only three salts were investigated, see Table 3.1. It turned out that the specific ion effects were slightly more pronounced than in the case of the C₃PO₂ mixtures.

Finally, Fig. 3.4 shows the influence of two different salts, both at a concentration of 0.041 moles per litre of water, on the CPs of different C₃PO₂/water compositions. The salt concentration was chosen so as to lie in the concentration range where Eqn. (3.1) is valid. As can be seen in Fig. 3.4 the salting-in and salting-out effects of the two salts appear at every composition investigated: for the ternary system containing the salting-in anion SCN⁻ all cloud points are shifted to higher temperatures. The shift is most pronounced near the LCST, whereas for higher and lower C₃PO₂ mass fractions the shift is smaller. By contrast, the addition of the salting-out salt Na₂SO₄ leads to monotonically decreasing cloud points with increasing C₃PO₂ mass fractions. For C₃PO₂ ratios up to the composition of the

a	Li^+	Na^+	K^+	Rb^+	Cs^+	NH_4^+	$\text{N}(\text{CH}_3)_4^+$	Gu^+	$\text{N}(\text{Bu})_4^+$
OH^-	-2.47	-3.55	-2.75		-2.91				
Ac^-	-3.25	-3.49	-3.80		-3.04	-3.04			0.42
Cl^-	-1.37	-2.07	-2.34	-1.49	-2.51	-1.46	-1.34	-0.357	
Br^-	-0.92	-1.02	-1.20	-1.13	-0.93	-0.50	-0.96		1.42
NO_3^-	0.09	-0.56	-0.38	-0.36	-0.26		-0.53	0.90	1.59
I^-		1.74							
ClO_4^-	2.87	2.38	4.13		4.45	3.80	4.42		2.00
SCN^-	2.80	3.17	3.13			2.89		2.56	1.85

Table 3.2: a coefficients for different 1:1 salts according to Eqn. (3.1) in $^\circ\text{C}$ per mmoles of salt added to a mixture of C_3PO_2 and water with a total liquid amount of 1 mole. The accuracy of the a coefficient is better than $0.2\text{ }^\circ\text{C}/\text{mmoles}$.

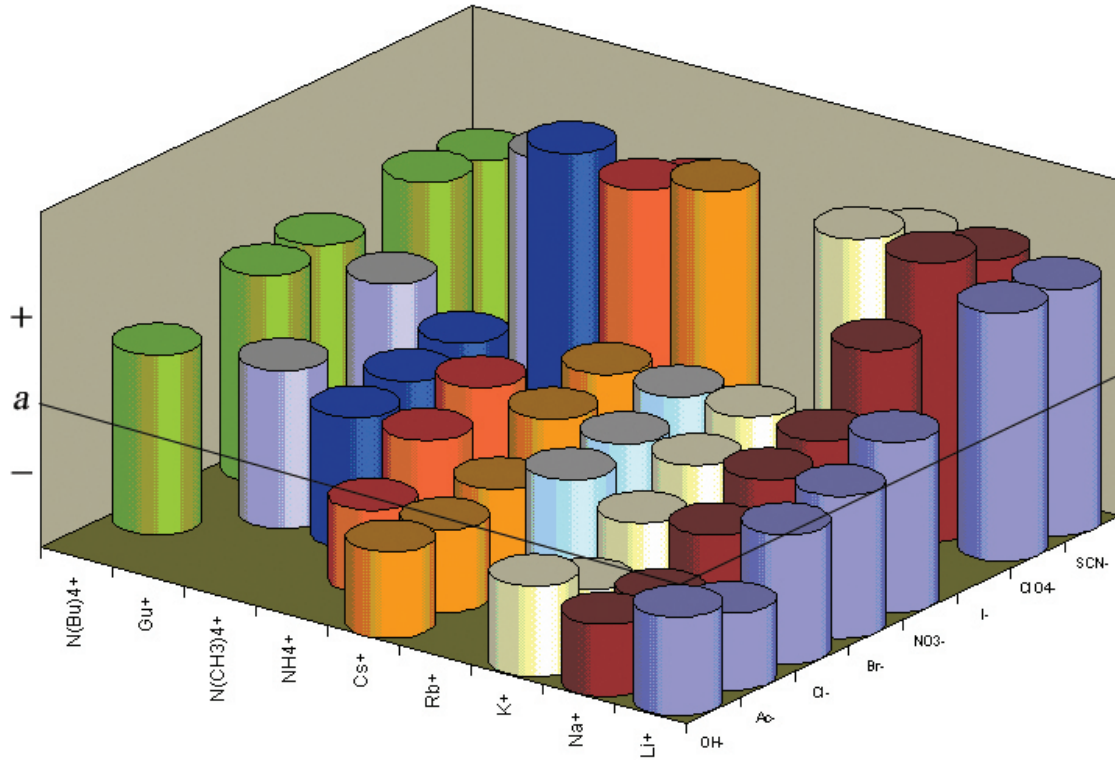


Figure 3.3: Representation of the a coefficients obtained with different 1:1 salts according to Eqn. (3.1) in $^\circ\text{C}$ per mmoles of salt added to a mixture of C_3PO_2 and water with a total liquid amount of 1 mole. The accuracy of the a coefficient is better than $0.2\text{ }^\circ\text{C}/\text{mmoles}$.

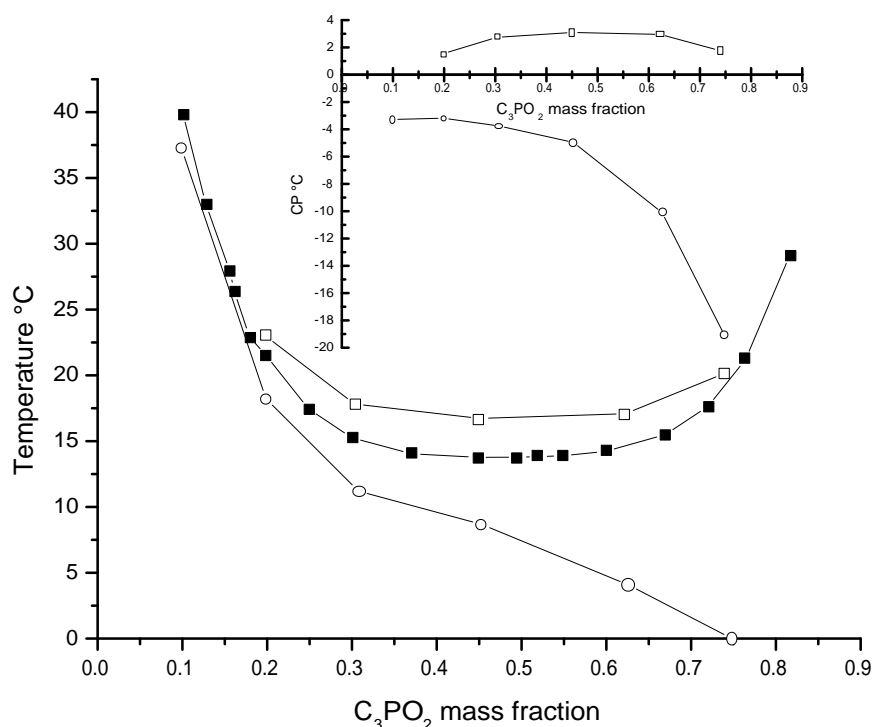


Figure 3.4: The phase diagrams of the pure binary C_3PO_2 /water mixture (■) is compared to the corresponding diagrams made from an aqueous solution containing an electrolyte at a fixed concentration of 0.041 M: Na_2SO_4 (○), which is a typical salting-out salt, and of $NaSCN$ (□), which is salting-in. The insert in the Figure shows the differences between the curves, ΔCP , i.e. the difference in the cloud points of the system with and without salt, in absolute values.

LCST, the shift is similar to the corresponding shift of the CPs in the presence of $NaSCN$, only in the opposite direction. However, for higher C_3PO_2 mass fractions, the CP shifts to smaller temperatures are much more pronounced compared to the corresponding CP shifts to higher temperatures in the presence of the thiocyanate salts.

3.4 Discussion

As remarked in the introduction numerous attempts have been undertaken to explain salting-in and salting-out effects and Hofmeister series. Do the ions “simply” change the water structure and hence the Gibbs energy of water or do they interact

directly with the organic phase close to the interface? Hofmeister himself in the conclusion of one of his later papers remained bemused on this issue. Our answer is: certainly both effects are involved. It is beyond the scope of this work to present a quantitative modelling. So we shall make only some qualitative comments. Salting-in ions are hydrophilic and at least slightly lipophilic. Note that this statement is not a contradiction. For example some quaternary ammonium salts are highly soluble both in water and in chloroform. Due to their slight hydrophobicity, the salting-in ions used in our study here, have a certain affinity or even solubility in the organic phase. This “surface solubility” will bring electrical charges into the organic phase thus rendering it more polar. As a result the organic phase becomes more water soluble and consequently the LCSTs go up: only at higher temperatures are the now stronger water- C_nPO_m interactions broken. C_3PO_1 is less hydrophobic than C_3PO_2 . Consequently, more ions can dissolve in C_3PO_1 and therefore the salting-in effect is higher, c.f. Table 3.1.

Salting-out ions are hydrophilic and not lipophilic. They are not necessarily more hydrophilic than salting-in ions: the solubility of their sodium salts and the Gibbs energy of solution in water can be similar for both types of ions. So the bulk properties alone cannot explain why ions or salts may be salting-out, although the ions studied in our case, such as sulphate and phosphate are highly charged and very hydrophilic.

At salt concentrations in the millimolar range, the bulk water properties will not be completely disturbed. However, in the C_3PO_2 /water mixtures, for which the LCST was found, there is probably no bulk water and the change in Gibbs surface energy is most relevant. For an interesting discussion of surface energy changes due to the presence of ions, see the works of L. Dang [22] and also E. Leontidis [23]. On average, eight water molecules surround one C_nPO_m molecule. Up to about 14°C the C_3PO_2 -water dipole interaction are strong enough to ensure miscibility. The addition of a small amount of “water withdrawing” salt is sufficient to disturb the C_3PO_2 hydration sphere and to induce a phase separation. The more ions are present the more will the effect be pronounced. Consequently, the linear dependence represented by Eqn. (3.1) and visualized in Fig. 3.2 seems reasonable. Na_2SO_4 salts C_3PO_1 more out than the less hydrophilic C_3PO_2 , c.f. Table 3.1. However, from the influence of a single salt it is difficult to draw a general conclusion.

Note that in a recent article Bowron and Finney argued very differently [24]. They suggest that the chloride ions are also salting-out, because they are partially dissolved in a hydrophobic alcohol. The chloride ions are supposed there to bridge the alcohol molecules and thus enhance the aggregation of the organic molecules which in turn leads to a reduced solubility of the alcohol in water. That salting-out ions favour the aggregation of hydrophobic alcohol molecules in water and that this effect follows the Hofmeister series, was also observed by NMR experiments [25]. Accordingly, salting-in ions were found to reduce the alcohol association tendency. However, we doubt that a bridging mechanism can generally explain the salting-out behaviour of various ions, because the anions partitioned between the organic molecules will also bring their electrical charges with them and so enhance the

polarity of the organic aggregates, which in turn would increase their water solubility.

Since salting-out is a surface effect and since the size of the hydrated C_3PO_2 aggregates and the number of aggregated C_3PO_2 molecules may vary, it is difficult to estimate or to predict the salt concentration that is necessary to induce a certain temperature shift of the LCST. In any case, it is remarkable that very small salt concentrations have such pronounced consequences for the LCSTs. According to Table 3.1, 1 mmole of Na_2SO_4 decreases the LCST of 1 mole of a C_3PO_2 /water mixture by more than 9 °C. In this mixture the number of moles of water is about 0.88. This means that there are 880 water molecules to one sulphate molecule. Such an enormous effect with so few sulphate ions leads us to the assumption of a strong cooperativity in the water structure that is globally changed by the ions, which act as defects in a solid, in much the same way that the austenite-martensite transition occurs in steel ³[26]. However, as long as there is no experimental confirmation, this conclusion must remain speculative.

For a detailed explanation computer simulations can probably not help. Even with many-body potentials it may be impossible to model the full water cooperativity as a function of solute. It seems to be more like a dynamic quasi crystal with every molecule in a predetermined place.

For the moment it is certain only that for salting-out phenomena the competition between ion-water and organic molecule-water interactions is decisive, whereas for salting-in effects the competition between ion-water and ion-organic molecule interactions will dominate. But what are the ion specific properties? Of course the size and the charge of the ions are important. The size of the ions is responsible for a dielectric cavity that strongly influences the structuring of the water molecules. According to the latest literature the polarizability of the ions leading to induced dipoles in the water and in neighbouring ions are also important. In all cases, it seems always the influence of the ions on the water, or in general, solvent structure at the interface that is important, much more than direct ion-interface interactions [11].

Now, how can we explain the changes in the whole phase diagram, once a certain concentration of salt is added to the binary system, c.f. Fig. 3.3? Let us first consider the phase diagram when the salting-in salt NaSCN is present: At the "wings" of the diagrams, i.e. for high and low C_3PO_2 mass fractions, the salting-in effect is small. At a great surplus of water molecules, the C_3PO_2 molecules are well hydrated and most of the water has certainly bulk behaviour. Most of the salt will be dissolved in the water bulk and consequently the salting-in effect of SCN^- is small. At high C_3PO_2 mass fraction the solution is more or less an organic system with an aqueous salt solution dissolved in it. The ions are partitioned between the water and the oil (pseudo-) phases. In this case a salting-in ion cannot have a pronounced effect either. Consequently, the highest salting-in effect can be expected close to the composition of the LCST, and that is indeed what is found experimentally.

In the case of salting-out ions the situation is different. At small C_3PO_2 mass

³Barry Ninham, private communication

fraction, there is still sufficient bulk water to dissolve the ions and hence the C_3PO_2 molecules do not experience a pronounced “water withdrawing” effect of the ions, although the overall polarity of the aqueous solutions is enhanced. With increasing C_3PO_2 mass fraction the bulk character of the aqueous solutions decreases more and more, and at high C_3PO_2 mass fractions the aqueous part of the mixture is more or less molecularly dissolved in the organic medium. When this is the case, the whole aqueous pseudo-phase is in close contact to the organic surrounding. Again, a high cooperativity of the water structure at the interface can be assumed, because there are 1300 times more water molecules than sulphate molecules. If only water molecules in the first two or three hydration shells of the ions were affected, there would still be most of the water molecules available to interact with the large excess of the C_3PO_2 molecules.

3.5 Conclusion

The addition of salts to binary C_3PO_m /water mixtures leads to the expected anion Hofmeister series in the shift of the LCST. As in the case of protein precipitation the cation specificity was found to be very slight [3]. Both salting-in and salting-out effects are observed much as in the case of mixtures of classical non-ionic surfactants with water. The specific ion effects are more pronounced for the more hydrophilic C_3PO_1 molecule. Whereas these shifts show certain symmetry of both effects, the binary phase diagrams of water/ C_3PO_2 mixtures in the presence of salting-in and salting-out ions are significantly different at high C_nPO_m concentrations, beyond the composition of the LCST. Qualitatively, the results can be interpreted by assuming:

- that salting-in ions are partially soluble in the organic phase,
- that salting-out ions modify significantly the water structure near the interface
- that there must be a huge cooperativity in the water structure near the interface.

Bibliography

- [1] J. Barthel, H.J. Gores, G. Schmeer, and R. Watcher. Non-aqueous electrolyte solutions in chemistry and modern technology. *Topics in Current Chemistry*, 111, 1983.
- [2] E. Leontidis. Hofmeister anion effects on surfactant self-assembly and the formation of mesoporous solids. *Current Opinion in Colloids and Interface Science*, 7:81–91, 2002.
- [3] F. Hofmeister. Zur lehre von der wirkung der salze. *Arch. Exp. Pathol. Pharmacol.*, 24:247, 1888.
- [4] G. Zoldak, M. Sprinzl, and E. Sedlak. Modulation of activity of nadh oxidase from thermus thermophilus through change in flexibility in the enzyme active site induced by hofmeister series anions. *European Journal of Biochemistry*, 271(1):48–57, 2004.
- [5] N. Papaiconomou, J. P. Simonin, O. Bernard, and W. Kunz. Description of vapor-liquid equilibria for co₂ in electrolyte solutions using the mean spherical approximation. *Journal of Physical Chemistry*, 107(24):5948–5957, 2003.
- [6] A. Kabalnov, U. Olsson, and H. Wennerstroem. Salt effects on nonionic microemulsions are driven by adsorption/depletion at the surfactant monolayer. *Journal of Physical Chemistry*, 99(16):6220–30, 1995.
- [7] W. Kunz, J. Henle, and B. Ninham. *Current Opinion in Colloids and Interface Science*, 2004.
- [8] Mathias Bostroem, David R. M. Williams, and Barry W. Ninham. Ion specificity of micelles explained by ionic dispersion forces. *Langmuir*, 18(16):8609, 2002.
- [9] Mathias Bostroem, David R. M. Williams, and Barry W. Ninham. Surface tension of electrolytes: Specific ion effects explained by dispersion forces. *Langmuir*, 17:4475–4478, 2001.
- [10] Barry W. Ninham and Vassili Yaminsky. Ion binding and ion specificity: The hofmeister effect and onsager and lifshitz theories. *Langmuir*, 13:2097–2108, 1997.

- [11] P. Jungwirth and D.J. Tobias. Ions at the air/water interface. *Journal of Physical Chemistry*, 106(25):6361–73, 2002.
- [12] W. Kunz, L. Belloni, O. Bernard, and B.W. Ninham. Osmotic coefficients and surface tensions of aqueous electrolyte solutions: Role of dispersion forces. *Journal of Physical Chemistry*, 108(7):2398–404, 2004.
- [13] Christine Holtzscherer and Francoise. Candau. Salt effect on solutions of non-ionic surfactants and its influence on the stability of polymerized microemulsions. *Journal of Colloid and Interface Science*, 125:97–110, 1988.
- [14] Hans Schott and Alan E. Royce. Effect of inorganic additives on solutions of nonionic surfactants. v: Emulsion stability. *Journal of Pharmaceutical Sciences*, 72:1427–36, 1983.
- [15] Hans. Schott. Comparing the surface chemical properties and the effect of salts on the cloud point of a conventional nonionic surfactant, octoxynol 9 (triton x-100), and of its oligomer, tyloxapol (triton wr-1339). *Journal of Colloid and Interface Science*, 205:496–502, 1998.
- [16] Gunnar Karlstroem, Anders Carlsson, and Bjoern. Lindman. Phase diagrams of nonionic polymer-water systems: experimental and theoretical studies of the effects of surfactants and other cosolutes. *Journal of Physical Chemistry*, 94:5005–15, 1990.
- [17] Nivedita Pandit, Troy Trygstad, Scott Croy, Maria Bohorquez, and Cody Koch. Effect of salts on the micellization, clouding, and solubilization behavior of pluronic f127 solutions. *Journal of Colloid and Interface Science*, 222:213–220, 2000.
- [18] W. F. McDevit and F. A. Long. The activity coefficient of benzene in aqueous salt solutions. *Journal of the American Chemical Society*, 74:1773–7, 1952.
- [19] A. Sokolowski. Chemical structure and thermodynamics of amphiphile solutions. 2. effective length of alkyl chain in oligooxyalkylenated alcohols. *Colloids and Surfaces*, 56:239–49, 1991.
- [20] P. Bauduin, L. Wattebled, S. Schrödle, D. Touraud, and W. Kunz. Temperature dependence of industrial propylene glycol alkyl ether / water mixtures. *Journal of Molecular Liquids*, 115:23–8, 2004.
- [21] S. Schroedle, R. Buchner, and W. Kunz. Automated apparatus for the rapid determination of liquid-liquid and solid-liquid phase transitions. *Fluid Phase Equilibria*, 216(1):175–82, 2004.
- [22] L.X. Dang. Computational study of ion binding to the liquid interface of water. *Journal of Physical Chemistry*, 160(40):10388–94, 2002.

- [23] E. Leontidis. Specific ion effects in the formation of inorganic colloids: insights from model systems. In *Proceedings of the ECIS meeting in Florence*, 2003.
- [24] D. T. Bowron and J. L. Finney. Structure of a salt-amphiphile-water solution and the mechanism of salting out. *Journal of Chemical Physics*, 118(18):8357–72, 2003.
- [25] Antonio Sacco, Francesca Maria De Cillis, and Manfred. Holz. Nmr studies on hydrophobic interactions in solution part 3 salt effects on the self-association of ethanol in water at two different temperatures. *Journal of the Chemical Society, Faraday Transactions*, 94:2089–2092, 1998.
- [26] M. Monduzzi, S. Murgia, and B.W. Ninham. Current opinion in colloids interface science (to be published).

4 Unified concept of solubilization in water by hydrotropes and co-solvents

In the present work a hydrophobic dye, *i.e.* disperse red 13 (DR-13): (2-[4-(2-chloro-4-nitro-phenylazo)-N-ethylphenylamino]ethanol, is solubilized in water with the help of different additives: acetone and 1-propanol as typical co-solvents; sodium xylene sulfonate (SXS) as a representative of a classical hydrotrope; sodium dodecyl sulfate (SDS) as a typical surfactant and finally some short amphiphiles: propylene glycol mono-alkylether derivatives (C_nPO_m) ($n = 1$; $m = 1$ and 3), ($n = 3$; $m = 1$ and 2), ($n = 4$ and tertio-butyl; $m = 1$) and 1-propoxy-2-ethanol (C_3EO_1). These solvo-surfactants are short amphiphiles that do not form well defined structures in water such as micelles. For all additives a sudden increase in the DR-13 solubilization was observed when their concentrations in water were increased. Except for the SDS solution, no difference in the overall shapes of the DR-13 solubilization curves (solubility against additive concentration) was observed. All the studied molecules were classified according to their hydrotropic efficiencies *i.e.* their abilities to solubilize a hydrophobic, sparingly soluble compound in water. The lower the concentration of the additive, at which the sudden increase in the dye solubilization occurs, the better is the hydrotropic efficiency. The volume of the hydrophobic parts of the studied additives, roughly evaluated by simple calculations, was found to influence strongly the hydrotropic efficiency, *i.e.* the larger the hydrophobic part of the additive, the better the hydrotropic efficiency. Taking the hydrophobic part of the molecules as the key parameter, the water solubilization efficiency of co-solvents, hydrotropes and solvo-surfactants can be described in a coherent way.

4.1 Introduction

At the beginning of the last century, the term hydrotropy was defined as the large increase in the water solubility of a variety of hydrophobic compounds brought about by the addition of certain water soluble organic compounds, named hydrotropes [1]. Hydrotropes comprise hydrophilic and hydrophobic moieties, with the hydrophobic moiety being typically too small to induce micelle formation [2]. Hydrotropes are usually anionic compounds and are composed of an aromatic ring substituted by a sulfate, sulfonate or carboxylate group, typical examples of hydrotropes being sodium xylene sulfonate (SXS) or sodium benzoate. This definition was later ex-

tended to cationic and neutral aromatic compounds [3]. Hydrotrope molecules are assumed to aggregate by a stacking mechanism of the planar aromatic ring present in their chemical structures. This type of aggregation is believed to be at the origin of the solubilization process of sparingly soluble hydrophobic compounds in water, in analogy to a micellization process. Nevertheless some aliphatic compounds such as short sodium alkanoates [4, 5] or alkyl sulfates [6] show also a hydrotropic behavior as it was observed for aromatic derivatives. For such aliphatic compounds the assumed stacking mechanism does not make sense.

It was observed that the hydrotrope concentration, at which the sudden solubility increase of a hydrophobic compound occurs, sometimes called minimum hydrotropic concentration (MHC), coincides with a change of the slope of the surface tension as a function of hydrotrope *concentration* [7]. And as pointed out by Da Silva et al. [8], cooperative aggregation such as micellization is accompanied by such a phenomenon. However, in hydrotrope-water mixtures such a micellization process does not occur. Further, typical critical micelle concentrations (CMC) are of the order of 10^{-2} - 10^{-3} M, and so far below the MHC of usual hydrotropes (≈ 1 M). Independently it was shown that for short amphiphiles, which present a high apparent high apparent CMC according to the plot of surface tension against molar concentration, the chemical activity has to be used instead of molar concentration [9]. If this is done, the break in the surface tension curve, which is supposed to indicate the sudden onset of aggregation, can completely disappear [9]. Usually this point is not considered in the studies concerning hydrotrope aggregation [7] but this must be taken into account to infer correct MHC values. Note that the MHC is not necessarily linked to a change in the slope of the surface tension. As Horvath-Szabo et al. [10] showed recently, in the plot of surface tension as a function of the logarithm of hydrotrope *activity* no break occurred at the activity at which the sudden increase in solubilization was found. In their study a pronounced association between lecithin, which was to be solubilized, and SXS, as the hydrotrope, was proposed to explain the sudden increase of lecithin solubility in water. No cooperative aggregation of the SXS molecules was considered.

It was also observed that the sudden increase in solubilization induced by hydrotropes after a certain threshold concentration (MHC) is sometimes followed by a level-off of the solubilities at higher hydrotrope concentrations [7, 11, 12, 13]. In such cases the solubilization curve as a function of hydrotrope concentration, plotted in a linear scale, has a sigmoidal shape. Balasubramanian et al. [7] attributed this sigmoidal curve to a cooperative process such as micellization. Aggregation would probably be the better word. Moreover, the fact that the MHC is rather insensitive to the nature of the hydrophobic compounds to be dissolved [7] supports the hypothesis of hydrotrope cooperative self-aggregation. Thus the mechanism of self-association of hydrotrope molecules is still under debate with both non-cooperative step-wise self-aggregation, *i.e.* in a pair-wise manner by formation of dimers, trimers and so on [14, 15, 16, 17], and cooperative self aggregation [7, 8] being suggested.

Balasubramanian et al. [7] differentiated clearly hydrotropy, showing typical sigmoidal solubilization profiles, from solubilization observed by co-solvency and by

salting-in effects showing a monotonic increase in the solubilizing ability with increasing co-solvent concentration. More generally, the solubilization of a hydrophobic compound in water by a co-solvent is known to increase slightly and monotonously at low and moderate co-solvent concentrations and to increase exponentially at very high concentrations [18].

In the present work we try a general classification of co-solvents and hydrotropes and related compounds (the solvo-surfactants). To this purpose we study spectrophotometrically the solubilization of a hydrophobic dye, *i.e.* disperse red 13 (DR-13), in water with the help of a typical hydrotrope, the SXS, by classical water co-solvents (acetone and 1-propanol) and using some short amphiphiles derived from propylene glycol (and ethylene glycol) mono-alkyl ether C_nPO_m (C_nEO_m) with $n < 5$. These short amphiphiles do not form well defined structures in water such as micelles and are usually considered as water co-solvents. Since they have also some features in common with surfactants, they are sometimes called “solvo-surfactants”. The solubilization of the DR-13 by a classical anionic surfactant, the sodium dodecyl sulfate (SDS) was also studied in order to assure that the DR-13 behaves like a classical solubilize in presence of surfactant *i.e.* the solubilization appears when micelles are formed at concentrations above the surfactant CMC. From these results all the studied compounds, whatever hydrotropes or co-solvents, were classified according to their “hydrotropic” efficiencies, which can be defined as their abilities to solubilize hydrophobic compounds at more or less low additive concentrations. Moreover, the volume of the hydrophobic parts of the studied solubilizing molecules, supposed to be the main factor influencing the hydrotropic efficiency, was roughly evaluated by simple calculations. According to these considerations the term of co-solvency and hydrotropy were discussed in a consistent way considering the usually admitted hydrotropy [2, 7, 17] and cosolvency [7, 18] definitions that were mentioned above.

4.2 Experimental

4.2.1 Materials

Sodium dodecyl sulfate (SDS, 99%), 1-propanol (99%), acetone (p.a.) were supplied by Merck and sodium xylene sulfonate (SXS, 40 wt% in water), 1-propoxy-2-ethanol (C_3EO_1 , 99.4%), disperse red 13 (2-[4-(2-chloro-4-nitrophenylazo)-N-ethylphenylamino]ethanol, DR-13, 95%) by Aldrich.

Except for the 1-tertobutoxy-2-propanol ($t-C_4PO_1$, >99%) which was supplied by Lyondell all the propylene glycol mono-alkylether derivatives were supplied by Dow Chemical with the following purity grades: 1-methoxy-2-propanol (C_1PO_1 , >99.5%), tripropyleneglycol mono-methylether (C_1PO_3 , >97.5%), 1-propoxy-2-propanol (C_3PO_1 , 99%), dipropyleneglycol mono-propylether (C_3PO_2 , >98.5%) and 1-butoxy-2-propanol (C_4PO_1 , >99%).

4.2.2 Solubilization experiments

All experiments concerning the solubilization process and the optical density measurements were done in a thermostated room at 25 ± 0.2 °C. All solutions to be measured, *i.e.* containing water and the studied compounds at an appropriate concentration, were saturated with a sufficient amount of DR-13 and left equilibrated 24 h. The solutions were then filtrated in order to separate the non-solubilized excess of DR-13 from the solutions. The optical density (O.D.) of the filtrated solutions were measured in 1 cm pathlength quartz cells with a UV-Visible Spectrophotometer Cary-3E at a wave length of 525 nm corresponding to the wave length λ_{\max} where DR-13 has its absorption maximum. Before each measure a zero absorbance was done with the corresponding solution without dye. For the studied hydrotropes and co-solvents λ_{\max} of the DR-13 was found to be not so sensitive to the chemical nature of these compounds (± 10 nm). When the measured O.D. was above a critical value, suitable dilutions were done by using the same solution but without dye. The resulting O.D.s reflect then, through the Beer-Lambert law, the concentration of the hydrophobic dye (DR-13) solubilized in the corresponding aqueous hydrotrope solutions or water co-solvent mixtures.

4.3 Modelling

For SXS, acetone, 1-propanol, C_3EO_1 and C_3PO_1 isoelectrondensity molecular surfaces were computed and color coded from electrostatic potentials. They were created with the software Molden based on ab initio-calculations with Gaussian 03 (RHF/6-311++G** or B3LYP/6-311++G**) using its cubegen utility. Red represents the most negative values, *i.e.* high electrondensity, increasing over green to blue which indicates the most positive values *i.e.* lower electrondensity.

4.4 Results and Discussion

4.4.1 Solubilization curves: comparison between hydrotrope, co-solvent and surfactant

The measured O.D.s as a function of molar concentration of surfactant, hydrotrope, co-solvent or solvo-surfactant in water are plotted in Fig. 1 for SDS, SXS, 1-propanol, C_3PO_1 , C_3EO_1 and acetone. In Fig. 1a the O.D. is plotted in a logarithmic scale in order to compare all solubilization curves over a large range of concentrations. In the case of 1-propanol, C_3PO_1 and C_3EO_1 the O.D. could be measured over the whole range of concentrations from pure water to pure solvents. The O.D. was measured in more restricted ranges of concentrations: for SXS (solid at room temperature) solutions, the O.D. was determined up to 2.248 mol/L (40 wt%) and for acetone up to 10.91 mol/L (80 wt%). In the case of acetone the DR-13 solubility becomes so high for acetone concentrations above 10.91 mol/L that

quantitative results could not be obtained for these compositions. This is a consequence of the extremely high solubility of the dye in acetone. In the case of the SDS the O.D. was measured until 1 mol/L (around 25 wt%) because a hexagonal phase appeared at higher concentrations (around 27 wt%).

The solubilities of the DR-13 in C_3EO_1 , C_3PO_1 and 1-propanol are, in the order of decreasing solvent power: 2519, 2106 and 815 (in O.D. unit), respectively. The DR-13 solubilization by SXS seems to be less efficient, in terms of the maximum solubilization, than in the case of the other studied additives: the O.D. at 2.248 mol/L (40 wt%) is only 347.4. The same is true for the dye solubilization by the anionic surfactant SDS: the maximum solubilization corresponds to an O.D. value of 331 at 1 mol/L (around 25 wt% SDS). The solubilization of a hydrophobic compound in water using a co-solvent is well known to be the most efficient solubilization method among the four common ones: micellar solubilization, complexation, hydrotrophy and co-solvency [18], and this is confirmed here. This point will not be further discussed here.

In order to compare to the SDS solubilization profile a double logarithmic scale was used, see Fig. 2. The DR-13 solubilization curve obtained with SDS exhibits the classical evolution observed in the case of micellar solubilization *i.e.* the DR-13 solubilization increases suddenly when micelles are formed for concentrations above the SDS CMC ($8.10^{-3}M$). Then, when SDS concentration further increases, the DR-13 solubilization increases linearly [19, 18]. Thus the DR-13 behaves like a classical hydrophobic compound in presence of a surfactant. The SXS and C_3EO_1 solubilization curves were added in Fig. 2. As expected the dye solubilization starts at much lower SDS concentrations compared to the hydrotrope and solvo-surfactant. The following discussions will be focused on the comparison between co-solvents, the hydrotrope and the solvo-surfactants.

For all these additives a sudden increase in the O.D., *i.e.* in the DR-13 solubilization, is observed when the additive concentration exceeds a certain threshold. The typical sigmoidal shape sometimes observed in the case of hydrotrope solubilization could not be detected here, even not in the case of the SXS, see Fig. 1b, in which the O.D. is plotted in a linear scale instead of a logarithmic one. On this linear scale an exponential increase in solubility with increasing concentration is observed for all compounds. This result is typical of co-solvent solubilization [18]. Moreover according to Balasubramanian et al. [7] the solubilization obtained in the case of co-solvents “shows a continuous and monotonic increase”. It is important to remark that Balasubramanian et al. [7] only considered one co-solvent to draw up their conclusions and that this co-solvent was polyethyleneglycol 400 (PEG-400) which is not representative of a water co-solvent.

Anyway, from our studies it can be inferred that the shape of the solubilization curves obtained in the cases of co-solvents, the hydrotrope and of solvo-surfactants, are similar. We conclude therefore that there is no need to distinguish between these different types, and in the following paragraphs we will use “co-surfactant” “solvo-surfactant” and “hydrotropes” as synonyms.

In all cases the additive concentration, at which there is a sudden onset of solubil-

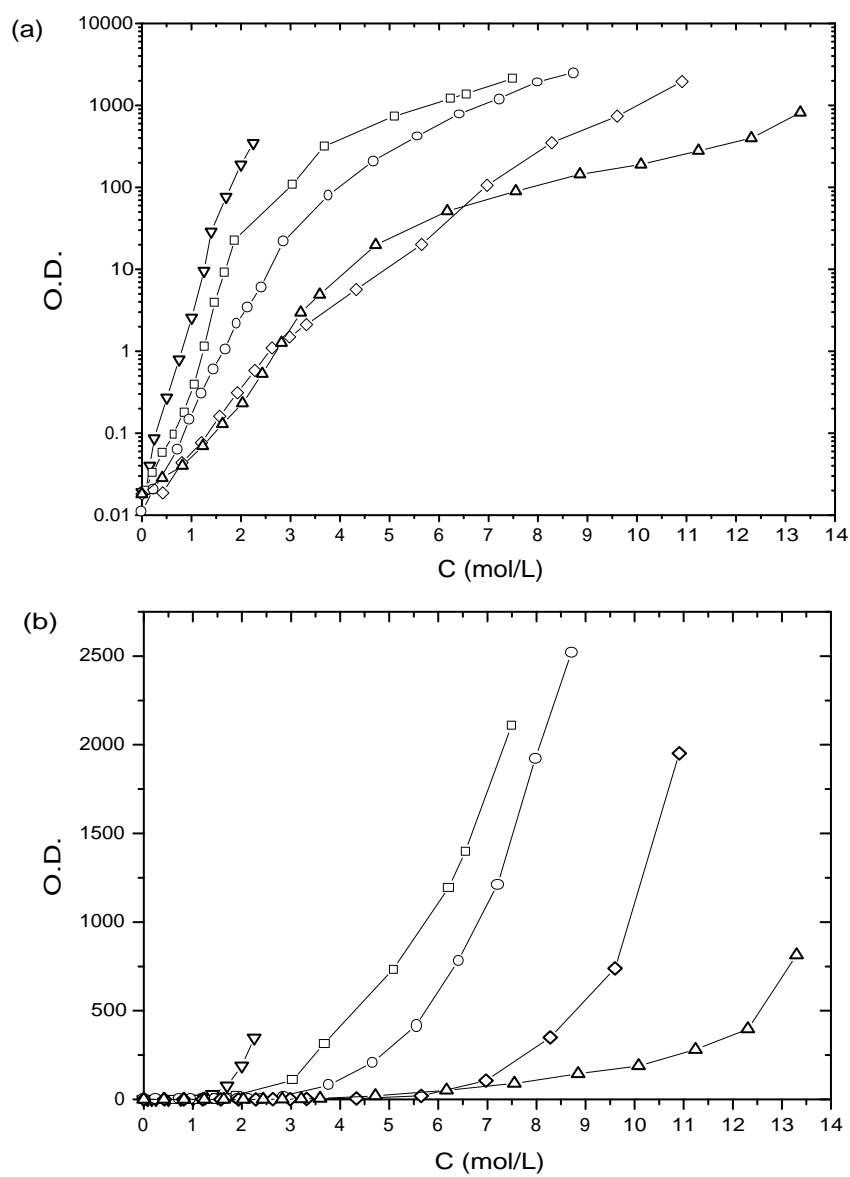


Figure 4.1: The optical density (O.D.), proportional to the amount of dissolved dye, versus the molar concentrations of hydrotropes (or co-solvents) in water: SXS (∇), 1-propanol (Δ), C_3PO_1 (\square), C_3EO_1 (\circ) and acetone (\diamond).

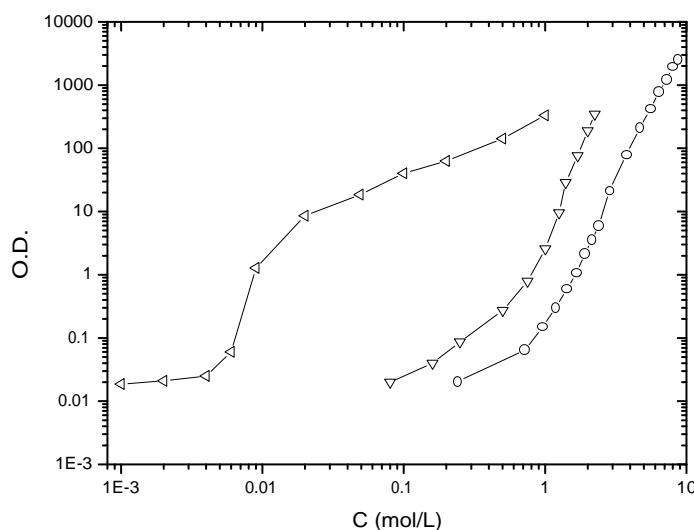


Figure 4.2: The optical density (O.D.), proportional to the amount of dissolved dye, versus the molar concentrations of SDS (\triangleleft) in water. This curve is compared to the ones obtained with SXS (∇) and C_3EO_1 (\bigcirc).

ity of hydrophobic compounds can be called MHC, as for typical hydrotropes. These MHC values characterize the hydrotropic efficiencies of the studied compounds (hydrotrope or solvent), *i.e.* the lower the MHC the more efficient the additive.

4.4.2 Aqueous solubilization in the water rich part: the hydrotropic behavior

So the only difference between the solubility curves obtained for the hydrotrope and the co- and solvo-surfactants remains in the concentrations, at which the sudden increase in solubility occurs. In Fig. 3a the solubilization curves of SXS, 1-propanol, C_3PO_1 , C_3EO_1 , acetone are zoomed in the low concentration range to allow for the MHC evaluation of these compounds. MHC values, by increasing values, *i.e.* by decreasing hydrotropic efficiency, are found to be about: 0.8, 1.2, 1.45, 1.8 and 2.1 mol/L, respectively for SXS, C_3PO_1 , C_3EO_1 , acetone and 1-propanol. First, it can be remarked that (1) the solubilization curves for concentrations below 3M obtained in the case of 1-propanol and acetone are very similar and that (2) it seems that the larger the molecules, the better their hydrotropic efficiency.

The only marked exception is SXS. The MHC obtained in the case of this aromatic hydrotrope SXS is lower than the MHC values the other linear non-ionic compounds. Very probably the aromatic rings in both the dye and the SXS molecules attract each other so that the dye is “salted-in” by this specific interaction. One might think that SXS molecules can self-aggregate due to the stacking of the aromatic

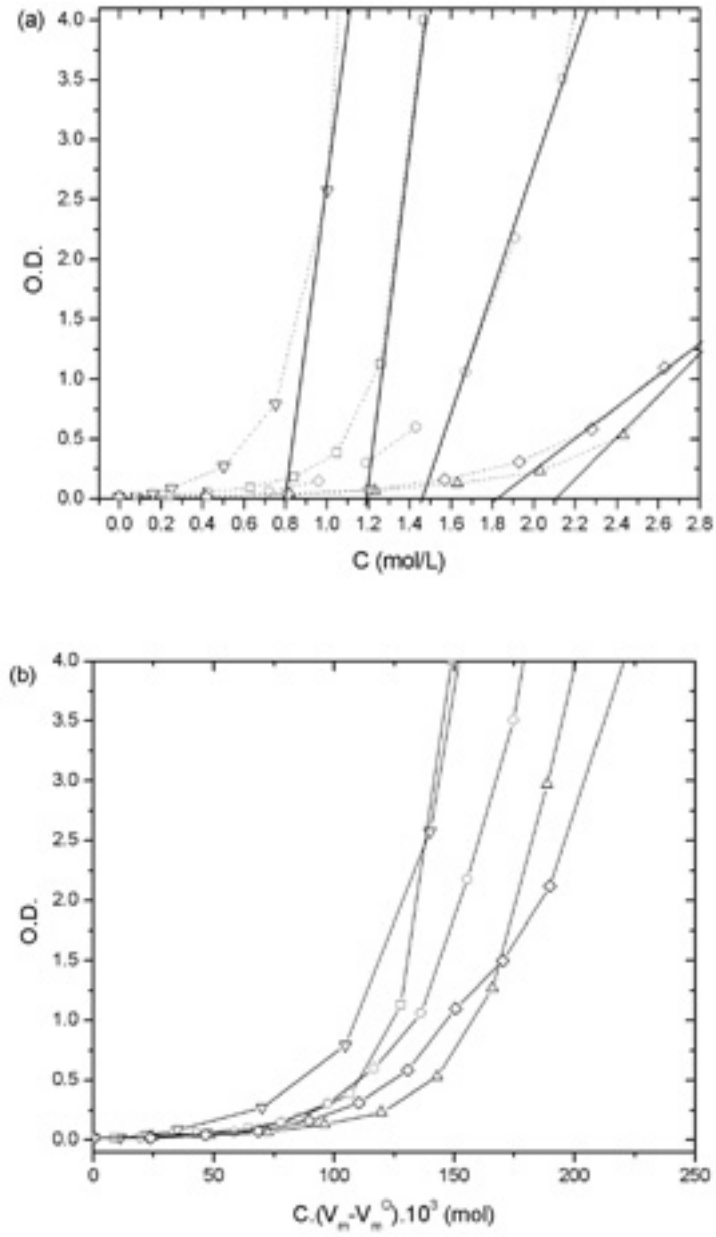


Figure 4.3: The optical density (O.D.) as a function of (a) molar concentrations of hydrotropes (or co-solvents) in water, (b) molar concentrations of hydrotropes (or co-solvents) in water multiplied by the evaluated molar volume of the hydrophobic part of the respective hydrotrope (or co-solvent) molecules; SXS (∇), 1-propanol (Δ), C_3PO_1 (\square), C_3EO_1 and acetone (\diamond).

rings. However, it was proven that such a formation of large SXS aggregates is not responsible for the sudden increase in hydrophobic compounds solubility [10].

4.4.3 The ordering of the hydrotropes

In Chapter 5 some non-ionic short amphiphiles, such as C_3PO_1 , C_3EO_1 and 1-propanol, have been studied in terms of their ability to lower the CMC of an ionic surfactant, *i.e.* to strengthen the hydrophobic interactions of surfactant molecules in solution (“co-surfactant” behaviour). The propylene glycol group appeared to be more efficient in lowering the surfactant CMC than the ethylene glycol group, which is less hydrophobic. Considering the polypropylene or polyethylene glycol alkyl ethers as the condensation of an n-alcohol and a certain number of propylene or ethylene glycol groups (PO or EO), the corresponding n-alcohol decreases less the surfactant CMC than the propoxylated or ethoxylated derivatives. Thus the hydrophobic behaviour of the studied amphiphiles was found to be in the following order: $C_3PO_1 > C_3EO_1 > 1\text{-propanol}$. Similar conclusions were drawn from the study of the adsorption of polypropylene and polyethylene glycol alkyl ethers at the water/air surface [20, 21]. The ordering of these additives according to their hydrotropic efficiency (or MHC), as inferred from the present study, is exactly the same ($C_3PO_1 > C_3EO_1 > 1\text{-propanol}$) as the ordering inferred from their interfacial behaviours [20, 21], see also Chapter 5.

Note that the dielectric constant of the hydrotrope is sometimes used as a parameter to estimate its hydrophobicity. Although this strategy can be dangerous, because the dielectric constant is a macroscopic parameter and its dependence on microscopic interactions is not straightforward, it was successfully used to classify the hydrotropic efficiencies of several co-solvents in the case of the solubilization of indomethacin [22]: ethanol > propyleneglycol (PG) > glycerol. This order is in agreement with our postulation, namely that the hydrotropic efficiency correlates with the hydrotropic hydrophobicity. To have a broader data basis, we also determined the DR-13 solubilization by some other polypropyleneglycol mono-alkylether derivatives in mixture with water. The solubilization curves, as a function of “hydrotrope” molality, obtained for C_3PO_2 , $t\text{-}C_4PO_1$, C_1PO_3 and C_1PO_1 are shown in Fig. 4a and compared to the ones already discussed for C_3PO_1 , C_3EO_1 and 1-propanol. The solubilization or hydrotropic efficiency appears to be in the following order: $C_3PO_2 > t\text{-}C_4PO_1 > C_3PO_1 \cong C_1PO_3 > C_3EO_1 > 1\text{-propanol} > C_1PO_1$. For the C_3 derivatives, including 1-propanol, the order is again in agreement with the one obtained from recent results which classified the studied molecules according to their hydrophobic behaviors [20, 21], see also Chapter 5. The DR-13 solubilization by C_4PO_1 , $t\text{-}C_4PO_1$ and C_3PO_2 water mixtures were measured up to the limits of solubility at 25°C which are respectively 5.3 wt% (0.42mol/Kg), 16.6 wt% (1.51mol/Kg), and 17.1 wt% (1.17mol/Kg) [23]. Since the aqueous solubility of C_4PO_1 is too low, no hydrotropic solubilization could be observed. By contrast, for $t\text{-}C_4PO_1$ and C_3PO_2 solutions, sudden increases in the solubilization appeared at concentrations below their limits of solubility. These two compounds have the

highest solubilization efficiencies, due to their pronounced hydrophobic character, among all studied compounds. Nevertheless, the maximum amount of solubilized dye remains limited in these two systems, at least in the water rich part of the phase diagram. The optimum solubility is given by a balance of a sufficiently high water solubility of the hydrotrope and a pronounced hydrophobicity. We propose that these are the two parameters to be optimized in parallel, and that compared to them, other properties of co-solvents or hydrotropes, such as the shape or the aromaticity are of minor importance.

A last point: it is interesting to compare C_1PO_3 and C_1PO_1 . The solubility efficiency is much higher in the case of C_1PO_3 . Obviously propylene glycol units are hydrophobic, and the more of such groups are present, the more the MHC is lowered and the higher is the solubility efficiency.

4.4.4 The extent of the hydrophobic part in hydrotrope molecules: a determining factor in the hydrotropic efficiency

It is our hypothesis that the “amount of hydrophobicity” is an important parameter for the hydrotropic efficiency of additives. To make a more quantitative estimation, some quantum calculations were done to estimate the electron densities in some selected hydrotropic molecules. The results can be seen in Fig. 5: the blue and green areas represent the low electron density parts in the molecules whereas the yellow and red ones display the high electron density parts. Roughly spoken, the yellow/red areas, *i.e.* the oxygen atoms in ether and hydroxyl groups, are responsible for the water solubility of the hydrotropic molecules, whereas the green/blue areas are the hydrophobic areas, hydrocarbon parts of the molecules. According to the extent of the hydrophobic parts, the following ordering is found: $SXS > C_3PO_1 > C_3EO_1 > 1\text{-propanol} \cong \text{acetone}$. This is in agreement with the order observed for the hydrotropic efficiency confirming thus the importance of the “amount of hydrotropic hydrophobicity” for the solubilization process.

To illustrate this fact in a more quantitative manner we proceed as follows. The volume of the hydrophobic parts of each studied compound is estimated by doing a simple calculation. The molar volume (V_m) of each studied pure compound at 25°C is calculated from density values. It was found to be 73.5, 75.125, 114.2 and 134.3 cm³/mol, respectively for acetone, 1-propanol, C_3EO_1 and C_3PO_1 . For SXS the molar partial volume was evaluated from the density of an aqueous solution at 40 wt% and was estimated to be about 188.4 cm³/mol.

As a first approximation the “hydrotropic” molar volume was assumed to be equal to the partial molar volume of the “hydrotrope” in solution in water. This approximation was checked in the case of C_3PO_1 , for which the partial molar volumes at different concentrations were determined at 25°C. In the diluted region the C_3PO_1 partial molar volume was found to differ from the molar volume of pure C_3PO_1 by not more than 9%. In the next step the molar volume of the hydrophobic part of

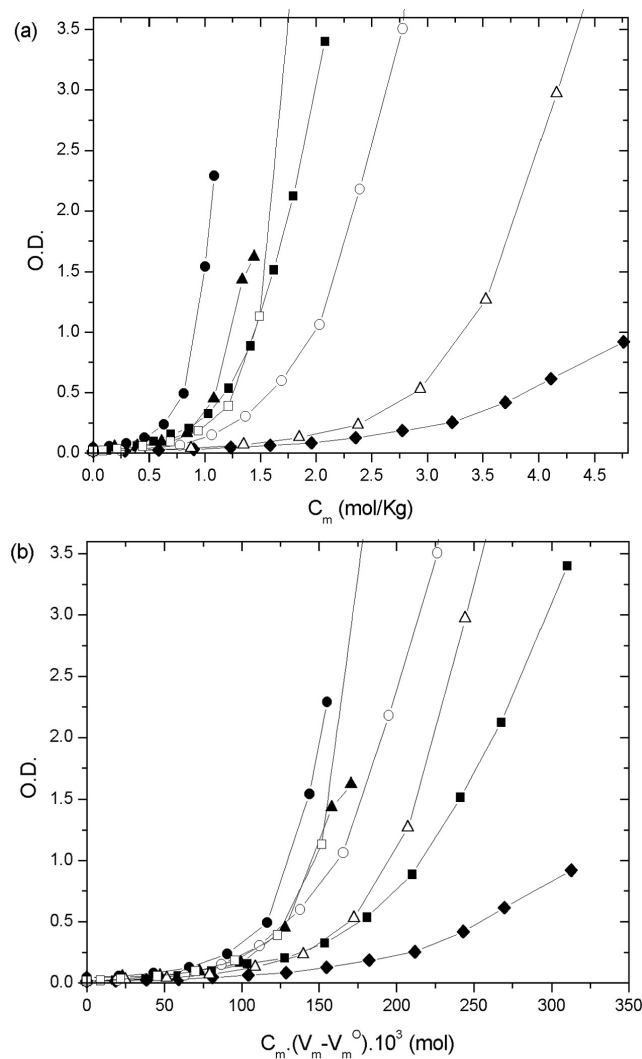


Figure 4.4: The optical density (O.D.) as a function of (a) molal concentrations of hydrotropes (or co-solvents) in water, (b) molal concentrations of hydrotropes (or co-solvents) in water multiplied by the evaluated molar volume of the hydrophobic part of the respective hydrotrope (or co-solvent) molecules; C_3PO_2 (●), $t-C_4PO_1$ (▲), C_3PO_1 (□), C_1PO_3 (■), C_3EO_1 (○), 1-propanol (△) and C_1PO_1 (◆).

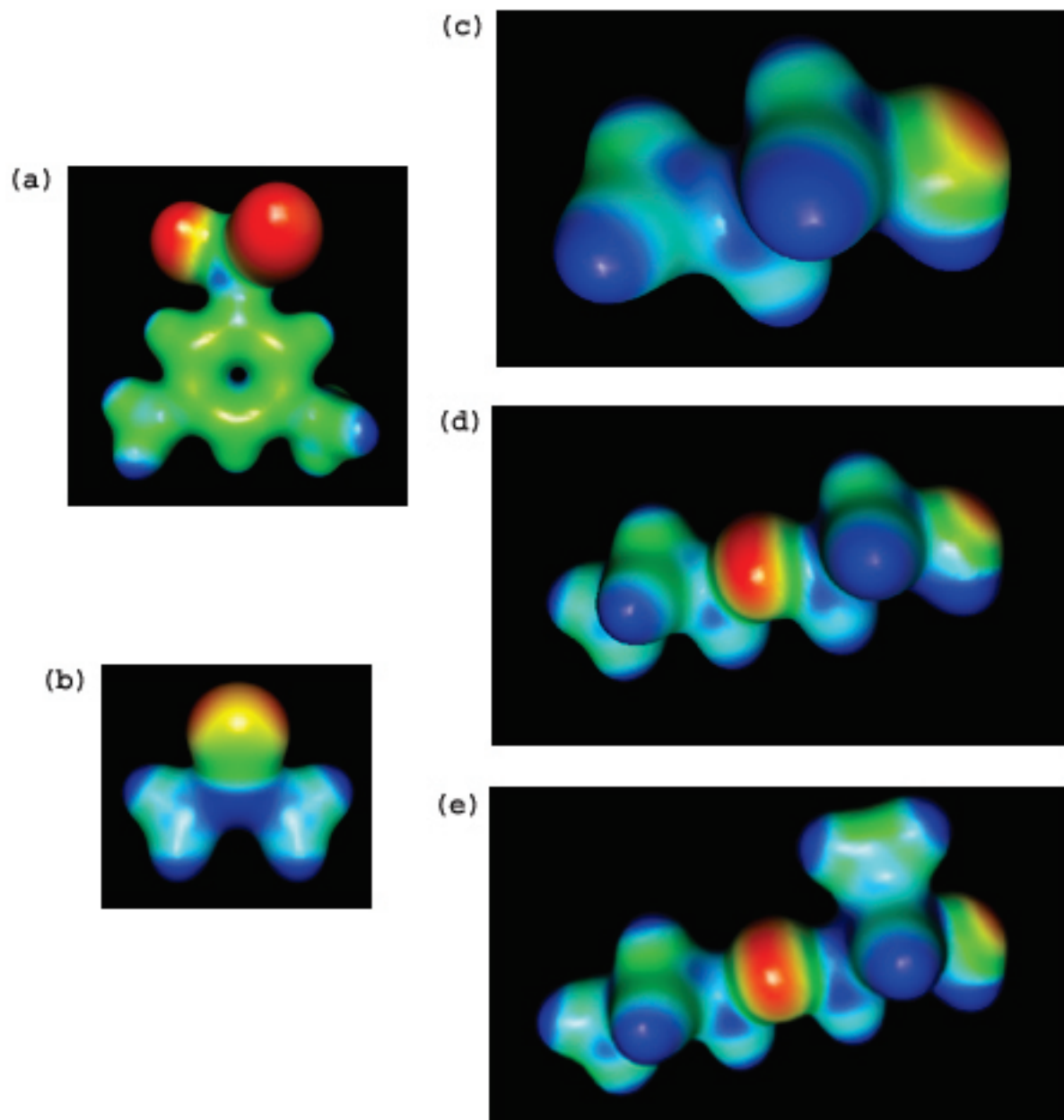


Figure 4.5: Representations of the electron density in hydrotrope and co-solvent molecules, green/blue and yellow/red areas represent respectively the low and high electron density parts in the molecules: SXS (a), acetone (b), 1-propanol (c), C_3EO_1 (d) and C_3PO_1 (e).

these molecules was evaluated by subtracting from V_m the molar volume V_m^O , *i.e.* the “molar volume” of the oxygen atom(s) contained in each molecule. The molar volume of one oxygen atom was roughly approximated to be 16 cm³/mol. With these approximations the optical densities given in Figs. 3a and 4a were plotted again, but this time as a function of the “hydrotrope” concentration multiplied by the molar volume of the hydrophobic part. The results are given in Figs. 3b and 4b. As expected the curves are much closer now, although a universal scaling law could not be detected. Partly, this is the consequence of the chemical specificity of each hydrotrope, partly it may come from the limited number of hydrotropic molecules considered in this study. Nevertheless, such calculations may help to give a first estimation of the solubility efficiency of a hydrotropic or co-solvent molecule. Note that the SXS curve is now much more in agreement with the other curves, despite the postulated specific association between the aromatic rings of SXS and DR-13.

Concerning the mechanism of the hydrotrope solubilization, it is interesting to remark that the short amphiphiles C_nEO_m , especially C_4EO_1 , have been recently studied by ultrasonic and dielectric spectroscopy and it results that such molecules form micro heterogeneous structures when mixed with water [24, 25, 26, 27]. The related aggregates appear at relatively high concentrations (around 1M) and these concentrations correlate well with the MHC observed in the case of C_3EO_1 and C_3PO_1 (chemical isomer of C_4EO_1). We have to bear in mind that at 1M the average distance between two molecules is only 18.8 Å assuming as a rough guide that the molecules are arranged on a cubic lattice and that the “length” of an SXS molecule is about 7 Å, the length of C_3PO_1 about 10 Å. Small hydrophobic association effects are then sufficient to bring the hydrotropic molecules together so that they can form bigger aggregates, in which hydrophobic molecules can be dissolved.

4.5 Conclusion

From the present study it is concluded that the solubility curves of a hydrophobic dye are all similar no matter if a co-solvent, a hydrotrope or a solvo-surfactant is used.

The less polar or the less hydrophilic the additive is, the lower is its minimum hydrotropic concentration (MHC) and the more efficient is its hydrotropic behavior.

The hydrophobic part of the hydrotrope or co-solvent molecules seems to be the major factor influencing the hydrotropic efficiency.

Other (second order) effects may enhance the hydrotropic efficiency, for example special attractions between aromatic rings. But these effects are neither at the origin of hydrotropy nor are they indispensable to the hydrotropic effect.

High hydrotropic efficiency does not mean that a large amount of hydrotropic molecules can be dissolved in water. If this is required, a hydrotrope must be used that is sufficiently soluble in water despite its necessarily high hydrophobicity. In this respect C_3PO_1 and C_1PO_3 offer a good compromise between a large hydrophobic part and a sufficient water co-miscibility. To overcome the problem of the poor

solubility of some potentially promising hydrotropes, it is preferable to mix them with other hydrotropes that are co-miscible with water. By doing so an optimum in solubilization is often achieved. This principle of solubilization is known as “facilitated hydrotrophy” [28].

The hydrophobicity of hydrophobic additives correlates well not only with the efficiency to dissolve hydrophobic particles in water, but also with surface tension measurements and the lowering of CMCs of classical surfactants in water. By contrast it does not correlate at all with the solubility of hydrophobic molecules in the pure hydrotropes. For example, the DR-13 dye used here is best soluble in pure acetone. However, the highest amount of dissolved dye in dilute water solutions is found with C_3PO_1 and C_1PO_3 . A similar conclusion is drawn up in Chapter 5: It can be misleading to extrapolate the behaviour of pure hydrotropic compounds or mixtures of them with only a small amount of water to the properties of dilute aqueous solutions.

Bibliography

- [1] Carl. Neuberg. Hydrotropic phenomena. i. *Biochemische Zeitschrift*, 76:107–76, 1916.
- [2] Annna. Matero. *Hydrotropes*, volume 1 of *Handbook of Colloid and Interface Science*, chapter 18, pages 407–420. Elsevier, London, 2002.
- [3] A. M. Saleh and L. K. El-Khordagui. Hydrotropic agents: a new definition. *International Journal of Pharmaceutics*, 24:231–8, 1985.
- [4] Ingvar Danielsson and Per. Stenius. Anion association and micelle formation in solutions of hydrotropic and short-chain carboxylates. *Journal of Colloid and Interface Science*, 37:264–80, 1971.
- [5] E. C. Lumb. Phase equilibria in mixtures of alcohols with aqueous hydrotropic salt solutions. *Transactions of the Faraday Society*, 47:1049–55, 1951.
- [6] P. Firman, D. Haase, J. Jen, M. Kahlweit, and R. Strey. On the effect of electrolytes on the mutual solubility between water and nonionic amphiphiles. *Langmuir*, 1:718–24, 1985.
- [7] D. Balasubramanian, V. Srinivas, V. G. Gaikar, and M. M. Sharma. Aggregation behavior of hydrotropic compounds in aqueous solution. *Journal of Physical Chemistry*, 93:3865–70, 1989.
- [8] Rodrigo C. da Silva, Marcos Spitzer, Luis H. M. da Silva, and Watson. Loh. Investigations on the mechanism of aqueous solubility increase caused by some hydrotropes. *Thermochimica Acta*, 328:161–167, 1999.
- [9] Reinhard Strey, Yrjoe Viisanen, Makoto Aratono, Josip P. Kratochvil, Qi Yin, and Stig E. Friberg. On the necessity of using activities in the gibbs equation. *Journal of Physical Chemistry B*, 103:9112–9116, 1999.
- [10] Geza Horvath-Szabo, Qi Yin, and Stig E. Friberg. The hydrotrope action of sodium xylenesulfonate on the solubility of lecithin. *Journal of Colloid and Interface Science*, 236:52–59, 2001.
- [11] Harold S. Booth and Howard E. Everson. Hydrotropic solubilities. i. solubilities in forty percent sodium xylenesulfonate. *Journal of Industrial and Engineering Chemistry (Washington, D. C.)*, 40:1491–3, 1948.

- [12] Harold S. Booth and Howard E. Everson. Hydrotropic solubilities. solubilities in aqueous sodium arylsulfonate solutions. *Journal of Industrial and Engineering Chemistry (Washington, D. C.)*, 41:2627–8, 1949.
- [13] Harold S. Booth and Howard E. Everson. Hydrotropic solubilities-solubilities in aqueous sodium o-, m-, and p-xylenesulfonate solutions. *Journal of Industrial and Engineering Chemistry (Washington, D. C.)*, 42:1536–7, 1950.
- [14] Stig E. Friberg. Hydrotropes. *Current Opinion in Colloid & Interface Science*, 2:490–494, 1997.
- [15] Brigitte. Schobert. The anomalous colligative properties of proline. *Naturwissenschaften*, 64:386, 1977.
- [16] Brigitte Schobert and Harald. Tschesche. Unusual solution properties of proline and its interaction with proteins. *Biochimica et Biophysica Acta*, 541:270–7, 1978.
- [17] Pasupati. Mukerjee. Micellar properties of drugs. micellar and nonmicellar patterns of self-association of hydrophobic solutes of different molecular structures. monomer fraction, availability, and misuses of micellar hypothesis. *Journal of Pharmaceutical Sciences*, 63:972–81, 1974.
- [18] Samuel H. Yalkowsky. *Solubility and Solubilization in Aqueous Media*. Oxford University Press, New York, 2000.
- [19] Stig E. Friberg and Chris. Brancewicz. *Hydrotropy*, volume 67 of *Science Surfactant Series*, chapter 2, pages 21–33. Marcel Dekker, New York, 1997.
- [20] A. Sokolowski and J. Chlebicki. The effect of polyoxypropylene chain length in nonionic surfactants on their adsorption at the aqueous solution-air interface. *Tenside Detergents*, 19:282–6, 1982.
- [21] Adam Sokolowski and Bogdan. Burczyk. Chemical structure and surface activity. viii. statistical evaluation of the influence of alkyl monoethers of polyoxyethylene glycols structure on their adsorption at the aqueous solution-air interface. *Journal of Colloid and Interface Science*, 94:369–79, 1983.
- [22] Mohamed Ahmed Etman and Aly Hassan. Nada. Hydrotropic and cosolvent solubilization of indomethacin. *Acta Pharmaceutica (Zagreb)*, 49:291–298, 1999.
- [23] P. Bauduin, L. Wattebled, S. Schrodle, D. Touraud, and W. Kunz. Temperature dependence of industrial propylene glycol alkyl ether/water mixtures. *Journal of Molecular Liquids*, 115:23–28, 2004.
- [24] U. Kaatze, K. Menzel, R. Pottel, and S. Schwerdtfeger. Microheterogeneity of 2-butoxyethanol/water mixtures at room temperature. an ultrasonic relaxation study. *Zeitschrift fuer Physikalische Chemie (Muenchen, Germany)*, 186:141–70, 1994.

- [25] U. Kaatze, M. Kettler, and R. Pottel. Dielectric relaxation spectrometry of mixtures of water with isopropoxy- and isobutoxyethanol. comparison to unbranched poly(ethylene glycol) monoalkyl ethers. *Journal of Physical Chemistry*, 100:2360–6, 1996.
- [26] K. Menzel, A. Rupprecht, and U.. Kaatze. Broad-band ultrasonic spectrometry of ciej/water mixtures. precritical behavior. *Journal of Physical Chemistry B*, 101:1255–1263, 1997.
- [27] Simon Schroedle. PhD thesis, University of Regensburg, Germany, 2005.
- [28] P. Simamora, J. M. Alvarez, and S. H. Yalkowsky. Solubilization of rapamycin. *International journal of pharmaceutics*, 213:25–9., 2001.

Part II

Co-surfactant properties of C_nPO_m s

5 Effect of non-ionic amphiphiles derived from ethylene and propylene glycol alkyl ethers on the CMC of SDS

Abstract

The effect of the short non-ionic amphiphiles: n-alcohol ($n = 3-6$), polypropylene glycol alkyl ether (C_nPO_m , for $n = 3, 4$; $m = 1-3$) and polyethylene glycol (C_nEO_m , for $n = 3$; $m = 1$ and $n = 4$; $m = 1-3$) on the critical micellar concentration (cmc) of sodium dodecyl sulfate (SDS) in aqueous solutions at 25°C has been determined experimentally by measuring the electrical conductance. The results show that there is a linear relation between the number of propylene glycol and ethylene glycol groups and the slope of the cmc decrease with amphiphile concentration. The propylene glycol group appears to be more efficient in lowering the cmc than the ethylene glycol group which is less hydrophobic. Considering the polypropylene glycol alkyl ethers as the condensation of an n-alcohol and a certain number of propylene glycol groups it was possible to classify these amphiphiles according to their efficiency to decrease the cmc of SDS: $C_4PO_3 > C_6PO_0 > C_4PO_2 > C_3PO_3 > C_4PO_1 > C_3PO_2 > C_5PO_0 > C_3PO_1 > C_4PO_0 > C_3PO_0$. This trend is different from the series of hydrophobicity of these compounds, inferred in Chapter 2 from water/ C_nPO_m binary phase diagrams: $C_6PO_0 > C_5PO_0 > C_4PO_3 > C_4PO_2 > C_4PO_1 > C_4PO_0 > C_3PO_3 > C_3PO_2 > C_3PO_1 > C_3PO_0$. The hydrophobicity of these compounds increases much more with the addition of one carbon in the alkyl chain than with the addition of one propylene glycol group. The co-surfactant behaviour of some of these molecules is also discussed and compared in terms of the topology of their ternary phase diagrams SDS/water/co-surfactant. Some striking differences in the co-surfactant behavior of the studied amphiphiles are found between their CMC decrease property and the topology of their corresponding ternary systems.

5.1 Introduction

The presence of amphiphilic additives is well known to decrease the critical micellar concentration (CMC) of surfactants [1, 2, 3]. The aggregation of surfactants involves contributions from both repulsive and attractive interactions. The addition of small amounts of amphiphilic additives strengthens the attractive interactions, also

called hydrophobic interactions, of surfactants molecules in solution leading thus to decrease the CMC. To measure this strengthening the initial rate of decrease of the CMC with the additive concentration, i.e. the $\ln(-d\ln\text{CMC}/dY_a)$ value, is taken as a valuable criterium [1, 2, 3]. The higher the $\ln(-d\ln\text{CMC}/dY_a)$ value, the more the additive or amphiphile strengthens the hydrophobic interaction of surfactants molecules. n-alcohols ranging from 1-butanol to 1-heptanol were already studied as amphiphilic additives, or co-surfactants, to sodium dodecyl sulfate (SDS) [2]. A linear relation between the carbon number of the n-alcohols and the $\ln(-d\ln\text{CMC}/dY_a)$ values was obtained. In the present work the effect of the short non-ionic amphiphiles: polypropylene glycol alkyl ether ($C_n\text{PO}_m$, for $n = 3, 4$; $m = 1-3$) and polyethylene glycol ($C_n\text{EO}_m$, for $n = 3$; $m = 1$ and $n = 4$; $m = 1-3$) on the CMC of SDS in aqueous solutions at 25°C has been determined experimentally by measuring the electrical conductance. The results are discussed in comparison to the ones obtained for n-alcohols ($n = 3-6$), which were redone. The choice of the $C_n\text{PO}_m$ as amphiphiles in the present study was mainly motivated by toxicological considerations. Indeed the n-alcohols, especially 1-butanol and 1-pentanol, which are the most widely used co-surfactants with ionic surfactants in the composition of microemulsions show acute toxicity limiting thus their applications¹. The use of short amphiphiles (co-surfactants) or solvents in combination with surfactants is of great importance in the formulation of cleaning products or in the increase of solubilization power [4, 5]. In comparison to the $C_n\text{EO}_m$, and obviously to the n-alcohols, very little attention is paid to the study of $C_n\text{PO}_m$ in the scientific literature [6, 7, 8, 9, 10, 11, 12]. As a result, the physico-chemical behaviors of these molecules are not yet well known. Nevertheless since 1980s toxicological studies showed that the solvents derived from ethylene glycol ether used in degreasing and cleaning process are hazardous to health and may present genotoxic activity [13, 14], see Section 1.2 for more details. All of these considerations reinforce the fact that the quest for new and less harmful low cost products with comparable physical and chemical properties is a current issue in the chemical industry. The short $C_n\text{PO}_m$ derivatives ($n < 5$, $m < 4$) present in this sense an attractive alternative to the alcohols or $C_n\text{EO}_m$ as solvent or co-surfactant.

5.2 Materials and Methods

Sodium dodecyl sulfate (SDS, 99%), 1-propanol (99.9%), 1-butanol (99.4%), 1-pentanol (99.5%), 1-hexanol (99.4%) were purchased from Merck, $C_3\text{EO}_1$ (99.4%), $C_4\text{EO}_1$ (99.9%), $C_4\text{EO}_2$ (99.2%) from Aldrich, $C_4\text{EO}_3$ (97%) from ABCR GmbH and $C_3\text{PO}_1$ (99%), $C_3\text{PO}_2$ (>98.5%), $C_3\text{PO}_3$ (97%), $C_4\text{PO}_1$ (>99%), $C_4\text{PO}_2$ (>98.5%) and $C_4\text{PO}_3$ (>95%) from DowChemical Company. All compounds were used as received without further purification. Purified water was taken from a Millipore Milli-Q system (electrical conductivity $<10^{-6}\text{S.m}^{-1}$). Critical micellar concentrations (CMC) of SDS at different concentrations of additives (at least three) were

¹This point shall be studied in more details in Chapter 6.

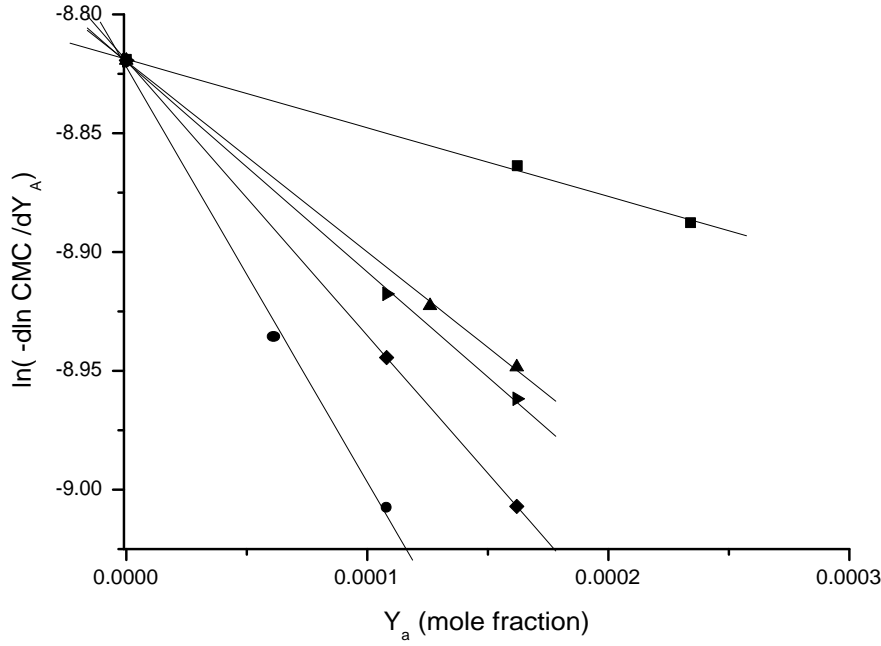


Figure 5.1: $-\ln(\text{CMC})$ values, for some of the studied amphiphiles, as a function of the amphiphile content Y_A , amphiphile mole fraction: (■) 1-butanol, (●) 1-hexanol, (▲) C_3PO_2 , (◆) C_3PO_3 and (►) C_4PO_1 .

determined by conductivity method at $25 \pm 0.1^\circ\text{C}$. Conductivities were measured with a self-made platinized electrode of known cell constant. The CMC values were classically determined at the break points of the two linear parts of the conductivity versus concentration plots. Results for some studied amphiphiles are shown in Figure 5.1, where $-\ln(\text{CMC})$ is plotted as a function of the amphiphile mole fraction Y_A . Note that in $-\ln(\text{CMC})$, CMCs are expressed in mole fraction.

The realm of existence of the monophasic and isotropic phase, i.e. micellar or microemulsion system, in the water/SDS/ C_4PO_3 system was determined at $25 \pm 1^\circ\text{C}$ according to the recommendations of *Clausse et al.* [15]. Mixtures of SDS and C_4PO_3 , at different ratios, were progressively enriched in water while being submitted to gentle agitation by means of a magnetic stirrer. Similar experiments were done from mixtures of water and C_4PO_3 with adding SDS. The concentrations of water at which turbidity-to-transparency and transparency-to-turbidity occurred were derived from precise weight measurements. In the low C_4PO_3 content part of the diagram, it was necessary to carry out static titration experiment.

5.3 Results and Discussion

Our strategy is to compare the hydrophilic/lipophilic behavior of the ethylene and propylene glycol alkyl ethers. As a criterium of this behavior we choose their $\ln(-\text{dlnCMC}/\text{dYa})$ values and compare them to the ones of n-alcohols. Indeed in comparison to 1-propanol and 1-butanol, the chemical structure of C_3PO_m , C_3EO_m , C_4PO_m and C_4EO_m can be regarded respectively as a 1-propanol (C_3PO_0 or C_3EO_0) or 1-butanol (C_4PO_0 or C_4EO_0) molecule condensed with propylene glycol or ethylene glycol groups. At first the $\ln(-\text{dlnCMC}/\text{dYa})$ values for n-alcohols from n-propanol to n-hexanol with SDS were determined and compared to the values obtained by Hayase *et al.* [2] for n-alcohols from n-butanol to n-heptanol, see Figure 5.2. The $\ln(-\text{dlnCMC}/\text{dYa})$ values for n-alcohols from n-propanol to n-hexanol show a linear evolution as a function of the alcohol carbon number. A similar evolution was found previously [2] for n-alcohols from n-butanol to n-heptanol. Nevertheless, a slight difference in the slope values between the data of Hayase *et al.* [2] and ours is found. This could be due to the fact that we use non-recrystallized SDS. For later calculations we will use our data on n-alcohols to compare them to the studied amphiphiles. The 1-propanol was studied in order to discuss the effect on the $\ln(-\text{dlnCMC}/\text{dYa})$ values of the addition of the first ethylene and propylene glycol unit, i.e. from 1-propanol to C_3EO_1 or C_3PO_1 .

In order to compare the studied amphiphiles their $\ln(-\text{dlnCMC}/\text{dYa})$ values were plotted, in a similar way as for n-alcohols, as a function of the number of the propylene and ethylene glycol units respectively in Figures 5.3 and 5.4. Such a representation is common; it was previously done in a similar study of α - ω diols ($\text{HO}-(\text{CH}_2)_n-\text{OH}$) [3]. The $\ln(-\text{dlnCMC}/\text{dYa})$ values were there plotted as a function of n , the number of methylene units and as in the case of the n-alcohols a linear evolution was found.

For C_3PO_m , C_4PO_m and C_4EO_m when $1 < m < 3$, linear evolutions of the $\ln(-\text{dlnCMC}/\text{dYa})$ values as a function of m are obtained. All linear expressions are inserted in Figures 5.3 and 5.4. From $m = 0$ to 1, the $\ln(-\text{dlnCMC}/\text{dYa})$ values change more significantly than it does from $m = 1$ to 2 and from $m = 2$ to 3. This means that the addition of the first propylene or ethylene glycol unit to 1-propanol or 1-butanol strengthens stronger the hydrophobic interactions of SDS molecules than the addition of a later unit. From this work this is confirmed at least for C_3PO_m , C_4PO_m and C_4EO_m when $m < 3$. The more hydrophobic nature of the first ethylene and propylene glycol unit in comparison to the later ones was already inferred previously from surface tension measurements on the same amphiphiles in binary water mixtures [10, 11]. The hydrophobic contribution of the second and the third ethylene and propylene glycol units seems to be comparable. This was also already observed in surface tension measurements [10, 11]. All $\ln(-\text{dlnCMC}/\text{dYa})$ values are given in Table 5.1.

In terms of the $\ln(-\text{dlnCMC}/\text{dYa})$ values, the equivalence of the EO and PO groups in comparison to methylene group ($-\text{CH}_2-$) of a n-alcohol were calculated by dividing the slope values of the linear parts in Figures 5.3 and 5.4 by the slope

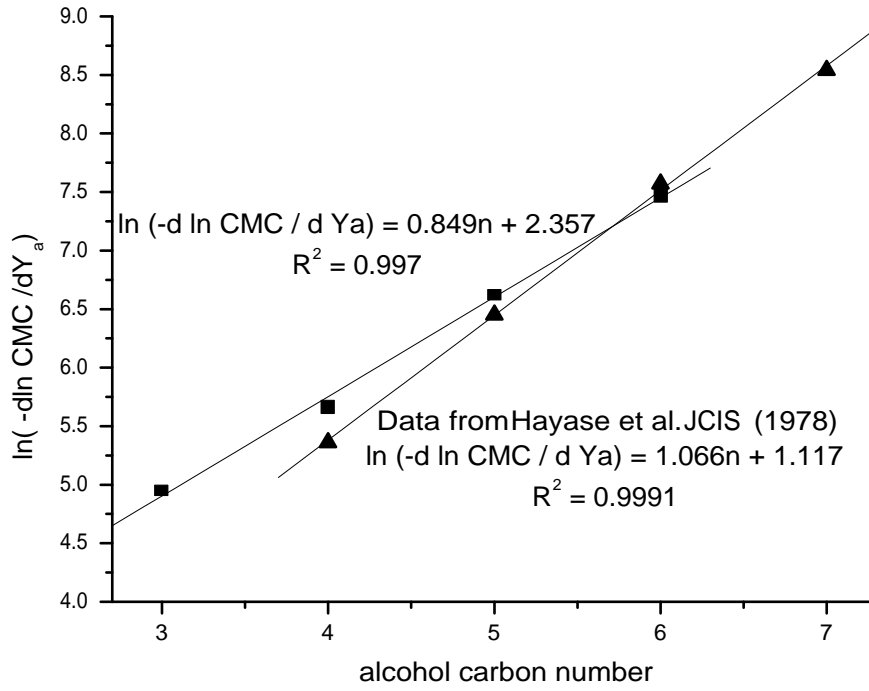


Figure 5.2: $\ln(-d \ln \text{CMC} / dY_a)$ values obtained for n-alcohols as a function of the carbon number of the alcohol: (■) from the present work and (▲) data from *Hayase et al.* [2].

amphiphile	$\ln(-d \ln \text{CMC} / dY_a)$	n_{eq}
1-propanol	4.96	/
1-butanol	5.67	/
1-pentanol	6.62	/
1-hexanol	7.47	/
C ₃ PO ₁	6.16	4.48
C ₃ PO ₂	6.69	5.10
C ₃ PO ₃	7.06	5.53
C ₄ PO ₁	6.78	5.21
C ₄ PO ₂	7.28	5.80
C ₄ PO ₃	7.75	6.35
C ₄ EO ₁	6.40	4.76
C ₄ EO ₂	6.73	5.15
C ₄ EO ₃	6.93	5.38
C ₃ EO ₁	5.46	3.66

Table 5.1: $\ln(-d \ln \text{CMC} / dY_a)$ values obtained for all the studied amphiphiles and their calculated n_{eq} (see text).

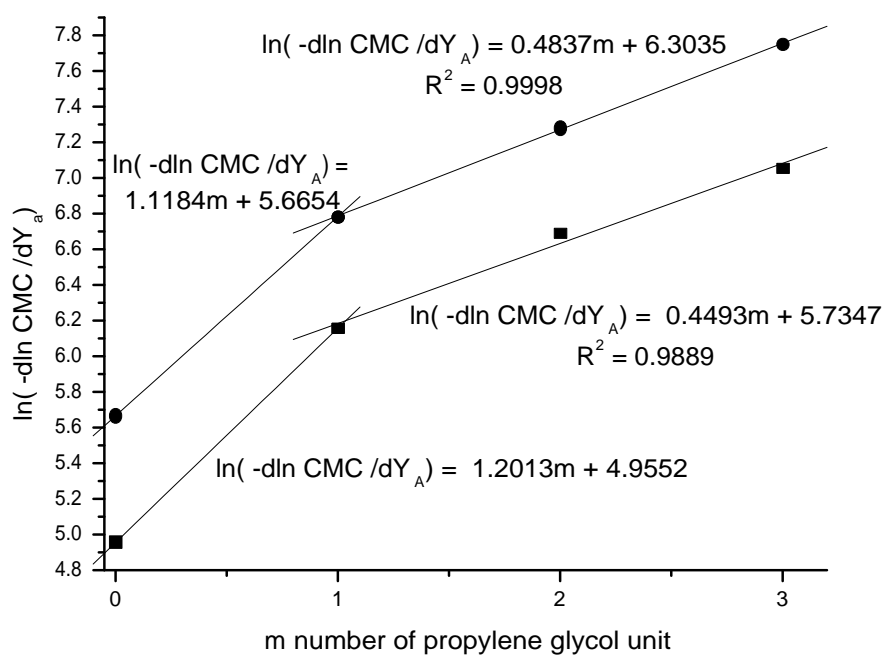


Figure 5.3: $\ln(-d\ln \text{CMC}/dY_A)$ values obtained C_4PO_m (●) and C_3PO_m (■) as a function of the number of propylene glycol units, m .

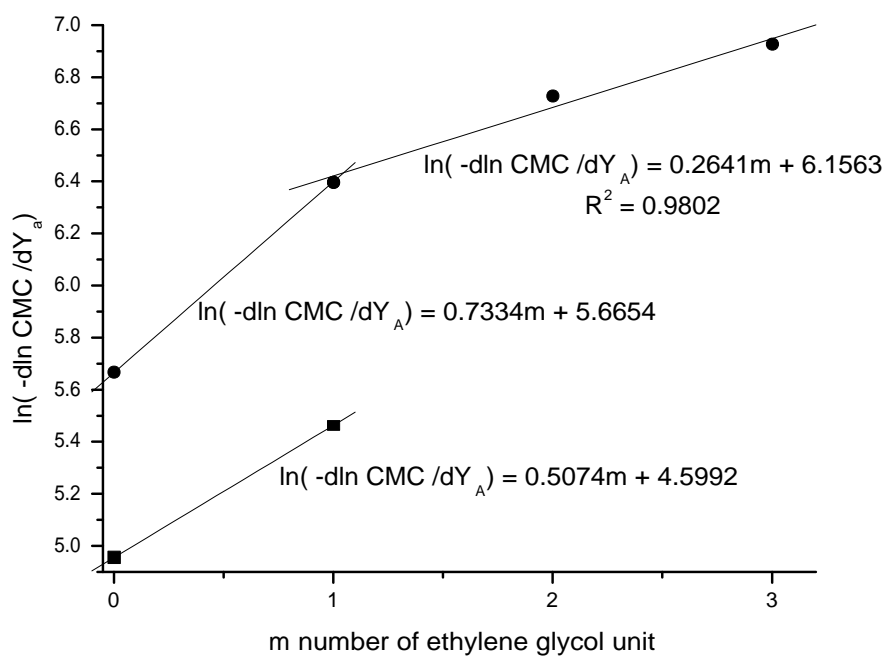


Figure 5.4: $\ln(-d\ln\text{CMC}/dY_A)$ values obtained C_4EO_m and C_3EO_m as a function of the number of ethylene glycol units, m .

obtained with n-alcohols, see Figure 5.2. These values of equivalents were found to be:

- for C_3PO_m and C_4PO_m , respectively 1.41 and 1.32 ($-CH_2-$) per first PO unit and 0.53 and 0.56 ($-CH_2-$) per PO unit for $1 < m < 3$,
- for C_3EO_m and C_4EO_m , respectively 0.6 and 0.86 ($-CH_2-$) per first EO unit and for C_4EO_m 0.31 ($-CH_2-$) per EO unit for $1 < m < 3$.

In a general way PO group brings more hydrophobicity than a EO group does. In order to compare all the studied amphiphiles between each others their $\ln(-d\ln CMC/dYa)$ values were plotted on the curve obtained for n-alcohols (Figure 5.2, square symbol), see Figure 5.5, the $\ln(-d\ln CMC/dYa)$ values of n-alcohols are represented by the full circle. From the linear equation in Figure 5.2 obtained for n-alcohols (square symbol) and from the $\ln(-d\ln CMC/dYa)$ values of the amphiphiles a n-alcohol equivalent carbon number n_{eq} was calculated for each amphiphile (Table 1). The n_{eq} obtained for an amphiphile represents the carbon number of a hypothetical n-alcohol having the same $\ln(-d\ln CMC/dYa)$ values i.e. having the same influence on the CMC decrease of SDS. An interesting discussion on the effect of the amphiphile on the SDS micelle formation can now be done. For instance, it can be seen in Figure 5.5 that C_3PO_2 , C_4EO_2 and C_4PO_1 have nearly the same effect as the 1-pentanol. Such a comparison could be a useful guide for a formulator whose aim is to replace a C_nEO_m or an alcohol from a formulation by an equivalent C_nPO_m , which do not present genotoxicity. Nevertheless this result has to be taken with care because the $\ln(-d\ln CMC/dYa)$ values are determined only for SDS at low co-surfactant and surfactant concentration. For more concentrated systems, for example microemulsions, or for other surfactant types the hydrophilic/lipophilic behavior of C_nEO_m , C_nPO_m and n-alcohols could be different.

To illustrate this the topology of ternary phase diagrams composed of water, SDS and short amphiphiles can be compared. Indeed the n-alcohols are known to present a significant difference in their co-surfactant behaviors when $n > 5$ and $n \leq 5$, n standing for the alcohol carbon number, with SDS or some other surfactants [15, 16]. This difference can be seen directly on the topology of ternary phase diagrams, see Figure 5.6. The black areas in these diagrams represent monophasic isotropic solutions being typically micellar solutions or microemulsions. L1 and L2 stand respectively for direct and reverse micelles or microemulsions i.e. oil in water and water in oil. The white areas represent polyphasic systems, i.e. liquid/liquid or solid/liquid systems, or ordered surfactant phases such as hexagonal or lamellar phases. No further details on the structure of the phases will be given. In the case of the system containing n-hexanol ($n > 5$) the phase diagram shows separate direct and reverse microemulsion regions. By contrast, for the systems containing n-butanol and n-pentanol ($n \leq 5$) a continuity between the direct and reverse microemulsion regions is observed, i.e. in region L. Such phenomena are often discussed in terms of the elasticity of the interfacial film [17].

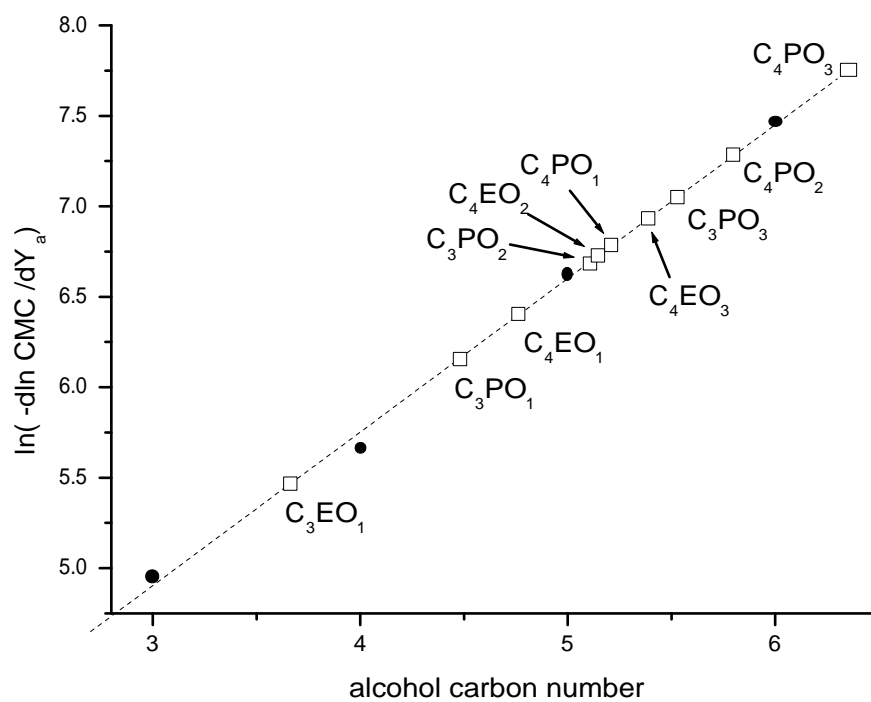


Figure 5.5: $\ln(-d\ln CMC/dY_a)$ values of some short amphiphiles derived from ethylene and propylene glycol ethers and of n-alcohols (●) versus the corresponding alcohol carbon number.

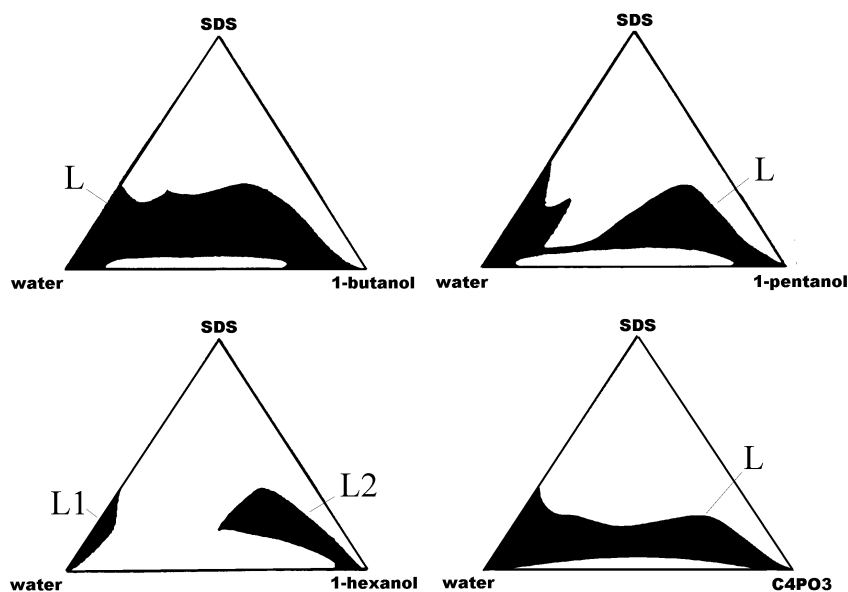


Figure 5.6: water/SDS/co-surfactant ternary phase diagrams, the co-surfactants being: 1-butanol, 1-pentanol, 1-hexanol and C_4PO_3 . The black areas represent monophasic isotropic solutions being typically micellar solutions or microemulsions. L1 and L2 stand respectively for direct and reverse microemulsions i.e. oil in water and water in oil. The white areas represent polyphasic systems, i.e. liquid/liquid or solid/liquid systems, or ordered surfactant phases such as hexagonal or lamellar.

The phase diagram obtained with C_4PO_3 belongs to the case of $n \leq 5$ and seems to be more similar to the one obtained with 1-butanol. This is in contradiction with the $\ln(-d\ln CMC/dY_a)$ values, indeed C_4PO_3 ($n_{eq} = 6.35$) appears there to be more hydrophobic than 1-hexanol. Thus there is no direct correlation between the $\ln(-d\ln CMC/dY_a)$ values of the amphiphiles and the topology of the water/SDS/amphiphiles ternary systems. It seems here that the determining factor which dictates the overall topology of the ternary phase diagram lies in the carbon number of the co-surfactant linear alkyl chain i.e. 1-butanol $\cong C_4PO_3$. Now considering the C_nPO_m and n-alcohols hydrophobicity obtained from the solubility data in water and from the lower critical solution temperature (LCST) inferred in Chapter 2 from water / C_nPO_m binary phase diagrams [18], it is possible to classify these amphiphiles: $C_6PO_0 > C_5PO_0 > C_4PO_3 > C_4PO_2 > C_4PO_1 > C_4PO_0 > C_3PO_3 > C_3PO_2 > C_3PO_1 > C_3PO_0$. This trend is different from the series of hydrophobicity of these compounds according to their efficiency to decrease the cmc of SDS (Figure 5.5): $C_4PO_3 > C_6PO_0 > C_4PO_2 > C_3PO_3 > C_4PO_1 > C_3PO_2 > C_5PO_0 > C_3PO_1 > C_4PO_0 > C_3PO_0$. The difference in hydrophobicity observed for these compounds between these two series lies in the presence of SDS in one case. The evolution of the previous ternary phase diagram topology according to the co-surfactant properties of the amphiphiles, i.e. $C_6PO_0 > C_5PO_0 > C_4PO_3 > C_4PO_0$, appears to follow the same evolution as the one obtained from the aqueous solubilities. Thus the topology of the ternary phase diagram seems to be related to the co-surfactant aqueous solubility as it is linked to the elasticity of the interfacial film. To elucidate this hypothesis more systems have to be studied.

5.4 Conclusion

In Chapter 2 and in some other works the hydrophilic/lipophilic behavior of C_nPO_m [18] and C_nEO_m have been regarded and classified in water by comparing the LCST values of the water/amphiphiles binary mixtures and the aqueous amphiphile solubilities. The main conclusion of these studies is that the presence of EO and PO groups respectively increase and decrease the hydrophilic property of amphiphiles. In the present work the comparison of these short amphiphiles was based on their ability to decrease the CMC values i.e. to strengthen the hydrophobic interactions of SDS. The more hydrophobic the amphiphile is, the bigger the CMC of SDS decreases. As expected a PO group brings more hydrophobicity than an EO group does. Moreover the equivalence of the EO and PO groups with a certain number of methylene groups ($-CH_2-$) of a n-alcohol was calculated. The first propylene or ethylene glycol unit added to 1-propanol or 1-butanol is found to give more hydrophobicity than the second and third units which bring comparable hydrophobicity. This observation correlates with some previous surface tension studies of the same amphiphiles in mixture with water. Another important point is that the $\ln(-d\ln CMC/dY_a)$ values are calculated at low additive content where the CMC decrease as a function of additive content remains linear. The comparison between

amphiphiles or co-surfactants from these values is then valid in the range of low surfactant and additive concentrations. At higher concentration, as in the case of the study of the ternary phase diagram topology, the evolution in the co-surfactant behavior is different from the one obtained from the $\ln(-d\ln\text{CMC}/dY_a)$ values. This shows that one has to be very careful when discussing the hydrophobicity of amphiphiles and that the notion of hydrophobicity depends strongly on the nature of the systems and on the concentrations of each species.

Bibliography

- [1] Kozo Shinoda. The effect of alcohols on the critical micelle concentrations of fatty acid soaps and the critical micelle concentration of soap mixtures. *Journal of Physical Chemistry*, 58:1136–41, 1954.
- [2] Kohji Hayase and Shigeo Hayano. Effect of alcohols on the critical micelle concentration decrease in the aqueous sodium dodecyl sulfate solution. *Journal of Colloid and Interface Science*, 63:446–51, 1978.
- [3] Mohammad Abu-Hamdiyyah and Christiane M. El-Danab. Strengthening of hydrophobic bonding and the increase in the degree of ionization of sodium lauryl sulfate micelles by amphiphiles and the micelle-water distribution coefficient. *Journal of Physical Chemistry*, 87:5443–8, 1983.
- [4] Patrick Durbut and Guy Broze. Liquid cleaning compositions. *U.S. Patent U.S. 5,834,413*, page 9 pp., 2001.
- [5] Patrick Durbut and Guy Broze. All purpose liquid cleaning compositions. *U.S. Patent U.S. 309,408*, page 7 pp., 2002.
- [6] H. L. Cox, Wm. L. Nelson, and L. H. Cretcher. Reciprocal solubility of the normal propyl ethers of 1,2-propylene glycol and water. closed solubility curves. ii. *Journal of the American Chemical Society*, 49:1080–3, 1927.
- [7] John Klier, Christopher J. Tucker, Thomas H. Kalantar, and D. P. Green. Properties and applications of microemulsions. *Advanced Materials*, 12:1751–1757, 2000.
- [8] L. F. Komarova and Y. N. Garber. Physical properties of dihydric alcohol ethers. *Zhurnal Organicheskoi Khimii*, 7:2507–9, 1971.
- [9] K. Lunkenheimer, H.-R. Holzbauer, and R. Hirte. Novel results on adsorption properties of definite n-alkyl oxypropylene oligomers at the air/water interface. *Progress in Colloid and Polymer Science*, 97:116–20, 1994.
- [10] A. Sokolowski and J. Chlebicki. The effect of polyoxypropylene chain length in nonionic surfactants on their adsorption at the aqueous solution-air interface. *Tenside Detergents*, 19:282–6, 1982.

- [11] Adam Sokolowski and Bogdan Burczyk. Chemical structure and surface activity. viii. statistical evaluation of the influence of alkyl monoethers of polyoxyethylene glycols structure on their adsorption at the aqueous solution-air interface. *Journal of Colloid and Interface Science*, 94:369–79, 1983.
- [12] R.M. Stephenson. *Journal of Chemical Engineering Data*, 38:134–142, 1999.
- [13] E. Degirmenci, Y. Ono, O. Kawara, and H. Utsumi. Genotoxicity analysis and hazardousness prioritization of a group of chemicals. *Water Science and Technology*, 42:125–131, 2000.
- [14] Z. Elias, M. C. Daniere, A. M. Marande, O. Poirrot, F. Terzetti, and O. Schneider. Genotoxic and/or epigenetic effects of some glycol ethers: results of different short-term tests. *Occupational Hygiene*, 2:187–212, 1996.
- [15] Marc Clausse, L. Nicolas-Morgantini, A. Zradba, and D. Touraud. in *Surfactant Science Series: Water-ionic surfactant-alkanol-hydrocarbon systems: influence of certain constitution and composition parameters upon the realms-of-existence and transport properties of microemulsion-type media.*, volume 24, pages 15–62. Marcel Dekker, NewYork, 1987.
- [16] R. Zana. Aqueous surfactant-alcohol systems: a review. *Advances in Colloid and Interface Science*, 57:1–64, 1995.
- [17] Thomas Zemb and Fabienne Testard. In *Handbook of Applied Surface and Colloid Chemistry: Solubilization.*, volume 2, chapter 32, pages 159–188. Wiley, John and Sons, Inc., 2002.
- [18] P. Bauduin, L. Wattebled, S. Schrodle, D. Touraud, and W. Kunz. Temperature dependence of industrial propylene glycol alkyl ether/water mixtures. *Journal of Molecular Liquids*, 115:23–28, 2004.

6 Design of low-toxic and temperature sensitive anionic microemulsions using short propyleneglycol alkylethers as co-surfactants

Abstract

The phase behavior of anionic microemulsions composed of water, sodium dodecyl sulfate (SDS), dodecane and short propyleneglycol monoalkylethers (C_nPO_m , $n = 3$; $m = 1$ and $n = 4$; $m = 2, 3$) is studied. From the pseudo-ternary phase diagrams it is inferred that C_nPO_m have co-surfactant behaviors comparable to those of 1-butanol and 1-pentanol, which are the most efficient and widely used co-surfactants. In contrast to these alcohols, the C_nPO_m co-surfactants induce high temperature dependences in the SDS microemulsion systems. Further, SDS / C_nPO_m microemulsions can be formed with small SDS concentrations (SDS / C_4PO_3 mass ratio of 1/6.26). These have a much lower toxicity than their 1-butanol or 1-pentanol counterparts or systems containing genotoxic short ethyleneglycol ethers (C_nEO_m) as co-surfactant. The strong temperature dependence can be favourable in the recovery of reaction products when the microemulsion is used as a reaction medium or in extraction processes.

6.1 Introduction

Microemulsions are isotropic solutions containing a surfactant or a mixture of surfactants and a co-surfactant that solubilizes considerable amounts of water and oil [1, 2]. This unique class of optically clear solutions has attracted much scientific [3, 4] and technological [5] interest over the past decades. This wide interest stems from their characteristic properties, namely ultra-low interfacial tension, large interfacial area and solubilization capacity for both water- and oil-soluble compounds. Owing to their ultra-low interfacial tensions microemulsions have found applications in oil recovery as well as in extraction processes, e.g. enhanced oil recovery [6], soil decontamination [7, 8] and detergency [9, 10]. The widespread use of microemulsions in pharmacy [11], food [12], cosmetics [13, 14], and textile dying [15, 16] is based on their high solubilization capacities for both hydrophilic and hydrophobic compounds.

Apart from these applications there has been a recent surge of interest in exploiting self assembled systems such as micellar solutions, microemulsions, and lipid bilayer systems as reaction media [17]. Among these systems, microemulsions have emerged as a popular choice for a number of diverse applications including bio-organic syntheses [17, 18, 19, 20, 21, 22]. Water-in-oil microemulsions have attracted attention as media for enzyme-catalyzed reactions because of their interesting properties as hosts for biocatalysts [20, 23, 24, 25]¹. The use of microemulsions as reaction media is sometimes favorable to give desired products in high yields [18, 21, 22].

For some practical purposes, e.g. for formulated products, it can be important to form temperature insensitive microemulsions, whereas for other applications, such as for extraction [26] and purification processes or organic synthesis, the temperature dependence of microemulsions can be desirable.

Usually non-ionic polyethoxylated surfactants (C_nEO_m) form efficient temperature sensitive microemulsions, most of the time without co-surfactant [27, 28, 29]. Nevertheless, when such microemulsions are used as reaction media, the purification of the reaction product from the non-ionic surfactant, usually hydrophobic, is intricate. In contrast, ionic surfactants form microemulsions which show much lower temperature dependence and when using single chain ionic surfactants a co-surfactant is always required. Single chain ionic surfactants, being usually very hydrophilic (high HLB), are more easily separated from the reaction product being usually hydrophobic.

In the present study the choice of C_nPO_m as co-surfactants was motivated by several points: i) these molecules are less toxic than their short-chain C_nEO_m analogues and also much less toxic than 1-butanol and 1-pentanol. C_nPO_m are already widely used, owing to their good solvent property, in industry and in formulation industries, e.g. in cleaning products, paints, inks or cosmetics. ii) in Chapter 4 we compared different hydrotropes and found that C_nPO_m s are excellent representatives of this class of molecules and should therefore be of interest also as co-surfactants [30]. Note that short C_nPO_m s were indeed recently found to be efficient co-surfactants in the formation of microemulsions [31], but the temperature dependence of such microemulsions was not pointed out. iii) The boiling points of the studied short C_nPO_m s are sufficiently low to remove them from the reaction medium under vacuum (see in Table 1.3), an important point for separation and purification processes.

It is remarkable that little attention is paid to the study of C_nPO_m in the scientific literature [31, 32, 33, 34, 35, 36], compared to C_nEO_m and n-alcohols.

In the following we investigate the phase behaviors of anionic microemulsions composed of water, sodium dodecyl sulfate (SDS), dodecane and short propyleneglycol monoalkylether derivatives (C_nPO_m , $n = 3$; $m = 1$ and $n = 4$; $m = 2, 3$). The temperature dependence of C_nPO_m /water mixtures was studied in Chapter 2 [37].

As a first step we study relevant parts of the realms of existence of the monophasic isotropic regions, which correspond to the microemulsion regions of such systems.

¹see in Chapter 8 where enzymatic reactions in water-in-oil microemulsions are largely reviewed and investigated.

This is done in order to study the ability of short C_nPO_m to form microemulsions with SDS. Comparisons to the usual SDS/*n*-alcohols based microemulsion systems are also done.

In the next step the temperature dependence of SDS/ C_nPO_m based systems is investigated. At first, water/SDS/ C_nPO_m systems are studied, and in particular, the cloud points of some C_nPO_m ($n = 3, 4$ and $m = 2, 3$)/water mixtures are measured as a function of SDS content. Then microemulsions composed of water/SDS/dodecane/co-surfactant, with C_3PO_2 , 1-butanol and 1-pentanol as co-surfactant, are investigated. To do so, the locations of the three-phase regions of these systems, which appear through addition of salt (NaCl), were determined at 13 and 69°C and at a fixed water to dodecane ratio (1/1), a fixed SDS content (3%wt) and by varying the molar ratio co-surfactant/SDS. By changing a) the salt content and b) the molar ratio co-surfactant/SDS, cartographies of the three phase regions of these systems are established. The high temperature sensitivity of microemulsions based on SDS/ C_nPO_m , in this case C_3PO_2 , is highlighted and compared to the much lower temperature sensitive microemulsions based on SDS/*n*-alcohols, in particular with 1-butanol and 1-pentanol.

Finally, the design of temperature sensitive microemulsions composed of water / dodecane / SDS / C_4PO_3 is elaborated from the knowledge of the temperature dependent binary and ternary systems composed of water/ C_4PO_3 and water/ C_4PO_3 /SDS.

6.2 Experimental Section

6.2.1 Materials

Sodium dodecyl sulfate (SDS, 99%), sodium chloride (NaCl, 99%), dodecane (99%), 1-butanol (99.4%), 1-pentanol (99.5%), 1-hexanol (99.4%) were purchased from Merck and C_3PO_1 (99%), C_3PO_2 (>98.5%), C_3PO_3 (>97%), C_4PO_1 (>99%), C_4PO_2 (>98.5%) and C_4PO_3 (>95%) from Dow Chemical Company. All compounds were used as received without further purification. Purified water was taken from a Millipore Milli-Q system (electrical conductivity $< 10^{-6} \text{ S m}^{-1}$). Water- and oil-soluble dyes were furnished by Lcw Company (France) under the name *Bleu soluble W6002* (blue dye, batch B1342) and *Jaune au gras W1201* (yellow dye, batch B0513).

6.2.2 Phase diagrams determination

The realms of existence of the monophasic and isotropic phases, i.e. micellar or microemulsion phase, in systems composed of water / dodecane / SDS / co-surfactant (see pseudo-ternary phase diagrams in Figs. 6.1b-d, 6.2c-e and 6.6c) were determined at 25°C (diagrams in Figs. 6.1 and 6.3) or 21°C (diagram in Fig. 6.6) ($\pm 1^\circ\text{C}$) according to the recommendations of Clausse et al. [38]. Two types of pseudo-ternary phase diagrams were established (1) at fixed SDS/ C_nPO_m mass ratio (K_M)

and (2) at a fixed SDS/dodecane mass ratio of 1/3. To mixtures of (1) dodecane / (SDS/ C_nPO_m), i.e. at fixed SDS/ C_nPO_m mass ratio (K_M) (Figs. 6.1b-d and 6.6c), and of (2) co-surfactant / (SDS/dodecane), i.e. at a fixed SDS/dodecane mass ratio of 1/3 (Fig. 6.2), water was progressively added during gentle agitation by means of a magnetic stirrer. The concentrations of water at which turbidity-to-transparency and transparency-to-turbidity occurred were deduced from precise weight measurements. In the pseudo-ternary phase diagrams (Figs. 6.1b-d, 6.2c-e and 6.6c) the dark areas represent the realms of existence of the monophasic and isotropic phases. The precision of the dark areas frontiers is evaluated to be about 3%.

The three phase regions in the brine/dodecane/SDS/co-surfactant systems, with C_3PO_2 , 1-butanol or 1-pentanol as co-surfactant, were determined visually. Slight amounts of water- and oil-soluble dyes, respectively blue and yellow, were used ($c \approx 10^{-5}$ - 10^{-6} M) to color the water and the dodecane. This helped the characterization of the 2- or 3-phase systems. According to Winsor's terminology [39, 40, 41], increasing salt (NaCl) concentration promotes the usual transition from Winsor I (WI) to Winsor III (WIII) to Winsor II (WII) systems. The third phase present in WIII systems, which is composed of large amounts of both water and dodecane, appeared as expected in green (blue + yellow). Series of tubes containing brine, dodecane, SDS and co-surfactant were prepared by weighing all the components. Water to dodecane volume ratio (1/1) and SDS content (3 wt%) were fixed. The molar ratio co-surfactant/SDS was varied as can be seen in Fig. 6.5 and the NaCl content in the brine varied from 0 to 12 wt%. After mixing, the tubes were very slightly agitated in order to avoid the formation of temporarily stable emulsions. Then the tubes were left without agitation and at fixed temperature during 24H in order to reach the thermodynamic equilibrium between the phases. The visual observations were then done at 16 and 69°C. Note that in the studied concentration range no lamellar crystal phase was observed in these three types of microemulsion systems. The boundaries WI/WIII and WIII/WII were determined with a precision in the NaCl concentration of 0.1wt%.

6.2.3 Phase transition determination by increasing temperature

The temperature at which liquid to liquid-liquid phase transition occurs, i.e. the cloud point, was precisely determined with the help of a self-made turbidity apparatus [42]. A constant heating rate of 2°C/hour was used in a range of temperature from 0 to 80°C. The temperature precision of the measures is estimated to be $\pm 0.05^\circ\text{C}$.

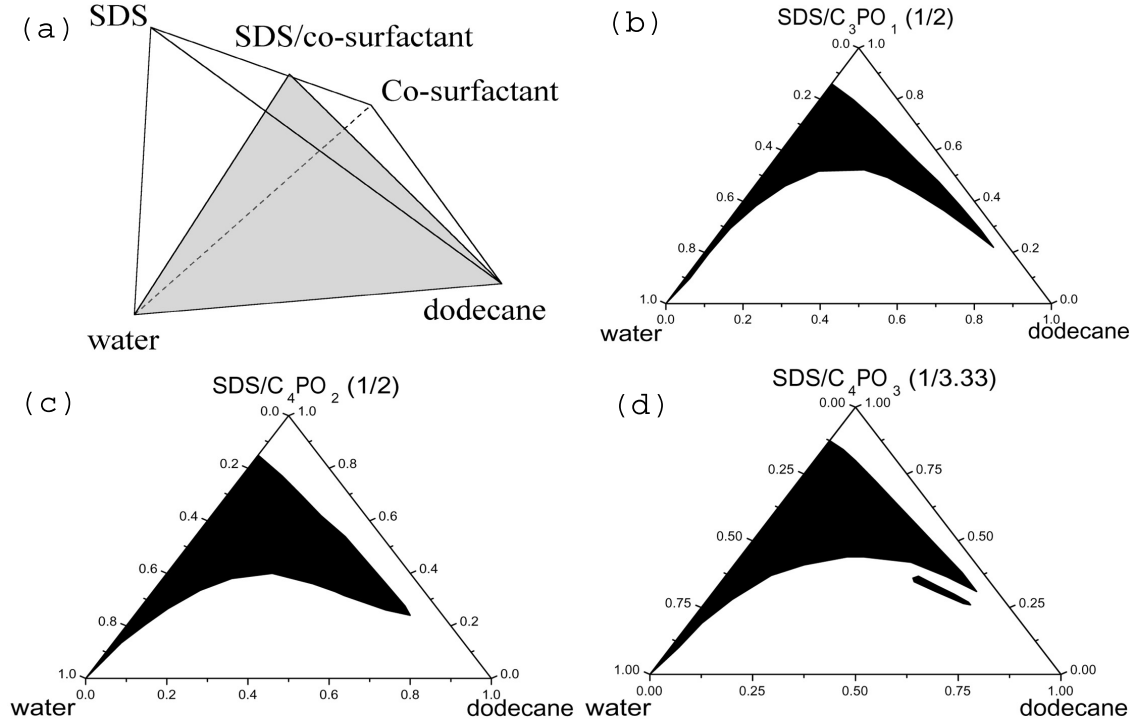


Figure 6.1: (a) Tetrahedral representation of quaternary systems composed of water / SDS / dodecane / co-surfactant, the grey triangle represents pseudo-ternary systems having a constant SDS/co-surfactant mass ratio (K_M), (b-d) pseudo-ternary phase diagrams of water / SDS / dodecane / C_nPO_m systems obtained for C_3PO_1 (b), C_4PO_2 (c) and C_4PO_3 (d) at SDS/ C_nPO_m mass ratio K_M of 1/2 (b), 1/2(c) and 1/3.33 (d). The dark areas represent the realms of existence of monophasic and isotropic phases. The diagrams were determined at 25°C.

6.3 Results and Discussion

6.3.1 C_nPO_m as co-surfactant in the formation of microemulsions

Figure 6.1 shows experimentally determined pseudo-ternary phase diagrams with C_3PO_1 , C_4PO_2 and C_4PO_3 with a SDS/ C_nPO_m mass ratio respectively of $K_M = 1/2$, $1/2$, $1/3.33$. These K_M values were chosen, because in the case of microemulsions based on SDS and on n-alcohols ($n = 3-6$) K_M values of around $1/2.5$, depending slightly on the length of the n-alcohol, give the largest microemulsion areas in the studied pseudo-ternary phase diagrams [38]. For a better comprehension a tetrahedral representation of such quaternary systems is given in Fig. 6.1a. The cut through the tetrahedron represents a typical pseudo-ternary phase diagram as considered in the present study.

Large monophasic zones of similar shapes are observed for the three studied sys-

tems (Figs. 6.1b-d). The shape and the extent of these monophasic regions are also similar to those observed in water/SDS/dodecane/n-alcohol (1-propanol, 1-butanol and 1-pentanol) systems at K_M around 1/2.5² [38]. From the similarity of the phase diagrams we infer that short C_nPO_m s can play, as well as n-alcohols ($n = 3-5$), the role of co-surfactants in the formation of SDS based microemulsions.

Although no quantitative comparison between the phase diagrams in Figs. 6.1b-d can be done, because of the different K_M values and the different molar masses of the C_nPO_m , it is interesting to note that the microemulsion zone observed in the case of C_3PO_1 is smaller than the others observed in the case of C_4PO_2 (c) and C_4PO_3 . This is analogue to the series of alcohols used as co-surfactants: 1-propanol is usually not considered as a “true” co-surfactant, its alkyl chain being too short [38]. Consequently the microemulsion region observed in the case of 1-propanol based systems is smaller than in the case of 1-butanol or 1-pentanol (“true” co-surfactants) based systems. 1-propanol is rather considered as a co-solvent. We conclude that C_3PO_1 obviously acts also partly as a co-solvent and partly as a co-surfactant, although no clear discrimination between both classes can be made [30]³. In the pseudo-ternary phase diagram obtained with C_4PO_3 (Fig. 6.1d) a very narrow isotropic phase of very high viscosity and having the shape of a lens is observed in the dodecane rich part. Such a highly viscous and isotropic phase is present in pseudo-ternary phase diagrams of water/SDS/dodecane/1-n-alcohol formed with 1-butanol and 1-pentanol at K_M values around 1/2.5 [43]. This phase of high conductivity was identified as a concentrated L1 phase, i.e. a direct microemulsion of high viscosity. In Chapter 5 the phase diagram topology of ternary systems composed of water/SDS/co-surfactant at 25°C was studied, C_4PO_3 was found to have a co-surfactant behavior that is intermediate between those of 1-butanol and 1-pentanol [44]. It can also be remarked that the co-surfactant behavior follows the aqueous solubility of the co-surfactant in water at 25°C, i.e. 1-butanol(7.35%)> C_4PO_3 (3.9%)>1-pentanol(2.20%) (see Table 2.1 or Ref. [37]). The presence of a concentrated L1 phase in the pseudo ternary phase diagram obtained with C_4PO_3 (Fig. 6.1d) confirms that C_4PO_3 has a co-surfactant behavior comparable to those of 1-butanol and 1-pentanol.

The systems water / SDS / dodecane / co-surfactant, with C_4PO_3 , 1-butanol and 1-pentanol as co-surfactant, were then studied by measuring another type of pseudo-ternary phase diagram. This time the SDS/dodecane mass ratio is kept constant at 1/3 (Figs. 6.2c-e). Fig. 6.2a gives a tetrahedral representation of the quaternary system. The cut inside the tetrahedron represents the studied pseudo-ternary phase diagrams (Figs. 6.2c-e). Another representation of the upper right face of the quaternary diagram is given in Fig.6.2, where the dark line is the projection of the studied pseudo-ternary phase diagrams with water (represented by the cut in Fig. 6.2a). The monophasic area for the C_4PO_3 system (Fig. 6.2c) is less extended

²For comparison see Fig. 8.1 where some pseudo-ternary phase diagrams with 1-butanol, 1-pentanol, 1-hexanol and 1-heptanol with a SDS/n-alcohol mol ratio of 1/6.54 are reproduced from the Ref. [38].

³This point was partly discussed in Chapter 4 where the co-solvent and hydrotrope properties of C_3PO_1 was investigated.

than those obtained with 1-butanol and 1-pentanol (Figs. 6.2d,e). This means that mixtures of C_4PO_3 /(SDS/dodecane(1/3)) cannot incorporate as much water as mixtures with n -alcohols ($n = 3, 4$)/(SDS/dodecane(1/3)). The fact that C_4PO_3 is much more bulky than 1-butanol and 1-pentanol is probably a reason for this difference in water solubilization.

For a more quantitative comparison of the co-surfactant behaviors of C_4PO_3 , 1-butanol, and 1-pentanol a representation in mole of co-surfactant is required. This was done by plotting the studied pseudo-ternary phase diagrams (Figs. 6.2c-e) in a binary representation having in abscissa x the number of mole of co-surfactant per 1g of SDS/dodecane mixture and as the ordinate the water content in wt%, see Fig. 6.3. The lower ability of the C_4PO_3 /(SDS/dodecane(1/3)) systems to incorporate water in comparison to n -alcohol systems can clearly be seen here. The observed maximum water solubilization is about 45 wt% in the case of 1-butanol and 1-pentanol systems and is only about 30 wt% in the case of C_4PO_3 systems. Interestingly, the maxima in water solubilization observed for 1-pentanol and C_4PO_3 systems appear at roughly the same x value ($x = 0.01$). In this respect, 1-pentanol and C_4PO_3 show a similar co-surfactant behavior.

To go further in the characterization of the C_nPO_m as co-surfactants and in their comparisons to n -alcohols a study of the microstructures present in C_nPO_m based microemulsions would be helpful. Nevertheless this is not the main aim of the present study and our interest will now focus on the study of the temperature dependence of systems based on C_nPO_m and SDS.

6.3.2 Temperature dependence of C_nPO_m /SDS based systems

Water/ C_nPO_m /SDS systems

The temperature dependence of binary C_nPO_m /water mixtures was studied in Chapter 2 [37]. As in the case of some C_iEO_j , lower critical solution temperatures (LCSTs) were measured for C_3PO_m ($m = 1-3$), whereas C_4PO_m s ($m = 1-3$) showed only partial co-miscibility with water between 0 and 100°C, i.e. $LCST < 0^\circ C$. The increase in the number of propylene glycol groups (PO) was found to decrease the hydrophilicity, i.e. to decrease the aqueous solubility and/or the LCST value. This is in contrast to the addition of an ethylene glycol group (EO), which is well known to increase the hydrophilicity of a component [27, 28, 29].

Keeping this difference between PO and EO groups in mind, the temperature dependence of water/ C_nPO_m /SDS systems was studied. To do so the cloud point of water/ C_nPO_m mixtures, for C_3PO_2 , C_3PO_3 , C_4PO_2 and C_4PO_3 , at a mixing ratio of 50 wt% was measured as a function of SDS content (SDS wt%), see Fig. 6.4.

For all studied C_nPO_m a gradual increase in the cloud point can be observed. In Chapter 3, the influence of adding electrolytes on the cloud point C_3PO_m /water mixtures was studied [45]. Salting-in salts were also found to increase the cloud points. Nevertheless here the observed increase in the cloud point is certainly rather due to the solubilization of the C_nPO_m in SDS micelles, i.e. co-surfactant co-micellization

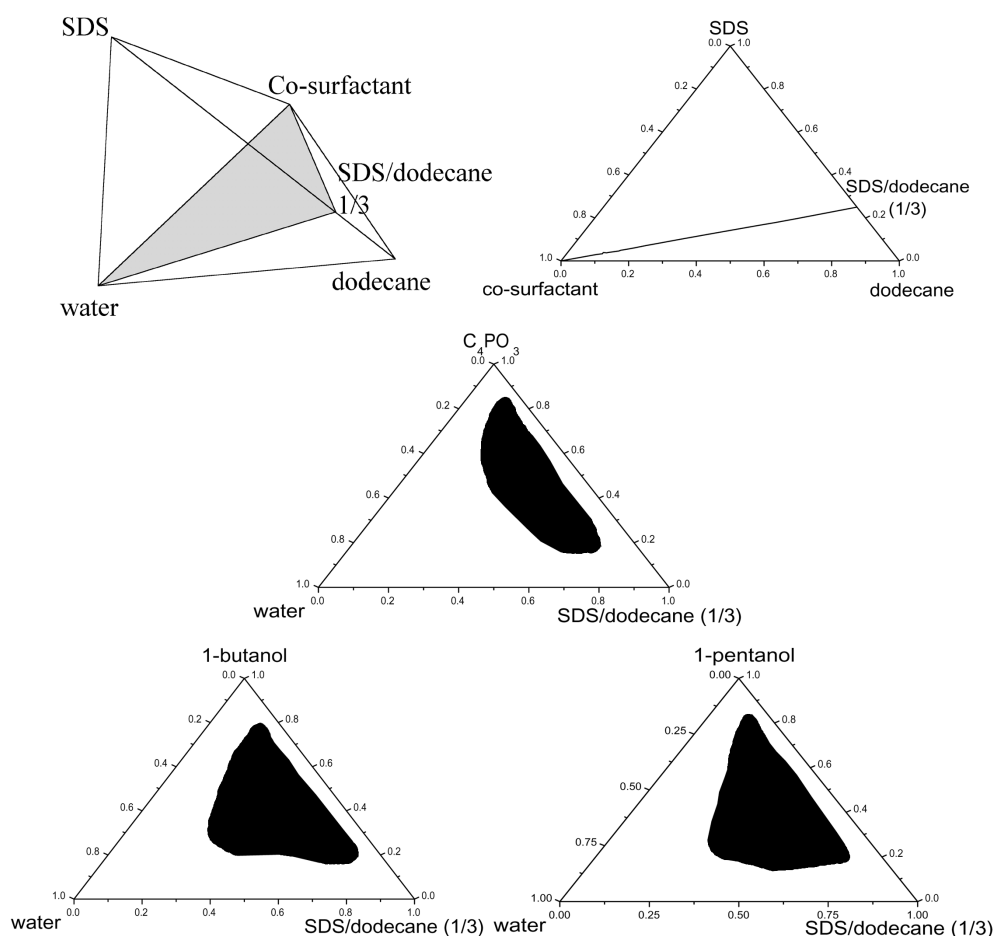


Figure 6.2: (a) Tetrahedral representation of the quaternary systems composed of water / SDS / dodecane / co-surfactant. The cut included in this tetrahedron represents the pseudo-ternary phase diagram of systems composed of water / co-surfactant / (SDS/dodecane) at a constant SDS/dodecane mass ratio of 1/3, (b) representation of the dodecane/SDS/co-surfactant ternary phase diagram, the dark line represents the projection of the studied pseudo-ternary phase diagram. (c-e) phase diagrams of water / SDS / dodecane / co-surfactant systems, with C_4PO_3 (c), 1-butanol (d) and 1-pentanol (e) as co-surfactants and at a constant SDS/dodecane mass ratio of 1/3. The dark areas represent the realms of existence of the monophasic and isotropic phases. The diagrams were determined at 25°C.

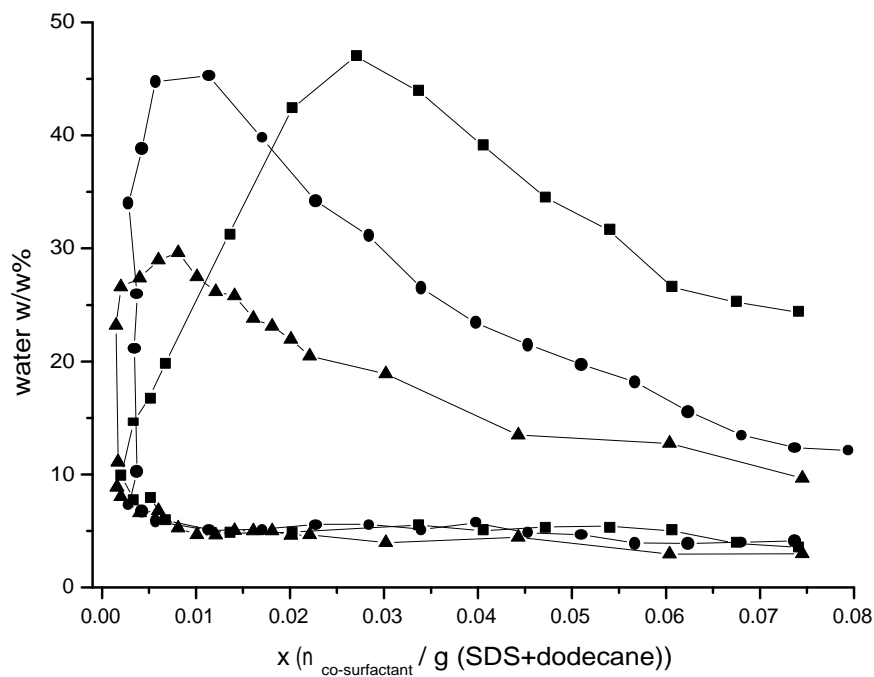


Figure 6.3: Binary representation of the monophasic areas shown in Figs. 6.2(c-e) with C_4PO_3 (▲), 1-butanol (■) and 1-pentanol (●) as co-surfactant; the abscissa and the ordinate represent respectively x , the number of mole of co-surfactant per 1g of SDS/dodecane mixture and the water solubility in wt%.

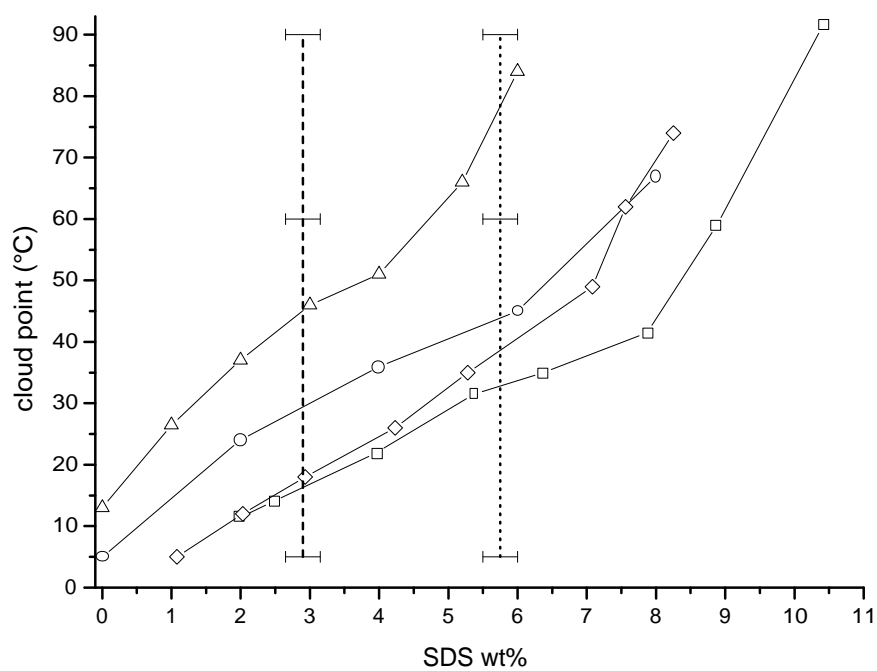


Figure 6.4: Cloud point of water/ C_nPO_m mixtures (mass ratio 1/1) as a function of SDS content in wt%: C_3PO_2 (Δ), C_3PO_3 (\bigcirc), C_4PO_2 (\diamond) and C_4PO_3 (\square). The dashed and dotted lines represent the water/*n*-alcohol (mass ratio 1/1) solubilization lines obtained with 1-butanol and 1-pentanol, respectively.

[38], than due to a salting-in solubilization process.

In Fig. 6.4 it can be observed that a decrease in the hydrophilic behavior of the C_nPO_m , i.e. an increase in n (from 3 to 4) or m (from 2 to 3), does not significantly influence the shape of the curves. The cloud points remain below 100°C up to relatively high SDS concentrations. In the case of the water/ C_4PO_3 system cloud points between 0 and 100°C can be measured even at SDS concentration as high as 10.5%. In contrast, the addition of a single chain ionic surfactant is known to increase very sharply the cloud point of a polyethoxylated surfactant [46, 47]. For instance the addition of SDS at a concentration as low as 10^{-4} mol/L ($\approx 0.003\%$!) leads to an increase of the cloud point of the Triton X-100 (iso- $C_8PhEO_{9.5}$) of 15°C.

Therefore, it is not convenient to use an ionic surfactant in order to tune the temperature dependence of the cloud points of polyethoxylated surfactants. For practical applications, e.g. for the formulation of reaction media, the system would be too sensitive to small amounts of SDS, and the amount of required nonionic surfactants would be too high. In contrast, the very moderate increase in the cloud points of the C_nPO_m /water mixtures by adding SDS gives the advantages that (1) the temperature dependence is tunable up to relatively high SDS concentrations and that (2) the cloud point can be easily adjusted to a wanted value by changing the SDS concentration.

For comparison, SDS was added to mixtures of 1-butanol / water and 1-pentanol / water at a mixing ratio of 50%. The results are indicated in Fig. 6.4 by the dashed (1-butanol) and dotted (1-pentanol) lines. The co-solubilization of 1-butanol and 1-pentanol with water appears abruptly at SDS contents of around 2.9 and 5.75 wt%. Consequently for these two systems no cloud points could have been measured.

The use of C_nPO_m as co-surfactants in water / SDS / co-surfactant ternary systems shows interesting properties: (1) in comparison with short n-alcohols used as co-surfactant, such as 1-butanol or 1-pentanol, a moderate temperature dependence is observed. (2) In comparison with polyethoxylated amphiphiles the temperature dependence is usable up to much higher SDS concentrations.

The temperature dependence of microemulsions, i.e. quaternary systems, containing C_nPO_m as co-surfactants is now investigated.

Brine/dodecane/ C_nPO_m /SDS systems

The location of the three phase microemulsion region, also called middle phase microemulsion, is a characteristic of the hydrophilic-lipophilic behavior of the surfactant or the co-surfactant/surfactant couple [48]. The surfactant and the oil being in the present study always SDS and dodecane, the location of the three phase region will serve us as a tool to characterize the co-surfactant behavior of C_3PO_2 and to compare it to the one of usual co-surfactants: 1-butanol and 1-pentanol.

To form three phase microemulsions with an ionic surfactant an electrolyte has to be added [2]. Note that electrolytes are often added to (or present in) microemulsions, e.g. to catalyze an organic reaction [18]. Thus cartographies of the three phase regions were made by changing the salt (NaCl) concentration and the co-

surfactant/surfactant molar ratio (see Section *Experimental Section*). The results are given in Figs. 6.5a,b for the systems containing C_3PO_2 , 1-butanol and 1-pentanol as co-surfactants and at 13 (Fig. 6.5a) and 69°C (Fig. 6.5b). Note that we tried to make a similar cartography using 1-hexanol as co-surfactant, but the presence of lamellar liquid crystal prevented the demixion of the polyphasic systems. Even after 6 months the thermodynamic equilibrium state was not achieved. Thus no VIII systems could be identified with 1-hexanol.

To the left and right sides of the three phase regions respectively, WI and WII systems were observed (Figs. 6.5a,b). At 13 and 69°C the three phase region obtained with 1-pentanol appears at salt concentrations lower than those observed with 1-butanol. This is not surprising because the salt concentration which is needed to reverse microemulsion systems, i.e. to come from WI to WII, is always lower when the surfactant or the co-surfactant/surfactant couple is more hydrophobic [2, 49]. The three phase regions obtained with 1-butanol and 1-pentanol appears to be only slightly affected by temperature. They shift a little towards the lower salt concentration regions when the temperature is increased from 13 to 69°C. Concerning the C_3PO_2 based microemulsions a strong influence of the temperature can be noted (Figs. 6.5a,b). Increasing the temperature from 13 to 69°C leads to an increase of the three phase region and to a shift towards the lower salt concentration regions. At 13°C the three phase region observed with C_3PO_2 is partly placed in the centre of the one of 1-butanol, whereas at 69°C it is shifted towards the three phase region of the 1-pentanol system. At this higher temperature the three phase region corresponding to the C_3PO_2 based microemulsions even covers completely the one corresponding to the 1-pentanol based microemulsions. It appears thus that the C_3PO_2 co-surfactant behavior in microemulsion systems is comparable to that of 1-butanol at low temperature and at higher temperature to that of 1-pentanol.

6.3.3 Design of an anionic monophasic temperature sensitive microemulsion using C_4PO_3 as co-surfactant

We present now an example of a specially designed anionic, temperature sensitive microemulsion using C_4PO_3 as co-surfactant. The different steps of this design are resumed in Fig. 6.6. The studied system is composed of water / dodecane / C_4PO_3 / SDS. It was shown above that useful temperature dependence in anionic microemulsions can be induced by taking C_nPO_m as co-surfactants instead of n-alcohols. The starting point is therefore the temperature dependent phase diagram of the binary water/ C_4PO_3 mixture, see Fig. 6.6a (taken from the Fig. 2.2 in Chapter 2 [37]). It shows that water and C_4PO_3 are only partially miscible between 0 and 100°C and consequently that the lower critical point is below 0°C. In Fig. 6.4 it was shown that the addition of SDS leads to a co-solubilization of water and C_4PO_3 , see also Fig. 6.6b, where the water/ C_4PO_3 mass ratio is 1/1. This co-solubilization does not appear abruptly, as it appears with mixtures of n-alcohol and water, and therefore the temperature of the cloud points, i.e of the phase transition from a one-liquid phase

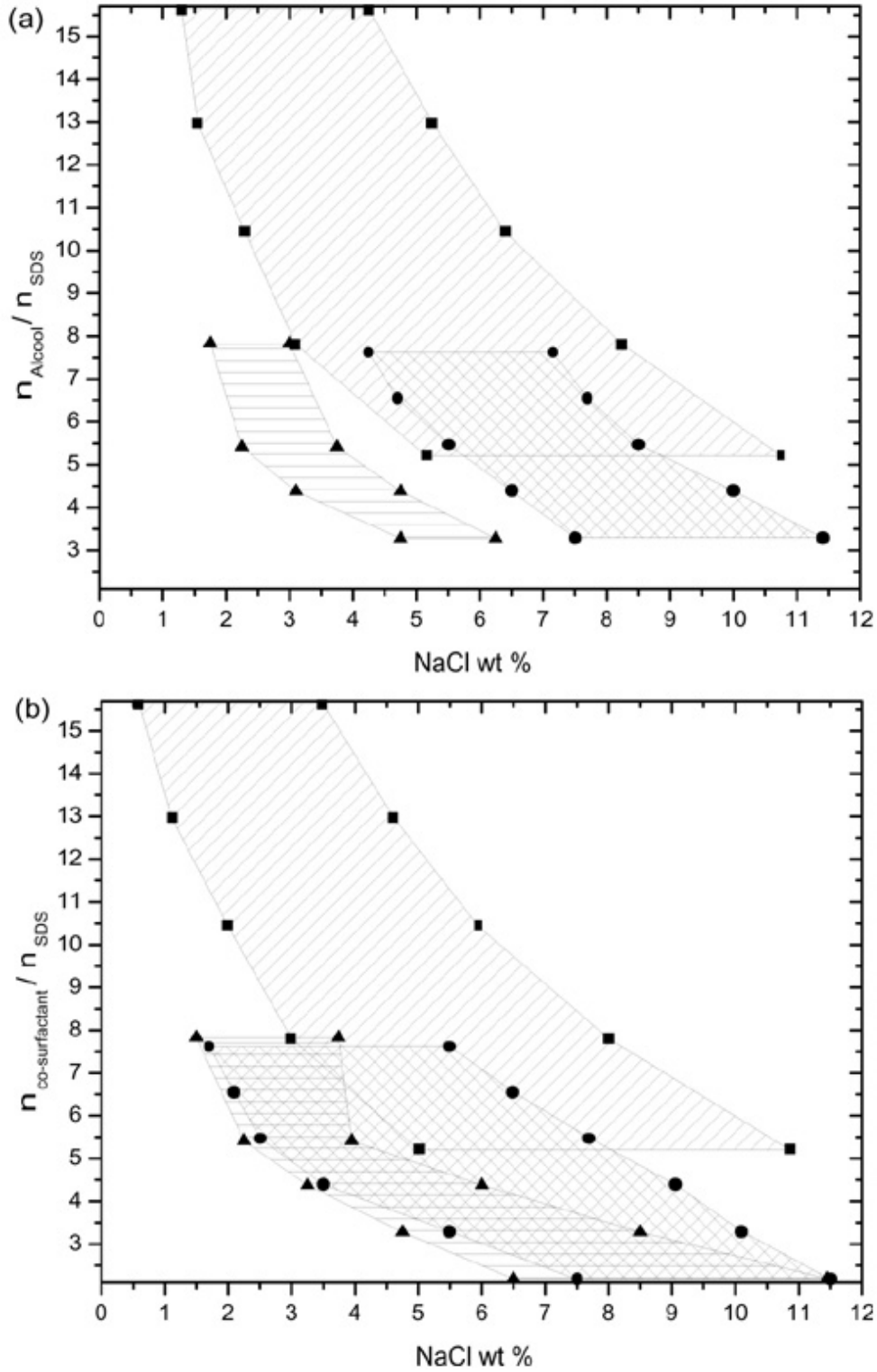


Figure 6.5: Representation of the realms of existence of the three phase region (Winsor III) of systems composed of brine (water+NaCl) / dodecane / SDS / co-surfactant (for the exact compositions see *Experimental Section*), obtained with C_3PO_2 (●), 1-butanol (■) and 1-pentanol (▲) as co-surfactant at 13°C (a) and 69°C (b).

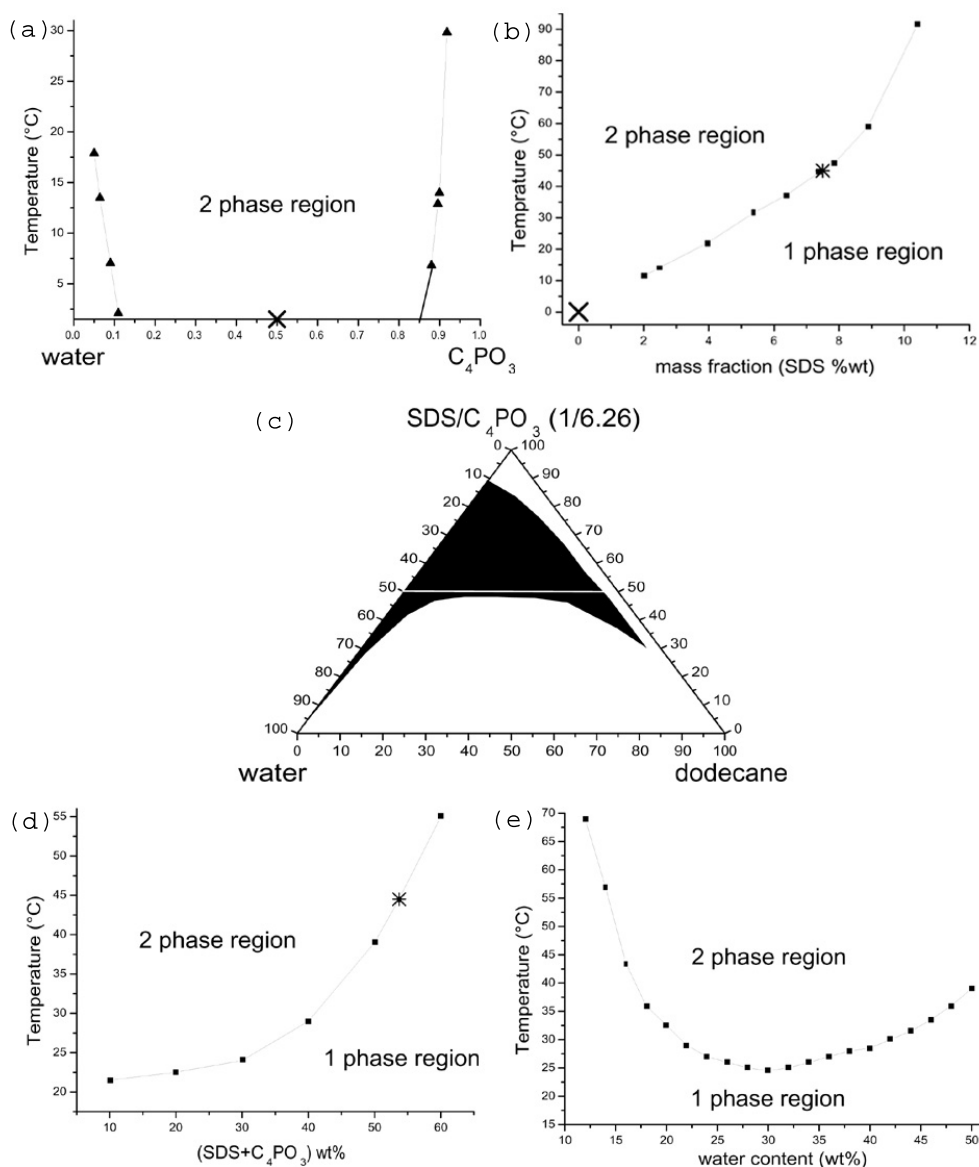


Figure 6.6: (a) Cloud points versus the C_4PO_3 mass fraction in the water / C_4PO_3 binary system, (b) cloud points of water / C_4PO_3 mixtures (mass ratio 1/1) as a function of SDS content in wt%, (c) pseudo-ternary phase diagram of the water / SDS / dodecane / C_4PO_3 system at SDS / C_4PO_3 mass ratio K_M of 1/6.26 and at 21 $^{\circ}C$. The dark area represents the realm of existence of the monophasic and isotropic phases. (d) Cloud points versus the pseudo-component (SDS+ C_4PO_3) content, at a SDS/ C_4PO_3 mass ratio of 1/6.26, in the (SDS+ C_4PO_3) / water system. This composition line corresponds to the left side of the pseudo-ternary phase diagram shown in (c). (e) Cloud points versus the water content along the white experimental path shown in (c). The cross and the asterisk marked in the diagrams represent similar compositions and temperatures.

system to a two-liquid phase system by increasing temperature, can be finally tuned. Considering for example that a chemical reaction has to be done at around 20°C, it would be interesting to induce phase transition by increasing the temperature to, say, 45°C to facilitate the recovery of the reaction product. According to Fig. 6.6b the cloud point at 45°C requires an SDS concentration of 7.5% and the resulting SDS/C₄PO₃ mass ratio is 1/6.26. At this SDS/C₄PO₃ mass ratio a pseudo ternary phase diagram was made at 21°C, see Fig. 6.6c. The typical SDS microemulsion phase diagram, as in Fig. 6.1b,c, appears. However, it is now strongly temperature dependent. To illustrate this, the cloud points were measured for this composition and the results are shown in Figs. 6.6d and e. Figure 6.6d gives the cloud points of the (pseudo-binary) (SDS+C₄PO₃)/water system as a function of the pseudo-component (SDS+C₄PO₃) weight content. These compositions correspond to the left side of the pseudo-ternary phase diagram (Fig. 6.6c). In Fig. 6.6e cloud points along the white experimental path indicated in the pseudo-ternary phase diagram (Fig. 6.6c) are indicated as a function of the water content.

So according to the special requirements of an application, the temperature dependence of classical ionic microemulsions can be adjusted by replacing the basic ionic surfactant by an appropriate amount of C₄PO₃. Note that in a recent review it was observed that for some applications, such as the formation of chemical reaction media, high surfactant levels may constitute contaminants that need to be removed, resulting in unacceptable process costs [31]. Here the studied microemulsion systems present the further advantage of having a low surfactant concentration (SDS/C₄PO₃ mass ratio of 1/6.26).

6.4 Conclusion

From the present study it can be inferred that short C_nPO_m can play the role of co-surfactants in the formation of SDS based microemulsions. Evidence appears from the observation of pseudo-ternary phase diagrams that C_nPO_m ($n = 3, 4$; $m = 1-3$) at room temperature have a co-surfactant behavior comparable to those of 1-butanol and 1-pentanol. This is true for all studied C_nPO_m except for C₃PO₁ which presents a co-surfactant behavior comparable to that of 1-propanol. Furthermore, it was demonstrated that a moderate temperature dependence in SDS based microemulsions can be induced by using C_nPO_m as co-surfactant. Such microemulsion systems present several advantages: low surfactant levels (e.g. SDS/C₄PO₃ mass ratio of 1/6.26), low toxicity and a temperature dependence which can be finely tuned and advantageously used for example in the recovery of reaction products or in extraction processes.

Bibliography

- [1] Kozo Shinoda and Hironobu. Kunieda. Conditions to produce so-called microemulsions. factors to increase the mutual solubility of oil and water by solubilizer. *Journal of Colloid and Interface Science*, 42:381–7, 1973.
- [2] Maurice Bourrel and Robert S. Schechter. *Microemulsions and Related Systems: Formulation, Solvency, and Physical Properties.*, volume 30 of *Surfactant Science Series*. Marcel Dekker, New York, 1988.
- [3] Henri L. Rosano and Marc Clausse. *Microemulsion Systems.*, volume 24 of *Surfactant Science Series*. Marcel Dekker, New York, 1987.
- [4] William M. Gelbart, Avinoam Ben-Shaul, and Didier Roux. *Micelles, Membranes, Microemulsions, and Monolayers*. 1994.
- [5] Conxita Solans and Hironobu Kunieda. *Industrial Applications of Microemulsions*, volume 66 of *Surfactant Science Series*. Marcel Dekker, New York, 1997.
- [6] D. O. Shah and R. S. Schechter. *Improved Oil Recovery by Surfactant and Polymer Flooding.*. Academic Press, New York, 1977.
- [7] Candida C. West and Jeffrey H.. Harwell. Surfactants and subsurface remediation. *Environmental Science and Technology*, 26:2324–30, 1992.
- [8] K. Stickdorn, M. J. Schwuger, and R. Schomaecker. Use of microemulsions in technical processes. *Tenside, Surfactants, Detergents*, 31:218–28, 1994.
- [9] Clarence A. Miller and Kirk H.. Raney. Solubilization-emulsification mechanisms of detergency. *Colloids and Surfaces, A: Physicochemical and Engineering Aspects*, 74:169–215, 1993.
- [10] F. Schambil and M. J.. Schwuger. Correlation between the phase behavior of ternary systems and removal of oil in the washing process. *Colloid and Polymer Science*, 265:1009–17, 1987.
- [11] D. Attwood. *Colloidal Drug Delivery Systems*, chapter 2, pages 31–71. Marcel Dekker, New York, 1994.

- [12] Stephanie R.. Dungan. *Microemulsions in foods: properties and applications.*, volume 66 of *Surfactant Science Series*, chapter 8, pages 147–174. Marcel Dekker, New York, 1997.
- [13] P. Erra, C. Solans, N. Azemar, J. L. Parra, D. Touraud, and M. Clausse. Reactivity of hair cystine in microemulsion media. *International Journal of Cosmetic Science*, 12:71–80, 1990.
- [14] J. L. Parra, J. J. Garcia Dominguez, F. Comelles, J. Sanchez, C. Solans, C. Pelejero, and F. Balaguer. Use of microemulsions as vehicles for nucleophilic reagents in cosmetic formulations. *International Journal of Cosmetic Science*, 7:127–41, 1985.
- [15] Klaus R. Wormuth, Linda A. Cadwell, and Eric W. Kaler. Solubilization of dyes in microemulsions. *Langmuir*, 6:1035–40, 1990.
- [16] Piero Savarino, Guido Viscardi, Pierluigi Quagliotto, Ermanno Barni, and Stig E.. Friberg. The role of cosurfactant and oil in the dyeing of cellulose acetate. *Journal of Dispersion Science and Technology*, 14:17–33, 1993.
- [17] Ray. von Wandruszka. *Reactions and Synthesis in Surfactant Systems*, volume 100 of *Surfactant Science Series*. Marcel Dekke,: New York, 2002.
- [18] Jean-Marie Aubry and Sabine. Bouttemy. Preparative oxidation of organic compounds in microemulsions with singlet oxygen generated chemically by the sodium molybdate/hydrogen peroxide system. *Journal of the American Chemical Society*, 119:5286–5294, 1997.
- [19] James F.. Rusling. Green synthesis via electrolysis in microemulsions. *Pure and Applied Chemistry*, 73:1895–1905, 2001.
- [20] Virinder S. Parmar, Kirpal S. Bisht, Hari N. Pati, Nawal K. Sharma, Ajay Kumar, Naresh Kumar, Sanjay Malhotra, Amarjit Singh, Ashok K. Prasad, and Jesper. Wengel. Novel biotransformations on peracylated polyphenolics by lipases immobilized in microemulsion-based gels and on carbohydrates by candida antarctica lipase. *Pure and Applied Chemistry*, 68:1309–1314, 1996.
- [21] Krister. Holmberg. Organic reactions in microemulsions. *Current Opinion in Colloid and Interface Science*, 8:187–196, 2003.
- [22] D. P. Green, J. Klier, C. J. Tucker, and M. S. Ferritto. Process for preparing chlorohydrins by the hypochlorination of alpha-olefins using a microemulsion. *US Patent 98-211284, 6051742, 19981214.*, 2000.
- [23] A.; Kopf A.; Touraud D.; Kunz W. submitted. 2005. Bauduin, P.; Renoncourt. submitted. 2005.

- [24] Slobodan Barbaric and Pier Luigi Luisi. Micellar solubilization of biopolymers in organic solvents. 5. activity and conformation of α -chymotrypsin in isooctane-aot reverse micelles. *Journal of the American Chemical Society*, 103:4239–44, 1981.
- [25] Karel Martinek, I. V. Berezin, Yu. L. Khmel'nitskii, N. L. Klyachko, and A. V. Levashov. Enzymes entrapped into reversed micelles of surfactants in organic solvents: key trends in applied enzymology (biotechnology). *Biocatalysis*, 1:9–15, 1987.
- [26] Karin Bonkhoff, Milan J. Schwuger, and Guenter. Subklew. *Use of microemulsions for the extraction of contaminated solids.*, volume 66, pages 355–374. Marcel Dekker, New York, 1997.
- [27] M. Kahlweit, E. Lessner, and R. Strey. Influence of the properties of the oil and the surfactant on the phase behavior of systems of the type water-oil-nonionic surfactant. *Journal of Physical Chemistry*, 87:5032–40, 1983.
- [28] M. Kahlweit, E. Lessner, and R. Strey. Phase behavior of ternary systems of the type water-oil-nonionic surfactant. *Colloid and Polymer Science*, 261:954–64, 1983.
- [29] Robert G. Laughlin. *The Aqueous Phase Behavior of Surfactants*. 1996.
- [30] P. Bauduin, A. Renoncourt, A. Kopf, D. Touraud, and W. Kunz. submitted. 2005.
- [31] John Klier, Christopher J. Tucker, Thomas H. Kalantar, and D. P. Green. Properties and applications of microemulsions. *Advanced Materials (Weinheim, Germany)*, 12:1751–1757, 2000.
- [32] K. Lukenheimer, H.-R. Holzbauer, and R. Hirte. Novel results on adsorption properties of definite n-alkyl oxypropylene oligomers at the air/water interface. *Progress in Colloid and Polymer Science*, 97:116–20, 1994.
- [33] A. Sokolowski and J. Chlebicki. The effect of polyoxypropylene chain length in nonionic surfactants on their adsorption at the aqueous solution-air interface. *Tenside Detergents*, 19:282–6, 1982.
- [34] Adam Sokolowski and Bogdan. Burczyk. Chemical structure and surface activity. viii. statistical evaluation of the influence of alkyl monoethers of polyoxyethylene glycols structure on their adsorption at the aqueous solution-air interface. *Journal of Colloid and Interface Science*, 94:369–79, 1983.
- [35] L. F. Komarova and Yu. N. Garber. Physical properties of dihydric alcohol ethers. *Zhurnal Organicheskoi Khimii*, 7:2507–9, 1971.

- [36] H. L. Cox, Wm. L. Nelson, and L. H. Cretcher. Reciprocal solubility of the normal propyl ethers of 1,2-propylene glycol and water. closed solubility curves. ii. *Journal of the American Chemical Society*, 49:1080–3, 1927.
- [37] A.; Kopf A.; Touraud D.; Kunz W. submitted. 2005. Bauduin, P.; Renoncourt. Temperature dependence of industrial propylene glycol alkyl ether/water mixtures. *Journal of Molecular Liquids*, 115:23–28, 2004.
- [38] Marc Clausse, L. Nicolas-Morgantini, A. Zradba, and D. Touraud. *Water-ionic surfactant-alkanol-hydrocarbon systems: influence of certain constitution and composition parameters upon the realms-of-existence and transport properties of microemulsion-type media.*, volume 24 of *Surfactant Science Series*, chapter 2, pages 15–62. Marcel Dekker, New York, 1987.
- [39] P. A.. Winsor. Hydrotropy, solubilization, and related emulsification processes. i. *Transactions of the Faraday Society*, 44:376–82, 1948.
- [40] P. A.. Winsor. Hydrotropy, solubilization, and related emulsification processes. ix. electrical conductivity and the water dispersibility of some solubilized systems. *Transactions of the Faraday Society*, 46:762–72, 1950.
- [41] P. A.. Winsor. Binary and multicomponent solutions of amphiphilic compounds. solubilization and the formation, structure, and theoretical significance of liquid crystalline solutions. *Chemical Reviews (Washington, DC, United States)*, 68:1–40, 1968.
- [42] Simon Schroedle, Richard Buchner, and Werner. Kunz. Automated apparatus for the rapid determination of liquid-liquid and solid-liquid phase transitions. *Fluid Phase Equilibria*, 216:175–182, 2004.
- [43] Marc Clausse, Abdallah Zradba, and Luc. Nicolas-Morgantini. Birefringence regions of the water/sodium dodecylsulfate/1-pentanol/n-dodecane system. *Comptes Rendus des Seances de l'Academie des Sciences, Serie 2: Mecanique-Physique, Chimie, Sciences de l'Univers, Sciences de la Terre*, 296:237–40, 1983.
- [44] P. Bauduin, A. Basse, D. Touraud, and W. Kunz. Colloids and surfaces a (accepted). 2005.
- [45] Pierre Bauduin, Laurent Wattebled, Didier Touraud, and Werner. Kunz. Hofmeister ion effects on the phase diagrams of water-propylene glycol propyl ethers. *Zeitschrift fuer Physikalische Chemie (Muenchen, Germany)*, 218:631–641, 2004.
- [46] B. S. Valaulikar and C. Manohar. The mechanism of clouding in triton x-100: the effect of additives. *Journal of Colloid and Interface Science*, 108:403–6, 1985.

- [47] Alireza Salehi Sadaghiania and Ali. Khan. Clouding of a nonionic surfactant: the effect of added surfactants on the cloud point. *Journal of Colloid and Interface Science*, 144:191–200, 1991.
- [48] Hironobu Kunieda and Conxita. Solans. *How to prepare microemulsions: temperature-insensitive microemulsions.*, volume 66 of *Surfactant Science Series*, chapter 2, pages 21–45. Marcel Dekker, New York, 1997.
- [49] J. L. Salager, N. Marquez, R. E. Anton, A. Graciaa, and J. Lachaise. Retrograde transition in the phase behavior of surfactant-oil-water systems produced by an alcohol scan. *Langmuir*, 11:37–41, 1995.

Part III

Enzymatic activity

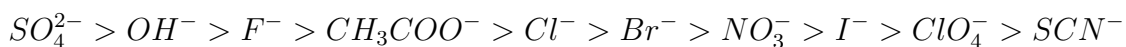
7 Hofmeister Specific-Ion Effects on Enzyme Activity and Buffer pH: Horseradish Peroxidase in Citrate Buffer

Abstract

Salt addition to enzymes in buffer induces always the problem of the respective influences of electrostatic interactions and anion specificity on buffer pH and enzyme kinetics. In the present work the influence of some sodium salts (Na_2SO_4 , NaCl , NaBr and NaNO_3) on the pH of a citrate buffer ($c = 0.025 \text{ M}$), and on the catalytic constants of Horseradish Peroxidase (HRP) is studied. First the pH changes due to the presence of salts in the buffer are examined, and second, catalytic constants K_{mABTS} , $V_{maxABTS}$ and $V_{maxABTS} / K_{mABTS}$, are studied as a function of pH in buffer with and without added salt, at various salt concentrations and different pH values due to the salt additions. With a simple electrostatic model, it is possible to show that the glass electrode yields reasonable pH values even in the presence of fairly high 1:1 salt concentrations. For the catalytic efficiency $V_{maxABTS} / K_{mABTS}$ a Hofmeister series is found with opposite deviations from the pure pH effect for salting-in and salting-out ions over a large range of salt concentrations. This usual Hofmeister series is a consequence of three, for the moment inseparable salt concentration and specific ion induced phenomena: global bulk effects, local active site effects and surface effects.

7.1 Introduction

The salt effects on enzyme kinetics and buffer are usually discussed in terms of electrostatic forces and correlated with the ionic strength of the buffer solutions [1]. However, there can be specific ion effects that cannot be explained neither by Coulombic interactions only nor by a specific chemical interaction between one chemical group on the enzyme and the ion. Such effects follow in general the so-called Hofmeister series, especially for anions. In this series the anions are classified according to their salting-out strength as follows:



Chloride usually represents a borderline case between salting-out (left-side) and salting-in (right-side). This series was discovered more than a hundred years ago for the precipitation of proteins [2]. It also seems to hold for enzymatic activities [3, 4, 5, 6, 7, 8]. The problem of the respective influences of electrostatic and anion specificity on buffer and enzyme kinetic is set. Sometimes the effect on pH buffer is taken into account [8]. Mostly, it is simply ignored so that the interpretation is at best dubious [3, 4, 7, 8]. But here another question arises [9]: does the pH electrode still indicate the bulk pH value at high salt concentrations? In order to bring more light into the above mentioned facts, the influence of four sodium salts (Na_2SO_4 , NaCl , NaBr and NaNO_3) on the pH of a citrate buffer ($c = 0.025\text{M}$), and on the catalytic constants of Horseradish Peroxidase (HRP) is studied for the classical enzymatically catalyzed oxidation reaction of 2,2'-azino-bis(3-ethylbenzothiazoline-6-sulfonic acid) diammonium salt (ABTS) by hydrogen peroxide. Although only four anions could be tested in this study, the results are supposed to reflect at least the trend of the Hofmeister series. First we determine in how far the influence of the ions on the measured pH is simply a consequence of the ionic strength in a citrate buffer ($c = 0.025\text{M}$), or if specific ion effects on the pH electrode must also be taken into account. To answer this question we will use a simple electrostatic model to estimate the proton concentration in the buffer in the presence of salts. Second, we examine if buffer pH modifications and electrostatic effects are sufficient to explain the variations of enzymatic constants. To do so we determine the kinetic constants K_{mABTS} and $V_{maxABTS}$ of the oxidation of ABTS (see section 7.2.2) at different pH values and with different salt at various salt concentrations. We assume that the activity of the substrate ABTS is not changed through the addition of the salts studied. Indeed, ABTS contains ammonium counter ions, but according to the ion pair dissociation constants of $(\text{NH}_4)_2\text{SO}_4$ and Na_2SO_4 , respectively 0.35 and 0.5 [10], the NH_4^+ ions are more strongly bound to sulfate than Na^+ , thus no replacement of NH_4^+ by Na^+ is supposed to occur. We also neglect any salt and pH effects on the H_2O_2 specific site of the enzyme and consider the two sites for H_2O_2 and ABTS as being completely independent. Then of course, all the determined affinity constants are only apparent ones. We are aware that the kinetic constants may be influenced by salt effects on the other catalytic site. HRP is a complex enzyme. Nevertheless, we stress that a FTIR study has shown that the active site retains the same conformation between $\text{pH} = 4$ and 7 [11]. All the results of the kinetics will be discussed with respect to the well-known Hofmeister series.

7.2 Materials and Methods

7.2.1 Materials

Purified water is taken from a Millipore Milli-Q system with an electrical conductivity less than 10^{-6} S.m^{-1} . The buffer contains citric acid monohydrate (purity $> 99.5\%$, Acros, concentration $c = 0.009 \text{ M}$) and citric acid trisodium salt dihy-

drate (purity > 99%, Acros, concentration $c = 0.016$ M), pH = 5.0. The different salts: Na_2SO_4 , NaBr, NaNO_3 and NaCl are purchased from Merck (purity > 99%). The enzyme is Peroxidase Type VI from horseradish (Sigma, HRP). The substrates chosen are hydrogen peroxide (Merck, 30% w/w medical, extra pure) and 2,2'-azino-bis(3-ethylbenzothiazoline-6-sulfonic acid) diammonium salt (Fluka, ABTS, purity > 99%).

7.2.2 Determination of the ABTS kinetic constants

The reaction mixtures are prepared by the addition of 10 mL of a ABTS solution at six different concentrations from 12 to 580 mM ABTS to 2.9 mL of the buffer solution with or without salt. Then 10 mL of a solution containing 26.2 mM H_2O_2 and finally 10 mL of a solution containing HRP (31.25 mg/L) are added. All the solutions are prepared using the citrate buffer at a precisely adjusted pH. The final addition of HRP initiates the enzymatic reaction. The kinetics of ABTS oxidation is studied spectroscopically at a constant temperature of $25 \pm 0.1^\circ\text{C}$ using a Varian Cary 3E spectrometer. The progress of the reaction is estimated from the absorption, i.e. optical density (OD), at 414 nm of the oxidized form of ABTS, which is detected during the first 4 min after the addition of HRP. The initial velocity, V in $\text{mol}\cdot\text{L}^{-1}\text{s}^{-1}$, of the enzymatic reaction is inferred from the slope of the absorption intensity versus time in seconds. This is linear at least during the first few minutes. For each of the different reaction compositions, at least three identical samples are prepared and the reaction velocities of these samples are measured independently at $25.0 \pm 0.1^\circ\text{C}$ to check the reproducibility of the results obtained. The error in the initial velocity is about 5%. A Lineweaver-Burk analysis [12] is used. The reaction follows always perfectly the Michaelis-Menton model and correct determinations of K_{mABTS} and $V_{maxABTS}$ are therefore possible. The precision of the kinetic constants is evaluated from five measures in pure buffer (pH = 5.0) without salt. The precision is found to be: $K_{mABTS} \pm 0.026 \text{ mol}\cdot\text{L}^{-1}$ and $V_{maxABTS} \pm 0.0027 \text{ mol}\cdot\text{L}^{-1}\text{s}^{-1}$.

7.3 Results

7.3.1 pH variation of a 0.025M citrate buffer with salt concentration

Figure 7.1 shows how the pH, measured with the help of a glass electrode, is influenced by the presence of salts. All added salts lead to a decrease in measured pH values. The higher the salt concentration the more pronounced is this effect. Furthermore, the 1-1-electrolytes do not show significant anion specificity, whereas the pH values are less influenced by sodium sulfate at higher ionic strengths.

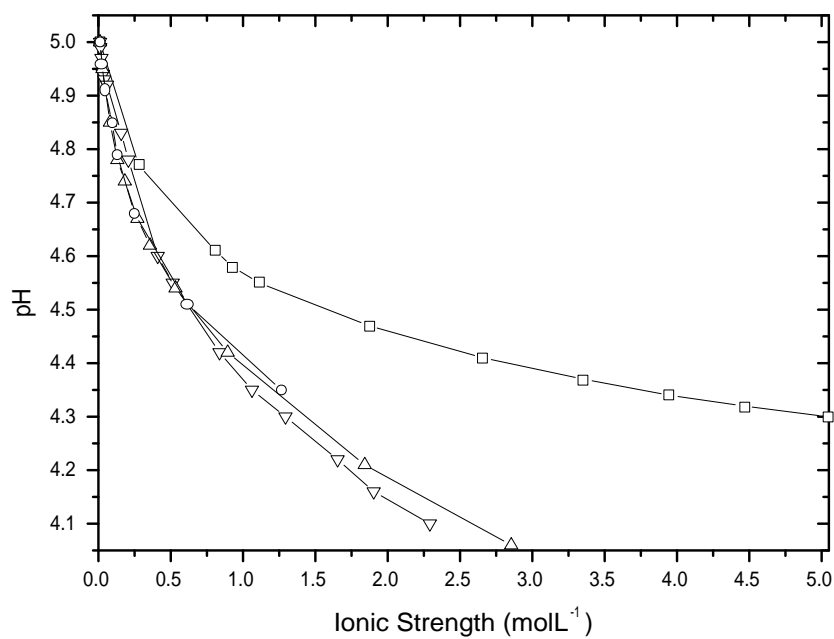


Figure 7.1: pH vs. ionic strength of a citrate buffer solution ($c = 0.025\text{M}$) containing different sodium salts: SO_4^{2-} (\square), Cl^- (\triangle), NO_3^- (\circ) and Br^- (∇).

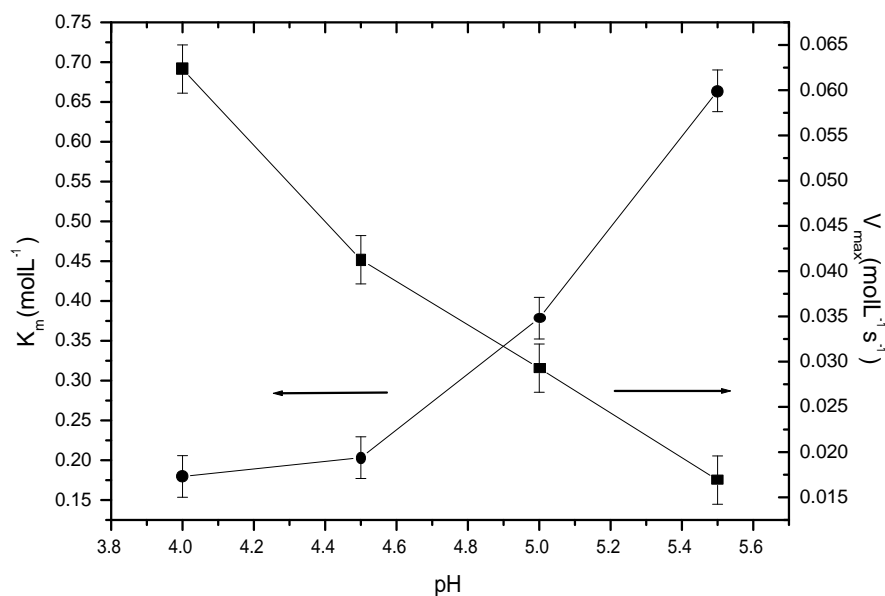


Figure 7.2: $V_{maxABTS}$ and K_{mABTS} vs. pH of a citrate buffer ($c = 0.025M$), the measured pH was adjusted by the addition of small amounts of NaOH or HCl.

7.3.2 K_{mABTS} and $V_{maxABTS}$ as a function of pH

K_{mABTS} and $V_{maxABTS}$ are determined at 4 different pH values between 4 and 5.5, see Fig. 7.2. The measured pH is adjusted by the addition of small amounts of NaOH or HCl. The K_{mABTS} and $V_{maxABTS}$ curves show an opposite trend as a function of pH. Whereas $V_{maxABTS}$ decreases with increasing pH, K_{mABTS} decreases with higher proton activity.

7.3.3 K_{mABTS} and $V_{maxABTS}$ as a function of salt concentration

We determine the K_{mABTS} and $V_{maxABTS}$ for two different concentrations of each salt. For the 1:1 salts, the lower concentration is chosen, because it should essentially reflect electrostatic interactions, whereas at the higher concentration, ion-specific effects should appear. In the case of the sodium sulfate solutions, the enzymatic reactivities are measured at the same salt concentrations, but at higher ionic strengths, because of the double charged anion. The results are illustrated in Figs. 7.3 and 7.4. For some salts the K_{mABTS} value increases at the lower salt concentration whereas it decreases for all studied salts at the higher salt concentration. No relation with the Hofmeister series is found. For all salts the $V_{maxABTS}$ values increase at the lower salt concentration and decrease at high salt concentration. Again, the results

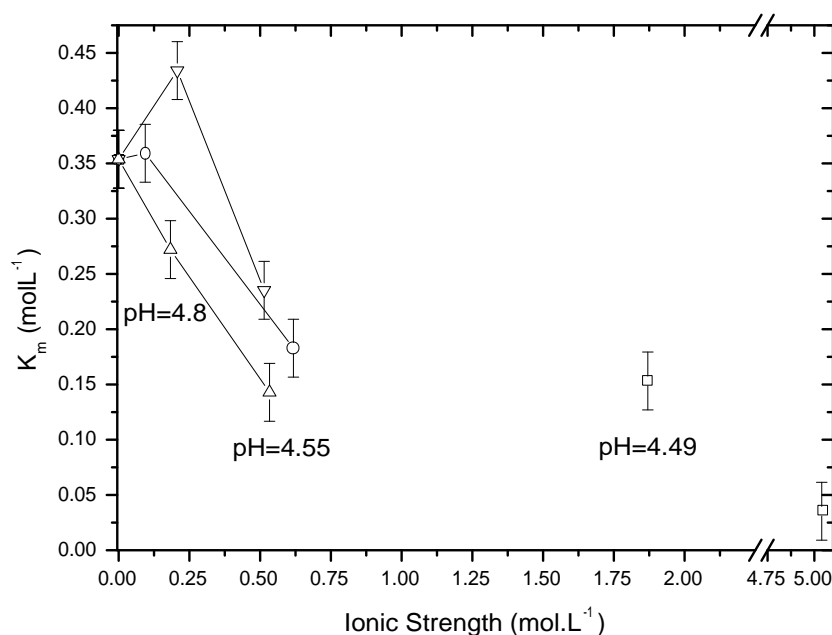


Figure 7.3: K_{mABTS} vs. ionic strength of a citrate buffer solution ($c = 0.025\text{M}$) containing different sodium salts: SO_4^{2-} (\square), Cl^- (\triangle), NO_3^- (\circ) and Br^- (∇).

do not follow the Hofmeister series.

7.4 Discussion

7.4.1 Can we trust our pH values?

We calculate the ionic-strength dependence of the pH value with the help of an extended Debye-Hückel model. The details of this calculation are given in the appendix. An aqueous solution of 0.025 molL^{-1} citric acid and 0.041 molL^{-1} sodium hydroxide is found to have a pH value of about 5.00. If one adds an inert salt to change the total ionic strength to 0.1 molL^{-1} , the pH-value calculated with the help of this model is 4.68. An ionic strength of 0.5 molL^{-1} changes the pH to a value of 4.53. An alternative estimation of the pH in this particular buffer system, also given in the appendix, give pH values of 4.65 and 4.47 for a total ionic strength of 0.1 molL^{-1} and 0.5 molL^{-1} , respectively, in good agreement with the values obtained with the help of the extended Debye-Hückel model. We can compare now the calculated values to the experimental ones. According to Fig. 7.1, the theoretical pH values for $= 0.1\text{ molL}^{-1}$ and $= 0.5\text{ molL}^{-1}$ are slightly smaller than the experimental

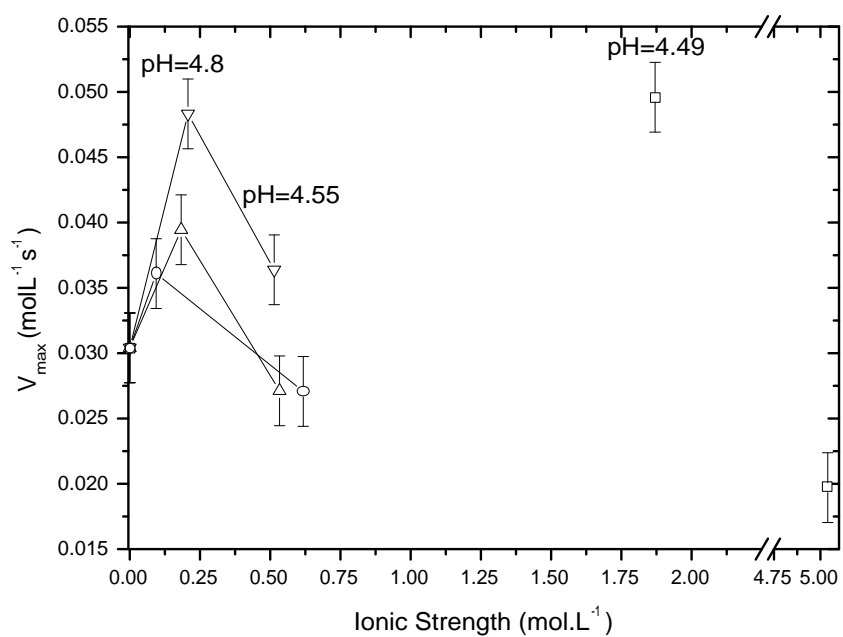


Figure 7.4: $V_{\max ABTS}$ vs. ionic strength of a citrate buffer solution ($c = 0.025\text{M}$) containing different sodium salts: SO_4^{2-} (□), Cl^- (△), NO_3^- (○) and Br^- (▽).

ones. This means that an even more pronounced effect on the pH could be expected from the preceding calculations. If there is a certain specific ion effect, it attenuates the pH shift due to the presence of ions rather than being at the origin of this shift. Of course, keeping in mind the simplicity of the model and all the approximations, no quantitative conclusion can be drawn. But at least at relatively low ionic strength the overall pH trend as a function of salt concentration is satisfactorily described by assuming only electrostatic interactions in the case of this citrate buffer system.

7.4.2 The catalytic constants K_{mABTS} and $V_{maxABTS}$

It is commonly accepted that the evolution of K_{mABTS} reflects structural changes at the active site of the enzyme and thus the modified affinity of the substrate, here ABTS, for the enzyme, here HRP. The higher the K_{mABTS} values, the lower is the affinity. According to Fig. 7.2, a negative pH shift results in decreasing K_{mABTS} values and consequently increasing substrate affinities for the enzyme. However, at the lower salt concentrations, an increase of K_{mABTS} is detected for NaBr and NaNO₃, c.f. Fig.7.3. These are the softest, most salting-in ions, that are included in our study. Specific adsorption or ion pair adsorption at the active site of the enzyme due to dispersion forces could be the reason for this finding, c.f. [13, 14, 15, 16]. Such an adsorption could lead either to a competition of ions and ABTS for the active site or to a denaturation of the latter. Na₂SO₄ and, to a less extent the “Hofmeister neutral” NaCl salt, increase the affinity with increasing salt concentrations. The extremely low K_{mABTS} value in the presence of a high Na₂SO₄ concentration is possibly the consequence of a strong reinforcement of the active site structure due to the strong water “structure-making” property of the highly charged sulfate ions. The velocity constant changes at the lower salt concentration are in agreement with the velocity constant changes due to pure pH variations but become smaller at the higher concentration, c.f. Fig. 7.4. Note, however, that the V_{max} values do reflect specific ion effects, even at low salt concentrations. These effects do not follow the standard Hofmeister series.

7.4.3 The catalytic efficiency ($V_{maxABTS} / K_{mABTS}$)

The catalytic efficiency $V_{maxABTS} / K_{mABTS}$ is supposed in standard conditions to yield the most complete information about the substrate-enzyme interactions, because it reflects both the local and the global effects in the buffer solution. In Figs. 7.5 and 7.6 the catalytic efficiencies are given as a function of ionic strength (and of salt concentration in molL⁻¹ in the insert of Fig. 7.5) and pH, respectively. In Fig. 7.6 the usual Hofmeister series clearly appears and also in the insert of Fig. 7.5. As can be seen from Fig. 7.5, all salts increase $V_{maxABTS} / K_{mABTS}$ and the higher the salt concentration the bigger the increase. Compared to the influence of the pH, c.f. Fig. 7.6, salting-in ions reduce the catalytic efficiency (NaBr and NaNO₃), the strongly salting-out salt Na₂SO₄ strongly increases further the efficiency, and the “Hofmeister neutral” NaCl indeed is close to the effect of pH

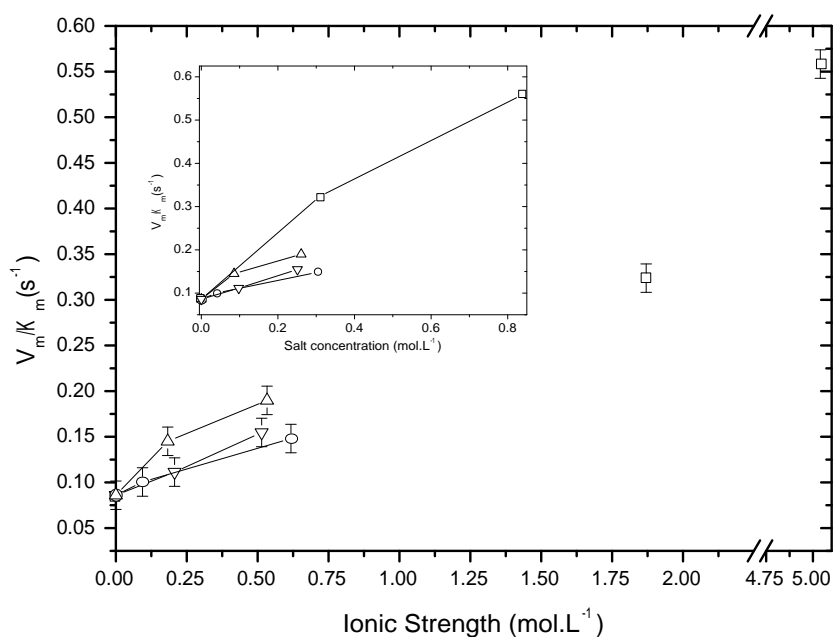


Figure 7.5: Catalytic efficiency $V_{maxABTS} / K_{mABTS}$ vs. ionic strength (and vs. salt molar concentration in the insert figure) of a citrate buffer solution ($c = 0.025\text{M}$) containing different sodium salts: SO_4^{2-} (□), Cl^- (△), NO_3^- (○) and Br^- (▽).

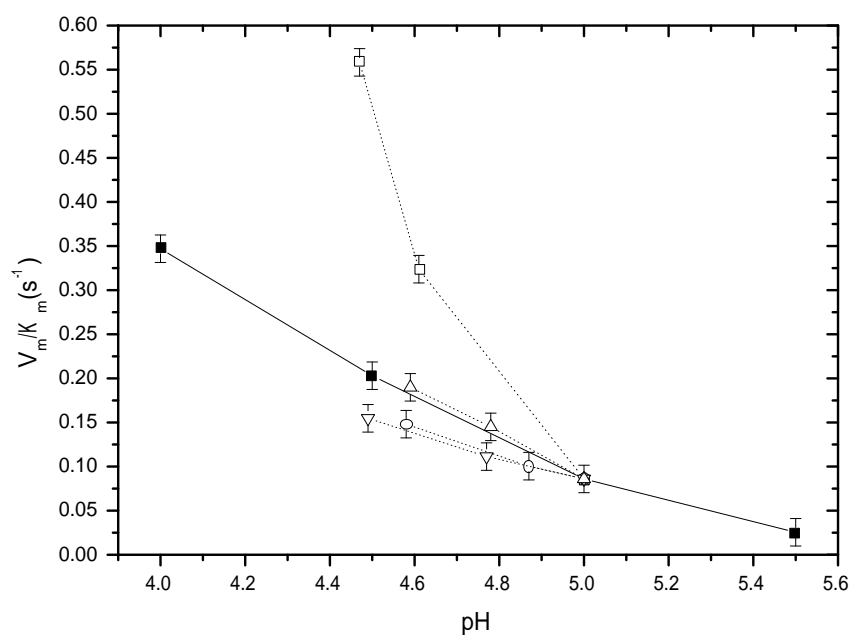


Figure 7.6: Catalytic efficiency $V_{maxABTS} / K_{mABTS}$ vs. pH of a citrate buffer solution ($c = 0.025\text{M}$) without additional salts (solid line) and containing different sodium salts (dotted lines): SO_4^{2-} (\square), Cl^- (\triangle), NO_3^- (\circ) and Br^- (∇).

changes. Note, however, that this “neutral” effect of NaCl is the consequence of a balance between pronounced K_{mABTS} and $V_{maxABTS}$ effects, whether there may be a specific ion effect (at 0.5 molL^{-1}) or only an electrostatic effect (at 0.25 molL^{-1}).

So, according to our analysis concerning K_{mABTS} , $V_{maxABTS}$ and $V_{maxABTS} / K_{mABTS}$, it appears that the observed Hofmeister series for the catalytic efficiency $V_{maxABTS} / K_{mABTS}$ is due to compensation phenomena on the active site and the surface of HRP. Of course, only four anions were considered and therefore care must be taken when an extrapolation to other ions is intended.

7.5 Conclusion

The catalytic activity of HRP in the oxidation process of ABTS is found to depend on the nature and the amount of added salt. The influence of the salt on the buffer pH can clearly be identified as one of the major reasons. This effect should not be overlooked in any discussion of salt effects on enzymatic activities. Most of biological or biotechnological studies involving enzymes disregard such considerations. The affinity of the substrate to the enzyme depends on the nature of the ions even for salt concentrations where the changes of pH can be attributed to electrostatic interactions only. The resulting catalytic efficiency $V_{maxABTS} / K_{mABTS}$ follows the usual Hofmeister series, its existence seems to be the result of a balance between the changes in $V_{maxABTS}$ and K_{mABTS} . This usual Hofmeister series is then a consequence of global bulk effects, of local active site effects and of surface effects. We can only speculate about the origin of these effects. Beyond electrostatics, changes in hydration water, induced dipoles and dispersion forces [13, 14, 15, 16, 17, 18] are certainly involved. More precise results may be obtained by separating salt effects at the two substrate sites of the HRP, but this work is outside the scope of the present study. Nevertheless, the present work shows that a simple electrostatic model, as also used in [1], can yield universal trends, but only at ionic strengths lower than $0.1\text{--}0.3 \text{ molL}^{-1}$ or so. Note that the ionic strength of physiological serum is about 0.15 molL^{-1} , but that the ionic strength in ion channels can be of several molL^{-1} .

7.6 Appendix

Citric acid, H_3A , dissociates according to the following equations



where the thermodynamic equilibrium constants of these reactions are

$$K_1 = \frac{[H^+][H_2A^-]}{[H_3A]} \cdot F_1 \quad (7.2a)$$

$$K_2 = \frac{[H^+][HA^{2-}]}{[H_2A^-]} \cdot F_2 \quad (7.2b)$$

$$K_3 = \frac{[H^+][A^{3-}]}{[HA^{2-}]} \cdot F_3 \quad (7.2c)$$

while the activity coefficient quotients are defined as

$$F_1 = \frac{y_{H^+}y_{H_2A^-}}{y_{H_3A}} ; \quad F_2 = \frac{y_{H^+}y_{HA^{2-}}}{y_{H_2A^-}} ; \quad F_3 = \frac{y_{H^+}y_{A^{3-}}}{y_{HA^{2-}}} \quad (7.3)$$

and the analytical concentration of the citric acid a is given by

$$a = [H_3A] + [H_2A^-] + [HA^{2-}] + [A^{3-}] \quad (7.4)$$

Solving this set of equations yields for the concentrations of the acid anions

$$[H_2A^-] = a \frac{[H^+]^2 K_1 F_2 F_3}{[H^+]^3 F_1 F_2 F_3 + [H^+]^2 K_1 F_2 F_3 + [H^+] K_1 K_2 F_3 + K_1 K_2 K_3} \quad (7.5a)$$

$$[HA^{2-}] = a \frac{[H^+] K_1 K_2 F_3}{[H^+]^3 F_1 F_2 F_3 + [H^+]^2 K_1 F_2 F_3 + [H^+] K_1 K_2 F_3 + K_1 K_2 K_3} \quad (7.5b)$$

$$[A^{3-}] = a \frac{K_1 K_2 K_3}{[H^+]^3 F_1 F_2 F_3 + [H^+]^2 K_1 F_2 F_3 + [H^+] K_1 K_2 F_3 + K_1 K_2 K_3} \quad (7.5c)$$

For an aqueous solution of citric acid and sodium hydroxide with analytical concentration b the condition of electrical neutrality leads to

$$[H^+] + b = \frac{K_w}{[H^+]} + [H_2A^-] + 2[HA^{2-}] + 3[A^{3-}] \quad (7.6)$$

where K_w is the ionization constant of water.

Inserting equations (5) in equation (6) yields a relationship between the proton concentration $[H^+]$, the equilibrium constants K_1 , K_2 , K_3 , the activity coefficients y_i of the different species i and the analytical concentrations of citric acid and sodium hydroxide a and b .

The activity coefficient of the undissociated citric acids, y_{H_3A} , is assumed to be unity, whereas the activity coefficients of individual ions, y_i , are approximated by the extended Debye and Hückel equation [19], which yields for aqueous solutions at 25°C [20]

$$\log y_i = - \frac{z_i^2 0.5115 \sqrt{I}}{1 + a_i 0.3291 \cdot 10^{-10} \sqrt{I}} \quad (7.7)$$

where z_i are the charges of ions, a_i are the ionic size parameters and I is the ionic strength. In accordance with the recommendations of Apelblat [21] we adopt an averaged ion size parameter of $a_i = 6.25 \cdot 10^{-10}$ m for our calculations.

We estimated the ionic-strength dependence of the pH-value in the following way. An aqueous solution of 0.025 molL^{-1} citric acid and 0.041 molL^{-1} sodium hydroxide shows a pH-value of about 5.00. If we add an inert salt to change the ionic strength to 0.1 molL^{-1} the pH-value calculated with the help of equations (5), (6) and (7) is 4.68. An ionic strength of 0.5 molL^{-1} changes the pH to a value of 4.53.

In a recent research Bénézech et.al. [22] determined the influence of added sodium chloride on the dissociation quotients, $K_i^{(c)}$, of citric acid.

$$K_1^{(c)} = \frac{[H^+][H_2A^-]}{[H_3A]} \quad (7.8a)$$

$$K_2^{(c)} = \frac{[H^+][HA^{2-}]}{[H_2A^-]} \quad (7.8b)$$

$$K_3^{(c)} = \frac{[H^+][A^{3-}]}{[HA^{2-}]} \quad (7.8c)$$

Using these dissociation quotients instead of equations (2) we get the following set of equations for the concentrations of the citric acid anions

$$[H_2A^-] = a \frac{[H^+]^2 K_1^{(c)}}{[H^+]^3 + [H^+]^2 K_1^{(c)} + [H^+] K_1^{(c)} K_2^{(c)} + K_1^{(c)} K_2^{(c)} K_3^{(c)}} \quad (7.9a)$$

$$[HA^{2-}] = a \frac{[H^+] K_1^{(c)} K_2^{(c)}}{[H^+]^3 + [H^+]^2 K_1^{(c)} + [H^+] K_1^{(c)} K_2^{(c)} + K_1^{(c)} K_2^{(c)} K_3^{(c)}} \quad (7.9b)$$

$$[A^{3-}] = a \frac{K_1^{(c)} K_2^{(c)} K_3^{(c)}}{[H^+]^3 + [H^+]^2 K_1^{(c)} + [H^+] K_1^{(c)} K_2^{(c)} + K_1^{(c)} K_2^{(c)} K_3^{(c)}} \quad (7.9c)$$

Together with equation (6) the equilibrium proton concentration can be calculated from the dissociation quotients, $K_i^{(c)}$, at different ionic strength from ref. [22].

If one adds sodium chloride to an aqueous solution of 0.025 molL^{-1} citric acid and 0.041 molL^{-1} sodium hydroxide (pH=5.00) to increase the ionic strength to $I=0.1 \text{ mol/dm}^3$ the pH is calculated to be 4.65 and at an ionic strength of $I=0.5 \text{ molL}^{-1}$ the pH is 4.47. This result is in good agreement with the calculations using the extended Debye-Hückel equation (pH=4.68 and pH=4.53). It shows, that at least in the low concentration range, the decrease of the pH-value with increasing ionic strength can well be described using appropriate expressions for the activity coefficients of the individual ions.

Bibliography

- [1] C. Park and R.T. Raines. Quantitative analysis of the effect of salt concentration on enzymatic catalysis. *Journal of the American Chemical Society*, 123:11472–9, 2001.
- [2] F. Hofmeister. *Arch. Exp. Pathol. Pharmacol.*, 24:247–260, 1888.
- [3] Peter Buenning and James F. Riordan. Sulfate potentiation of the chloride activation of angiotensin converting enzyme. *Biochemistry*, 26:3374–7, 1987.
- [4] E. M. Wondrak, J. M. Louis, and S. Oroszlan. The effect of salt on the michaelis menten constant of the hiv-1 protease correlates with the hofmeister series. *FEBS letters*, 280:344–6, 1991.
- [5] J. S. Nishimura, R. Narayanasami, R. T. Miller, L. J. Roman, S. Panda, and B. S. Masters. The stimulatory effects of hofmeister ions on the activities of neuronal nitric-oxide synthase. apparent substrate inhibition by l-arginine is overcome in the presence of protein-destabilizing agents. *Journal of biological chemistry*, 274:5399–406, 1999.
- [6] H.-K. Kim, E. Tuite, B. Norden, and B. W.. Ninham. Co-ion dependence of dna nuclease activity suggests hydrophobic cavitation as a potential source of activation energy. *European Physical Journal E: Soft Matter*, 4:411–417, 2001.
- [7] A. Ruggia, J. L. Gelpi, M. Busquets, M. Cascante, and A. Cortes. Effect of several anions on the activity of mitochondrial malate dehydrogenase from pig heart. *Journal of Molecular Catalysis B: Enzymatic*, 11:743–755, 2001.
- [8] Gabriel Zoldak, Mathias Sprinzl, and Erik. Sedlak. Modulation of activity of nadh oxidase from thermus thermophilus through change in flexibility in the enzyme active site induced by hofmeister series anions. *European Journal of Biochemistry*, 271:48–57, 2004.
- [9] Mathias Bostroem, Vince S. J. Craig, Ryanna Albion, David R. M. Williams, and Barry W. Ninham. Hofmeister effects in ph measurements: Role of added salt and co ions. *Journal of Physical Chemistry B*, 107:2875–2878, 2003.
- [10] W. L. Masterton and L. H. Berka. Evaluation of ion-pair dissociation constants from osmotic coefficients. *Journal of Physical Chemistry*, 70:1924–9, 1966.

- [11] Ines E. Holzbaur, Ann M. English, and Ashraf A. Ismail. Infrared spectra of carbonyl horseradish peroxidase and its substrate complexes: Characterization of ph-dependent conformers. *Journal of the American Chemical Society*, 118:3354–3359, 1996.
- [12] Hans Lineweaver and Dean. Burk. Determination of enzyme dissociation constants. *Journal of the American Chemical Society*, 56:658–66, 1934.
- [13] M. Bostroem, D. R. M. Williams, and B. W. Ninham. Specific ion effects: Why the properties of lysozyme in salt solutions follow a hofmeister series. *Biophysical Journal*, 85:686–694, 2003.
- [14] M. Bostroem, D. R. M. Williams, and B. W. Ninham. Specific ion effects: The role of co-ions in biology. *Europhysics Letters*, 63:610–615, 2003.
- [15] Mathias Bostroem, David R. M. Williams, and Barry W. Ninham. Influence of hofmeister effects on surface ph and binding of peptides to membranes. *Langmuir*, 18:8609–8615, 2002.
- [16] Barry W. Ninham and Vassili. Yaminsky. Ion binding and ion specificity: The hofmeister effect and onsager and lifshitz theories. *Langmuir*, 13:2097–2108, 1997.
- [17] W. Kunz, B. W. Ninham, and LoNostro P. *Current Opinion in Colloid and Interface Science*, 9:1–18, 2004.
- [18] W. Kunz, L. Belloni, O. Bernard, and B. W. Ninham. *Journal of Physical Chemistry*, 108(7):2398–2404, 2004.
- [19] R. A. Robinson and R. H. Stokes. *Electrolyte Solutions*. 2nd ed. Butterworths, London, 1959.
- [20] Herbert S. Harned and Benton B. Owen. *The Physical Chemistry of Electrolytic Solutions*. 3rd ed. Am. Chem. Soc. Monograph No. 137. Reinhold Publ. Corp., New York., 1958.
- [21] Alexander Apelblat and Josef. Barthel. Conductance studies on aqueous citric acid. *Zeitschrift fuer Naturforschung, A: Physical Sciences*, 46:131–40, 1991.
- [22] Pascale Benezeth, Donald A. Palmer, and David J. Wesolowski. Dissociation quotients for citric acid in aqueous sodium chloride media to 150 degc. *Journal of Solution Chemistry*, 26:63–84, 1997.

8 The influence of structure and composition of a reverse SDS microemulsion on enzymatic activities

Abstract

The activity of the enzyme horse radish peroxidase (HRP) is studied in a series of reverse microemulsions composed of dodecane, aqueous buffer, sodium dodecyl-sulfate (SDS) and alcohols of the homologous series 1-butanol to 1-octanol. The HRP catalysed reaction is the oxidation of a classical water soluble substrate, the 2,2-azino-bis(3-ethylbenzothiazoline-6-sulfonic acid) diammonium salt (ABTS) by hydrogen peroxide. In parallel electric conductivity measurements are performed on the same solutions. The structural changes in the microemulsions, as inferred by the conductivity measurements, correlate remarkably well with the changes in the enzymatic activities. In particular it is found that a) the maximum activity of the enzyme is always related to its optimum hydration and that this hydration can be related to the microemulsion structures, b) the enzyme inhibition caused by the alcohols in microemulsions is a consequence of both the solubility of the alcohols in the buffer and the rigidity of the interfacial film. Consequently, it can be concluded that enzymatic activity measurements are a valuable tool to study confined systems such as microemulsions and that enzymatic activities can be finely tuned by small changes in microemulsion structures, probably in a predictive way.

8.1 Introduction

Enzymes have extensive application as catalysts for organic reactions. They work at ambient temperatures with large selectivity, specificity and minimal side-product formation [1, 2]. But an understanding of the influence of local physico-chemical conditions on enzymatic activity is still lacking. In this connection, the peroxidases have been much studied [3], especially horseradish peroxidase (HRP). Its activity has been tested in various media - in ionic liquids [4], sol-gel hosts [5, 6], biphasic systems [7, 8], organic solvents [9], microemulsions, reverse micelles [10, 11, 12, 13, 14, 15, 16], supercritical CO₂ [17], and emulsions [18, 19]. Reverse micellar systems provide model systems in which aqueous solution properties in confined media can be varied [10, 11, 12, 13, 14, 15, 16]. For the much explored water/AOT system current

knowledge concerning the physical-chemical properties is summarised elsewhere [20]. The present paper is concerned with HRP activity in reverse SDS microemulsions. The HRP catalysed reaction is the oxidation of a classical water soluble substrate, namely the 2,2-azino-bis(3-ethylbenzothiazoline-6-sulfonic acid) diammonium salt (ABTS) by hydrogen peroxide. As HRP and ABTS are completely insoluble in oil and in the *n*-alcohols used in this study, the enzymatic reaction takes place in the aqueous nanodroplets. Our reverse microemulsion reactor comprises aqueous buffer, SDS, *n*-alcohol in the homologous series from 1-butanol to 1-octanol, and dodecane. These systems are well described in the literature [21]. The main effect of varying the *n*-alcohol carbon number is to change the flexibility of the interfacial film which is usually expressed in terms elastic constant or eleastic modulus [22]. These systems are different to the usual AOT systems in they contain alcohols as co-surfactant. While that complicates matters, it has the compensating advantage that the microstructure can be widely varied. Furthermore, such systems have been studied previously as a reaction medium for organic reactions and syntheses [23, 24, 25, 26, 27, 28, 29, 30, 31, 32]. The main aim of the present study is focused on enzymatic activity as a function of microstructure. First the presence of the enzyme, and of the citrate buffer ($c = 0.025\text{M}$) in our systems, are shown not to significantly alter the phase behaviour and the microstructures. Preliminary enzymatic activity tests in bulk aqueous buffer solutions are then performed with the different *n*-alcohols and as a function of SDS concentration. The influence of pH in pure buffer and in microemulsions is also reported. Finally, enzymatic activity in the microemulsion systems is explored along experimental paths with different water (buffer) to dodecane ratios, but with constant surfactant/alcohol mass percentage and ratio, c.f. Fig. 8.1. The change of the buffer to dodecane ratio, i.e. this is equivalent to the mass percent of buffer aqueous solution in the microemulsion, this shall be refer in the present study as buffer content, affects the local curvature and hence surface hydration and microstructure. The electric conductivities of the studied microemulsion systems were measured along the same experimental paths used for enzymatic activities to illuminate microstructures. The different results, compared step by step, allowed the drawing of some conclusions on the influence of the different reaction medium microstructures on the enzymatic activity. In preceding studies on horse liver alcohol dehydrogenase (HLADH) in a ternary system of nonionic surfactants [33, 34] it was concluded that HLADH can be used as a structural probe. In the same vein, an interesting work on the enzymatic activity of lipase in a reverse microemulsion composed of pentanol/cetyltrimethylammonium bromide/water/hexane has been published recently [35].

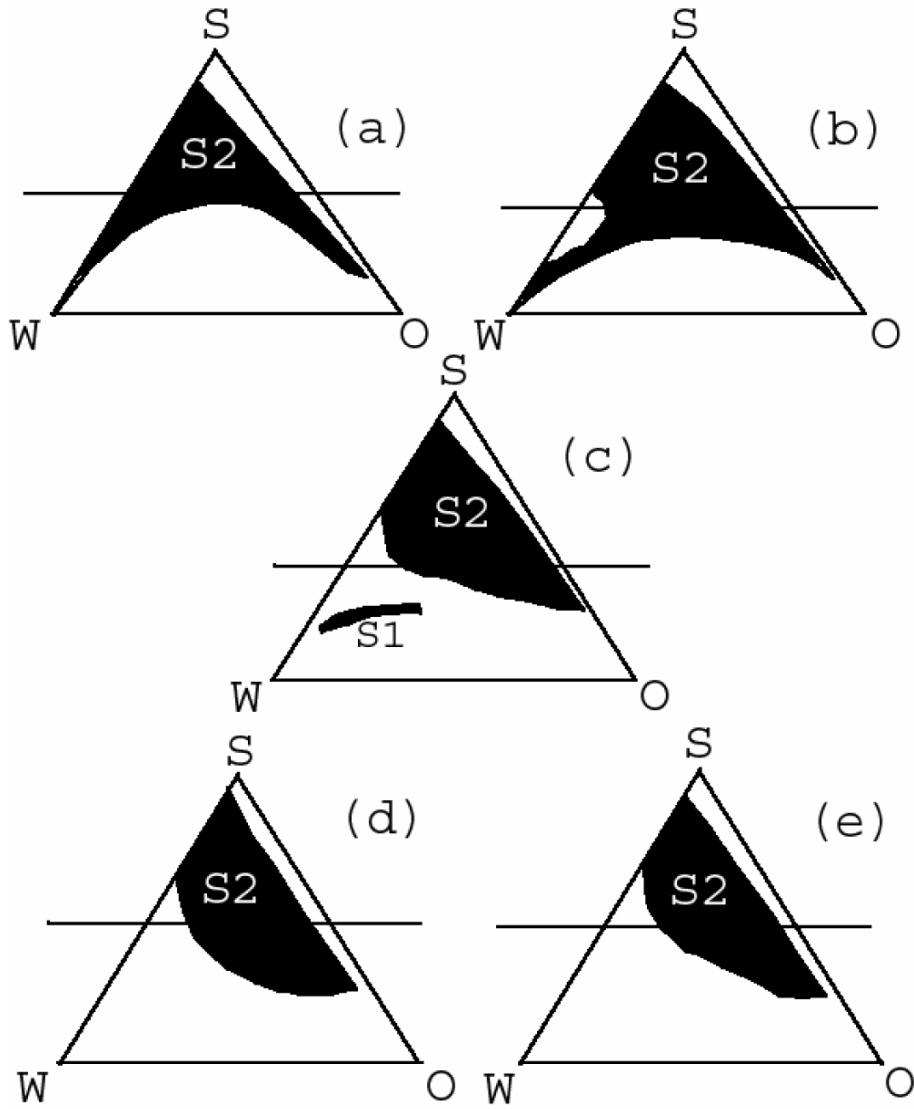


Figure 8.1: The phase diagrams of pseudo-ternary water/SDS/dodecane/n-alcohol systems (S stands for SDS/n-alcohols, W for water, and O for dodecane) taken from [21], (a) 1-butanol, (b) 1-pentanol, (c) 1-hexanol, (d) 1-heptanol and (e) 1-octanol. In every case the molar ratio K_M between surfactant and alcohol of 1/6.54. The full lines indicate the chosen compositions of the reaction media. The mass percents of SDS+alcohol are: $P_{s_{SDS+1-butanol}}=0.5$, $P_{s_{SDS+1-pentanol}}=0.4$, $P_{s_{SDS+1-hexanol}}=0.424$ and $P_{s_{SDS+1-heptanol}}=0.447$. This means that we worked at comparable SDS+alcohol content in the different alcohol systems, except in the case of 1-butanol, where we had to use a slightly higher SDS+alcohol molarity in order to have a sufficiently extended monophasic range, see Fig. (a).

8.2 Materials and Methods

8.2.1 Materials

Purified water was taken from a Millipore Milli-Q system (electrical conductivity $< 10^{-6} \text{ Sm}^{-1}$). The buffer contained citric acid monohydrate (purity $> 99.5\%$, Acros, concentration $c = 0.009 \text{ M}$) and citric acid trisodium salt dihydrate (purity $> 99\%$, Acros, concentration $c = 0.016 \text{ M}$), $\text{pH} = 5.0$. The various alcohols used in this work are listed in Table 8.2.1. SDS was purchased from Merck (purity $> 99\%$). The enzyme was Peroxidase Type VI from horseradish (Sigma, HRP, batch 10K7430). The substrates chosen were hydrogen peroxide (Merck, 30% w/w medical, extra pure) and 2,2-azino-bis(3-ethylbenzothiazoline-6-sulfonic acid) diammonium salt (Fluka, ABTS, purity $> 99\%$). The oxidation of ABTS with hydrogen peroxide (Merck) catalyzed by peroxidase is a classical reaction for the study of HRP initial velocities [36]. Note that all alcohols are completely miscible with dodecane.

8.2.2 Conductivity Experiments

The conductivity measurements were performed with a Consort Ion/EC Meter C733 conductivity meter using a Consort SK41T electrode cell placed in the sample. The temperature of the sample was held at 25°C by a thermostatic bath with an accuracy of $\pm 0.1^\circ\text{C}$.

8.2.3 Preparation of the Reaction Mixtures

The reaction mixtures were prepared by the addition of 10mL of a solution containing 0.012 M ABTS to 2.9 mL of the buffer solution or microemulsion media. Then 10mL of a solution containing 0.0262 M H_2O_2 and finally 10mL of a solution containing HRP (31.25 mg/L) were added. All the solutions were prepared using the citrate buffer. The final addition of HRP initiates the oxidation of the ABTS.

8.2.4 Determination of Enzyme Activity

The kinetics of ABTS oxidation was studied spectroscopically at a constant temperature of 25°C using a Varian Cary 3E spectrometer. The progress of the reaction was estimated from the absorption at 414 nm of the oxidized form of ABTS, which was detected during the first 4 min after the addition of HRP. The initial velocity, V , of the enzymatic reaction was inferred from the slope of the absorption intensity versus time, which was linear at least during the first few minutes. In order to reduce the uncertainty of the measured results due to the variable reproducibility of the mother enzyme solutions, the activity, A , was defined with respect to the initial velocity, V_0 , of the same enzyme reaction in the standard buffer solution. The activity is expressed as $A = V/V_0$ and was determined under the same experimental conditions for different reaction media compositions, for the exact compositions

Name	purity [%]	Solubility [37, 38, 39, 40] at 25°C		viscosity (Pa.s) 25°C	purchased from
		n-alcohol in water	water in n-alcohol		
1-butanol	> 99.7	0.0735	0.2027	≈ 0.026 [41]	Merck
1-pentanol	> 99	0.0220	0.0746	≈ 0.034 [42, 43, 44]	Aldrich
1-hexanol	> 98	0.0057	0.0073	≈ 0.045 [44, 45]	Merck
1-heptanol	> 98	0.0010	0.0055	≈ 0.059 [46]	Elf Atochem
1-octanol	> 99	0.00059	0.0025	≈ 0.074 [46]	Aldrich

Table 8.1: Used alcohols

see the discussion of the phase diagrams and the experimental paths in the next paragraph. For each of the different reaction compositions, at least three identical samples were prepared and the reaction velocities of these samples were measured independently at $25.0 \pm 0.1^\circ\text{C}$ to verify the reproducibility of the results. It is about 5%. Note that Gebicka et. al [11] demonstrated, for the present enzymatic system and for similar HRP, H_2O_2 and ABTS concentrations as we use here, that the observed reaction rate in aqueous reverse AOT micelles should be the same as in homogeneous aqueous solution. Thus it should also be valid here for the studied reverse SDS micelles.

8.3 Results

8.3.1 Phase diagrams of microemulsions

The phase diagrams of pseudo-ternary systems, water/SDS/dodecane/n-alcohols, are shown in Fig. 8.1 for various alcohols from 1-butanol to 1-octanol [47] for a value of the surfactant / alcohol molar ratio $K_M = 1/6.54^1$. The dark areas (S, S1, S2) represent regions of existence of monophasic, isotropic, and thermodynamically stable liquids of low viscosity. The bright areas correspond to other phases or mixtures but are not marked here in detail, because the experiments were carried out in the monophasic isotropic areas. The experimental paths tracked along the dark straight lines. In order to confirm the weak effect on the phase diagram topology due to the replacement of the water by the citrate buffer solution, the phase diagram of the citrate buffer solution/SDS/dodecane/1-pentanol system [48] was also determined, see Fig. 8.2. It can be seen that the two phase diagrams are essentially identical. The same is true for microemulsions containing the other alcohols.

8.3.2 Conductivity Measurements

The conductivity was measured along the experimental paths defined above, with an increasing amount of buffer in the microemulsions, i.e. buffer content, and for the different alcohol systems from 1-butanol to 1-octanol; see Fig. 8.3. In this figure the ratio of water to surfactant molecules for the 1-butanol system and the other alcohol systems is added to facilitate discussion on the states of hydration in the reverse microemulsions. Three different profiles of the conductivity were observed in the curves according to the carbon number of the alcohol. The 1-butanol and 1-pentanol curves could be separated into two parts: There was first a sharp increase of conductivity from 5 to 14% of buffer content (bc), followed by a softer increase for higher buffer contents. In the case of 1-heptanol and 1-octanol the conductivity values were very low and there was a very limited increase of conductivity with

¹For comparison, similar phase diagrams for water/SDS/dodecane/ C_nPO_m systems are given in Fig. 6.1.

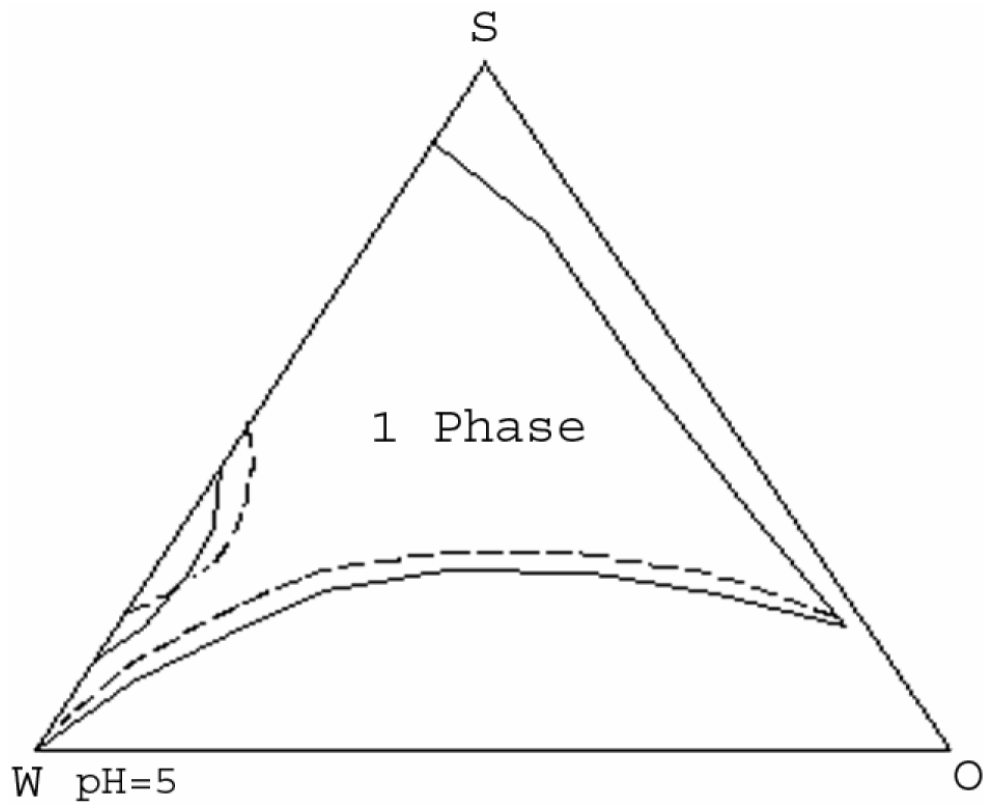


Figure 8.2: Pseudoternary diagram of the citrate buffer solution ($c = 0.025\text{M}$) / SDS / 1-pentanol / n-dodecane ($K_M = 1/6.54$, $T = 25^\circ\text{C}$) in comparison with the water system indicated by the dashed line.

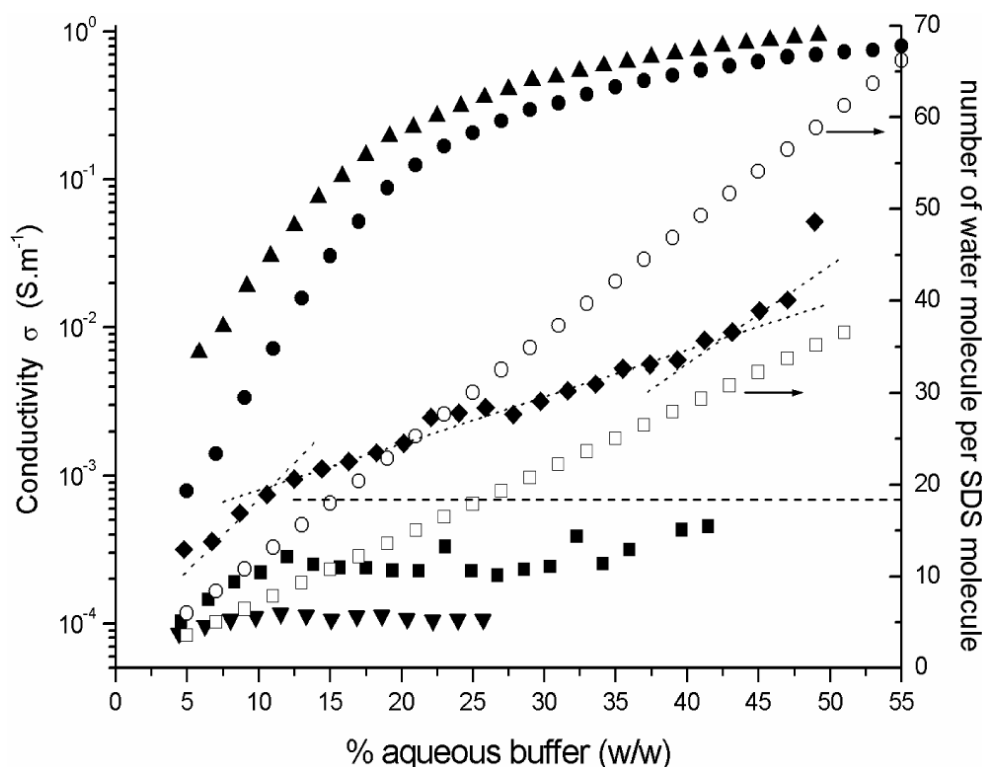


Figure 8.3: Variations of citrate buffer/SDS/n-alcohols/n-dodecane microemulsion conductivity (expressed in S.m^{-1} , $T = 25^\circ\text{C}$) with the citrate buffer content in mass percent, along the composition paths, for different n-alcohols: 1-butanol (▲), 1-pentanol (●), 1-hexanol (◆), 1-heptanol (■) and 1-octanol (▼). Also given is the ratio of water to surfactant molecules for the 1-butanol system (□) and the other alcohol systems (○), see Fig. 8.1 and the discussion of the phase diagrams. The dashed line refers to the number of water molecules per surfactant molecule at the percolation point of the 1-pentanol system.

increasing bc. Beyond approximately 11% bc the conductivity was found to be nearly independent of the composition.

Finally, for the 1-hexanol system, an intermediate behaviour was observed, where three regions can be distinguished. For low bc (5 to 12%) the conductivity increased rapidly, for intermediate buffer contents (12 to 40% bc) the rate of increase leveled off and finally, for high buffer contents, a sharper, non-linear increase of conductivity was found. The conductivity measurements for 1-butanol and 1-pentanol were carried out a second time by replacing the buffer solution with millipore water, see Fig. 8.4. This procedure was performed in order to confirm the weak influence of the citrate buffer ($c = 0.025\text{M}$) on the conductivity and hence on the microstructures. The enzyme concentration used is so low ($\approx 10^{-9}\text{M}$) that no influence of the enzyme on conductivity and on the liquid structure is expected.

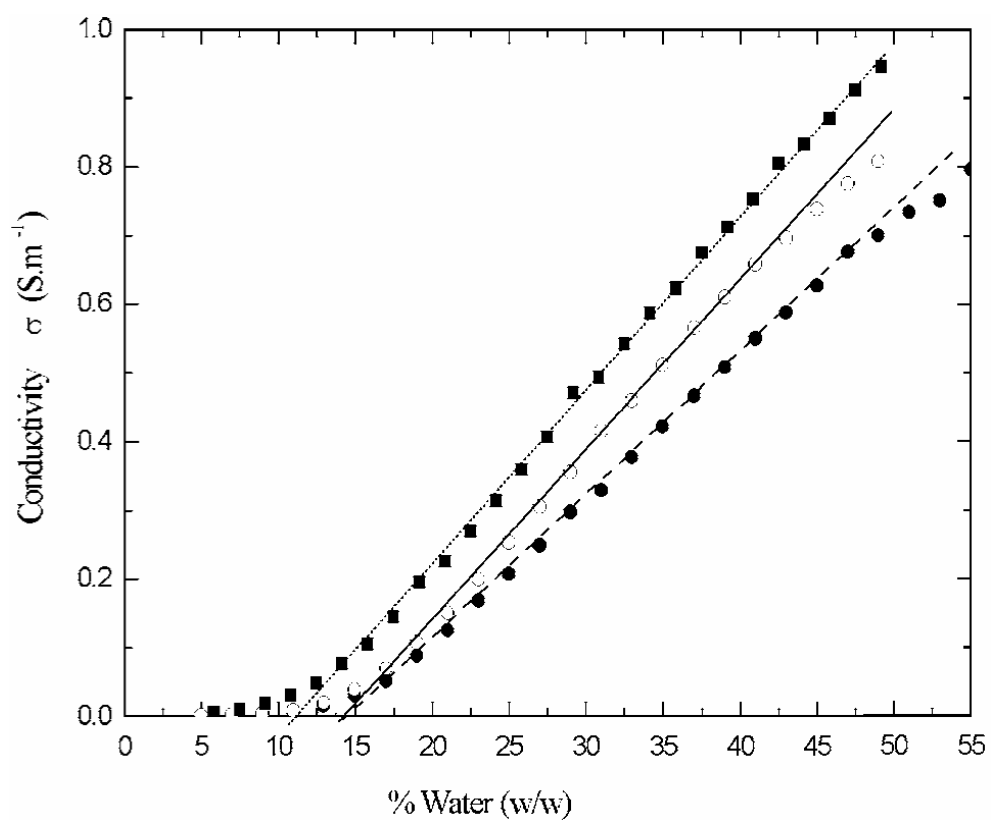


Figure 8.4: Variations of conductivity along the experimental path in the system: citrate buffer solution ($c = 0.025\text{M}$)/SDS/1-pentanol/n-dodecane (●) ($K_M = 1/6.54$, $T = 25^\circ\text{C}$) in comparison with the water system (○), and the 1-butanol system with buffer solution (■).

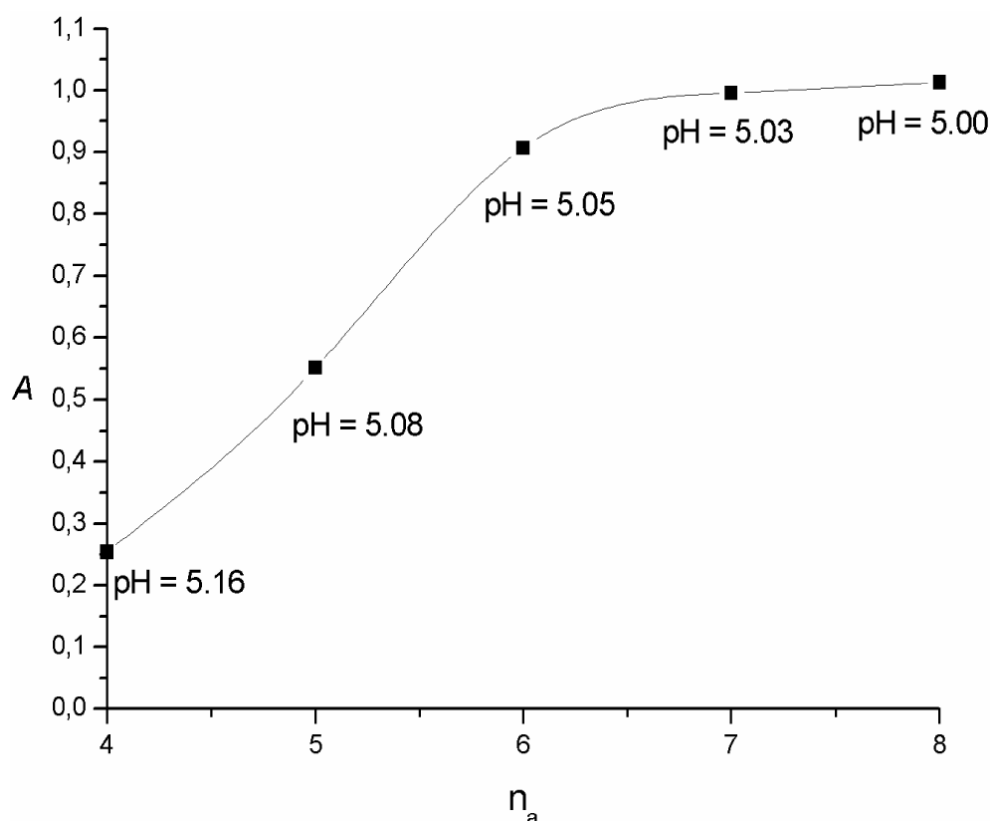


Figure 8.5: Enzymatic activities of HRP in citrate buffer solutions ($c = 0.025\text{M}$, $\text{pH} = 5$) saturated with different n -alcohols from 1-butanol to 1-octanol where n_a is the number of carbon atoms in the alcohol. The corresponding measured pH values are also given.

8.3.3 Preliminary Enzymatic Tests

Enzymatic Activities in n -Alcohol Saturated Buffer Solutions

Enzymatic activities in buffer solutions, saturated with different n -alcohols, were measured and the results are reported in Fig. 8.5. This was done to evaluate the maximal enzymatic inhibitions caused by each alcohols. A partial inactivation of the enzyme was observed for 1-butanol, 1-pentanol and also a small one for 1-hexanol solutions. For solutions saturated with 1-heptanol and 1-octanol the enzymatic activity was comparable to that in the pure buffer solution ($A = 1$). We remark that the different alcohols slightly change the measured pH values.

Enzymatic Activities in buffer with various SDS concentrations

Figure 6 gives the SDS concentration dependence of the catalytic activity of HRP. The first part of the curve, $\% \text{ SDS} = 0$ to 4, shows a large increase of enzymatic activity, and for $\% \text{ SDS} = 4$ to 10 a constant enzymatic activity ($A = 1.6$). For higher SDS concentrations the activity decreases slowly.

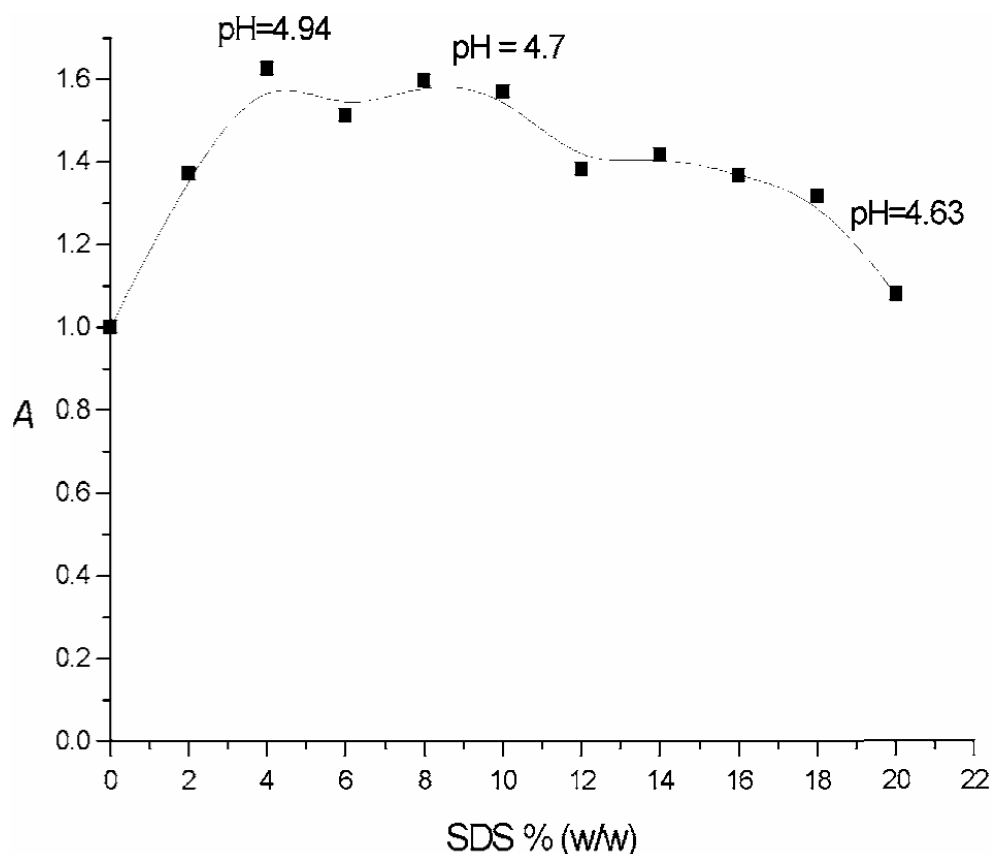


Figure 8.6: Enzymatic activities of HRP versus SDS concentration (mass percent) in citrate buffer ($c = 0.025\text{M}$, initial buffer pH = 5).

Influence of SDS concentration on the buffer pH

In Fig. 8.6 the buffer pH as a function of the SDS concentration is also displayed. The pH were measured with a glass electrode. With increasing SDS concentrations the measured buffer pH is always decreasing. A similar pH decrease in this buffer was already observed by increasing the concentration of inorganic sodium salts [49].

8.3.4 Dependence of the enzymatic activity on the alcohol carbon number for various buffer contents

The influence of the alkyl chain length of n-alcohols on the enzymatic activity was tested in microemulsions, along the experimental paths given in Fig. 8.1. The results are reported in Fig. 8.7.

1-butanol

For the 1-butanol systems the enzymatic activities have very low values ($0.1 < A < 0.47$) for all buffer contents. One observes two linear parts, first in the region between

6 and 25% bc, where the enzymatic activity increases, and then in a second region between 25 and 50% bc, where the enzymatic activity decreases with a slope similar to the first region. The maximum enzymatic activity ($A = 0.47$) is determined for a buffer content of 25%.

1-pentanol

Here, the dependence of the enzymatic activity on the buffer content clearly shows three different regions: the first one is characterized by a sharp increase between 5 to 14% bc ending up with a maximum enzymatic activity of $A = 1.35$. A slight decrease between 14 and 42% bc defines the second region; and finally the third region exhibits a sharp linear decrease between 42% and 55% bc.

1-hexanol

As for 1-pentanol one can observe three distinctive regions in the activity curve, but the middle range is smaller. The first region is between 5 and 12% bc, the second one ranges from 12 to 31% bc and the third one from 31% up to 50% bc. Note that 1-hexanol systems show the highest enzymatic activities of all microemulsions with $A_{max} = 1.6$ at bc = 12%.

1-heptanol

Finally, the 1-heptanol systems exhibit only two regions: a large increase of activity for buffer contents from 5 to 11% ($A_{max} = 1.4$) followed by a less pronounced decrease between 11 and 42% bc. For reasons explained in the discussion section, it was not possible to obtain reliable values for 1-octanol systems.

8.4 Discussion

8.4.1 Phase Diagrams

The different phase diagrams shown in Fig. 8.1 for the water/SDS/dodecane/n-alcohol systems are monophasic along the experimental paths. That is the main reason for the choice of these systems. Nevertheless, for the 1-butanol system it was necessary to alter the value of $P_{SDS+1-butanol}$ in order to shift the experimental path into a sufficiently large range of microemulsion. The differences between the extent of microemulsion areas in the phase diagrams have already been discussed in previous papers [21], according to the influence of the various alcohols. It was also shown that the alcohols must have at least four carbon atoms to play the role of a co-surfactant of SDS, independently of the oil.

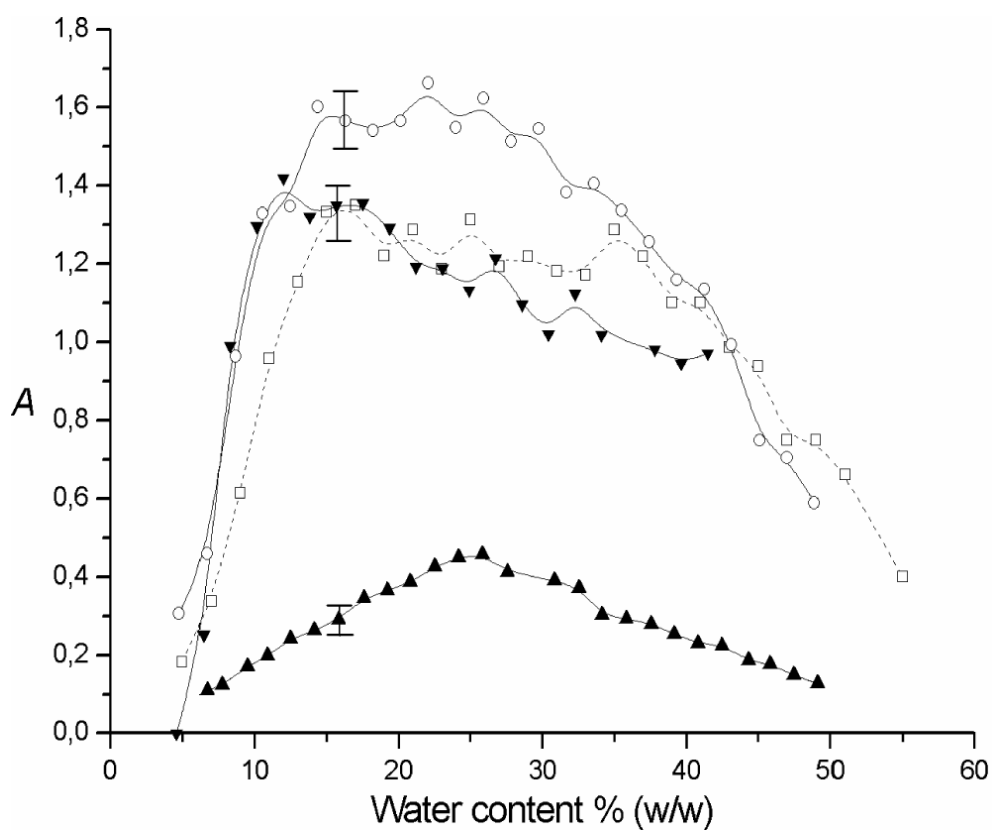


Figure 8.7: Enzymatic activities in microemulsions (citrate buffer solution / SDS / dodecane / n-alcohol ($K_M = 1/6.54$)) as a function of the buffer content. 1-butanol (▲), 1-pentanol (□), 1-hexanol (○) and 1-heptanol (▼). Typical error bars are also included.

8.4.2 Conductivity measurements

The conductivities of microemulsions are related to the microstructure of the solution [50]. Electrical conductivity reflects the ability of ions to move in the aqueous phase of the microemulsion, where the movements depend on the local environment surrounding the charge carriers. According to the results given in Fig. 8.3 three types of behavior induced by the alcohols can be distinguished: the two short-chain alcohols, 1-butanol and 1-pentanol, the intermediate case of 1-hexanol and the low conducting systems containing 1-heptanol and 1-octanol. For the 1-butanol and 1-pentanol systems, the percolation thresholds, where the aqueous droplets begin to merge, are determined following the method of *Lagourette et al.* [51]. The values obtained are 11% water content in the presence of 1-butanol, and 14% of water or buffer content in the case of the 1-pentanol systems, c.f. Fig. 8.4. It is known that no percolation phenomena occur either in the case of 1-heptanol [21] or in 1-octanol reverse microemulsions. The very low conductivities measured for these two systems indicate that the reverse micro droplets behave as hard objects with highly rigid interfacial films (very limited or no clustering and no merging processes). Increasing amounts of added water only lead to a swelling of the reverse micelles, but the ions remain tightly bound to the interface. Comparing 1-butanol and 1-pentanol microemulsions on the one hand and 1-heptanol or 1-octanol containing microemulsions on the other hand, the 1-hexanol microemulsion appears as the intermediate case with a hybrid trend of electrical conductivity variations, see Fig. 8.3. In the 1-hexanol system no percolation occurs. For a more detailed interpretation of these conductivity data see [21]. At higher water contents the 1-butanol and 1-pentanol systems can be described with the percolation and effective medium theories [51, 52, 53], which are consistent with the existence of reverse micro droplets clustering and merging processes. The occurrence of reverse bicontinuous structures is reflected by a significant deviation of the conductivity curves from a linear slope at high water contents. Such a deviation is found in the 1-pentanol system, at about 46% bc, see Fig. 8.4. By contrast, in the 1-butanol microemulsion system, only the last point at 49% bc may correspond to a reverse bicontinuous structure. This observation is in keeping with the results of *Clausse et al.* [47], who had performed the conductivity measurements in the ternary system water/SDS/1-butanol ($K_M = 1/6.54$). Since the ions are quite mobile in the region between the percolation point and the point of change to the bicontinuous structure, additional water simply dilutes the ions so that the increase of conductivity is less pronounced in the bicontinuous region. Our interpretation of the conductivity data is qualitatively in agreement with studies on various other microemulsions. For example it was argued by *Riter et al.* [54, 55, 56] that in AOT systems water molecules have only a weak mobility in reverse micelles, because the small ions are mainly bound to the interfacial film and strongly hydrated so that the water mobility is highly reduced as long as the water concentration is not high enough to form a sufficient amount of “free” or “bulk-like” water. This picture has recently been confirmed by a dielectric spectroscopic study for the proposed system along a similar experimental path

[57]. Furthermore the change to a reverse bicontinuous microemulsion structure in parallel with a complete hydration of all the implicated molecules, and especially the counter-ions, was previously reported by *Yao et al.* for a water/n-alcohol/cetyl trimethyl ammonium bromide/n-alkane system [58]. The 1-hexanol systems show a characteristic change in the slope of the conductivity curve at about 40% of water. No well-defined reverse bicontinuous microemulsion structure is known for this system as encountered in the 1-butanol or 1-pentanol system [21]. Finally, neither 1-heptanol nor 1-octanol show any change to a bicontinuous system or a fusion of droplets. The interfacial film is too rigid to allow such a structural transition to occur [21]. These results are in agreement with the calculations of the elastic moduli in these systems [22, 59, 60, 61] also suggesting an increase of interfacial rigidity with the number of carbon atoms in the n-alcohols. The interfacial film rigidity will play an important role in the interpretation of the enzymatic activities shown in the last section. It should be noted that alternatively the discussion of packing factors and parameters would lead to the same conclusion. Replacement of water by a citrate buffer solution has only a small effect both on the phase diagrams (Fig. 8.2) and on the microstructure of the systems (Fig. 8.4). The structuring properties of n-alcohols may therefore be considered to be similar with and without buffer. In the following we will try to relate the models of structure and hydration, as inferred from conductivity measurements, to the enzymatic activity curves.

8.4.3 Preliminary Enzymatic Tests

Enzymatic activities in buffer solutions saturated with n-alcohols

The denaturation of enzymes such as chymotrypsin, lactase and lysosyme by alcohols has been extensively studied [62, 63, 64, 65, 66, 67]. Our own results can be partially explained by these previous works. As an increase of inhibition was observed with the increase of the lipophilic behaviour of n-alcohols from methanol to 1-propanol [65, 66, 67], it was postulated that the denaturation is due to a hydrophobic binding of the alcohol molecules with the lipophilic parts of the enzyme. In the case of the present study the poor water solubility of the used alcohols (Table 8.2.1) limits the contacts between alcohols and enzymes. Therefore, Fig. 8.5 reflects mainly the different alcohol solubilities.

Enzymatic Activities in buffer with various SDS concentrations

Several studies of the influence of SDS on HRP structure and activities have already been carried out [68, 69, 70, 71, 72, 73, 74]. It was shown there that important interactions occurred between SDS and HRP. The change in HRP activity observed by addition of SDS to citric buffer (see Fig. 8.6) could be related to these HRP/SDS interactions. In addition to such considerations bulk effects were found to play an important role in the HRP activity [49, 75]. Indeed the addition of sodium sulfate or of some sodium salts was found to increase the HRP activity in citric buffer [49].

Note that this effect can be seen as a enzymatic superactivity. The main explanation for this effect is that the addition of salts leads to a decrease of the pH of the citric buffer which is favourable to the HRP activity. This pH decrease through addition of salt was quantitatively modelled at low salt concentration and was confirmed experimentally at high salt concentration [49]. The addition of SDS leads to a decrease of the citric buffer pH much as the addition of conventional inorganic electrolytes does. Thus the superactivity observed in the case of SDS addition can be partially explained by the pH decrease of the citric buffer. In reverse micelles the ionic strength is high due to the presence of SDS. Thus with the same reasoning the superactivity in microemulsions could qualitatively be explained. We are aware that pH values in such systems as measured with a simple glass electrode might be erroneous. However, there is one experimental result that gives us some confidence concerning the validity of such pH measurements: we compared the pH-enzymatic activity relation both in simple buffer solutions and in the reverse microemulsions and we found exactly the same curve. This means that on both the enzyme and the electrode surfaces exactly the same specific adsorption effects occur - a fact that is not very probable. A better explanation is certainly that the electrode still indicates the “right” pH value and that the enzyme is still as sensitive to pH changes as in the neat buffer solution without oil, surfactant and alcohol.

8.4.4 Microemulsions: the dependence of the enzymatic activity on the number of carbon atoms in the alcohols at different water contents

Before discussing the different alcohol systems, it should be stressed that the HRP concentrations used in the present study are typical for bioconversions and are much lower than the SDS concentrations. Only a very small part of the reverse buffer droplets contain HRP molecules. As a consequence, the enzyme should not significantly influence the structure of the medium. This is in contrast to other studies, e.g. those carried out in Pileni’s group [76, 77] where a protein such as cytochrome C was able to reorganize the reverse micelles in percolating systems. As the HRP has a similar structure and hydropathy as cytochrome C, a certain adaptation of the reverse micelles around a HRP molecule cannot be completely excluded.

The SDS/1-butanol/dodecane/buffer/system

The very low enzymatic activity values (Fig. 8.7) in this system can be explained by the relatively high solubility of 1-butanol in the aqueous buffer system, c.f. Table 8.2.1. Due to the low polarity of dodecane, 1-butanol is essentially dissolved in the aqueous droplets leading to a strong inhibition of the water soluble enzyme. Furthermore, 1-butanol acts as a co-surfactant with the particular feature that the SDS/1-butanol film is highly flexible. As a consequence, the micelles begin to merge and percolate at a very low concentration ($\approx 11\%$ bc, c.f. Fig. 8.4), even before the hydration of all components in the film and in the aqueous buffer droplets is

complete. Therefore, the buffer content at the percolation threshold is lower than the necessary buffer content at which the enzyme activity has its maximum ($\approx 25\%$ bc, c.f. Fig. 8.7). At all concentrations there is a competition of SDS, 1-butanol and HRP for hydration water. If we assume that optimal hydration correlates with maximal activity this is only achieved at 25% bc. At lower buffer concentrations, hydration water is shared between SDS, 1-butanol and HRP. Note that at 25 % bc, the solution contains about 18 molecules of water per SDS molecule. According to dielectric relaxation measurements on SDS in water it was found that the hydration of SDS ion pair is completed for a mole ratio of water/SDS around 20 [78]. There is also a balance between the hydrophobic inhibitor binding of 1-butanol and the SDS-HRP interactions, which is favourable to the HRP activity (see Section 8.4.3 Discussion Preliminary Enzymatic Tests). The decreasing activities for buffer contents larger than 25% can be explained by two different phenomena: (i) According to our experimental strategy (section Materials and Methods), always the same amount of ABTS, H_2O_2 and finally HRP is added to the previously prepared microemulsions. This means that the higher the buffer content of the microemulsions the more diluted are the reverse buffer droplets with respect to these three components. On the other hand, it can be supposed that the buffer droplets are always saturated with 1-butanol. As a consequence, the molar ratio 1-butanol/HRP increases and so does the inhibition. This is true both for competitive and non competitive inhibition. (ii) It is also possible that HRP has a certain affinity to the interface. The hydrophobic behaviour of HRP and its capacity to link to biological membranes [79, 80, 81] support this hypothesis. Therefore, the alcohol concentration “seen” by the enzyme is dependent on the film composition. The interfacial alcohol concentration increases with increasing buffer content as it was found by *Yao et al.* [58], so that the local alcohol concentration around the HRP molecules near to the interface is higher than the bulk water saturation concentration of 1-butanol. Note that in this study [58] cetyltrimethylammonium bromide is used as surfactant. Nevertheless CTAB and SDS give similar phase diagrams, so the two surfactant systems are assumed to be comparable. Finally, the affinity of the enzyme to the highly flexible film also exposes the enzyme to the denaturing dodecane phase, a fact which further decreases the activity. These two facts explain why the measured activities for buffer contents above 35% in the microemulsions are lower than in 1-butanol saturated buffer ($A = 0.26$, Fig. 8.5).

The SDS/1-pentanol/dodecane/buffer/system

In the 1-pentanol reverse microemulsion system the buffer concentration for the percolation threshold value and for the maximum enzymatic activity are very similar (bc $\approx 14\%$). A new dielectric study of this system [57] shows that the hydration of SDS and of 1-pentanol reaches its maximum just at the percolation threshold. The difference between the elastic moduli of the interfacial films formed with 1-butanol and 1-pentanol explains the difference between the two percolation thresholds (Fig. 8.4, see also Section 8.4.2 Discussion: Conductivity measurements), the interfacial

film obtained with 1-pentanol being more rigid. In the case of the 1-pentanol system, the hydration of both SDS and alcohol must be complete for the onset of percolation, whereas in the case of the 1-butanol microemulsion the hydration is only complete at buffer contents more than twice as high (25%) as the buffer content at the onset of percolation (11%). These results are also in agreement with the well-known co-surfactant behaviour of 1-pentanol [82]. As a consequence, it seems probable that the optimum hydration is the decisive factor for the maximum enzyme activity and it is achieved when all the other components are sufficiently hydrated (at $bc = 14\%$ there are about 18 water molecules per SDS molecule in solution, c.f. the dashed line in Fig. 8.3). The observed enzymatic superactivity ($A_{max} \approx 1.35$, see Fig.7) is very probably the consequence of the high ionic strength in the aqueous droplets and the resulting pH decrease (see Section 8.4.3 Discussion Preliminary Enzymatic Tests). For the sake of clearness our arguments are summarized in Fig. 8.8.

It is interesting to compare the A_{max} obtained in the case of 1-pentanol to the ones obtained using 1-butanol and 1-hexanol as cosurfactant. Since the solubility of 1-pentanol in the buffer solution is smaller and the interfacial film is more rigid than in the case of 1-butanol, the inhibiting influence of 1-pentanol is less pronounced than that of 1-butanol, c.f. Fig. 8.5. In the same vein, since the solubility of 1-hexanol ($A_{max} \approx 1.6$, see Fig.7) in the buffer solution is smaller than in the case of 1-pentanol, the inhibiting influence of 1-hexanol is less pronounced than that of 1-pentanol. Thus, subject to sufficient hydration, alcohol-enzyme interactions are important to understand the HRP activity. The decreasing activity from 14% to 42% bc is less pronounced than in the case of 1-butanol. Probably, this is also due to the lower solubility of 1-pentanol and a higher incorporation of 1-pentanol in the interfacial film, when compared to 1-butanol. The local environment of the enzyme seems not to be changed significantly by simple dilution with buffer. There is a large decrease of HRP activity beyond 46% bc. This concentration value corresponds to a cross-over of the system to the reverse bicontinuity phase (see Section 8.4.2 Discussion: Conductivity measurement and Fig. 8.3). At this point the buffer content is large enough to stabilize a bicontinuous structure. Following this argument, enzyme and substrates are much more diluted than in the reverse micelles phase, they are embedded in a quasi-bulk water solution, and consequently the activity goes down. In addition, the inhibition by 1-pentanol still persists and the sum of the two effects tends towards a steeper activity decrease than for bc smaller than 46%. It is interesting that the A value for the highest bc is about 0.42, which is significantly smaller than the values measured in the 1-pentanol saturated buffer solution, cf. Fig. 8.5. This is another hint at a certain affinity of the enzyme to the interfacial film where the inhibiting alcohol molecules are incorporated. It should also be noted that similar enzyme activity curves with a sudden rise in activity followed by a decrease with bc was found for several other enzymes in the well-known AOT(sodium bis(2-ethylhexyl sulfosuccinate))/alkane/water [83, 84, 85] system. But in contrast to these works we think that a combination of hydration and dilution effects, as suggested in the present paper, does account better for, and is the source of this enzymatic behaviour. If, as these authors argue, the SDS molecules pushed the

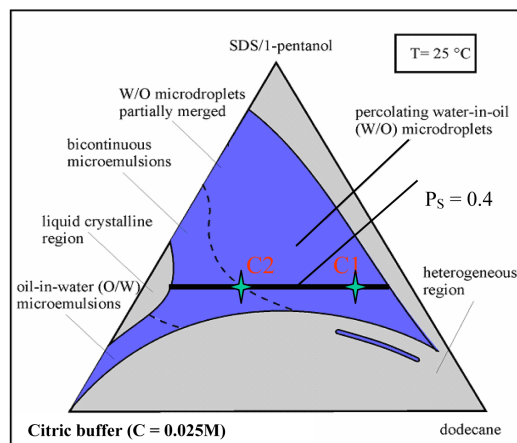


Figure 8a

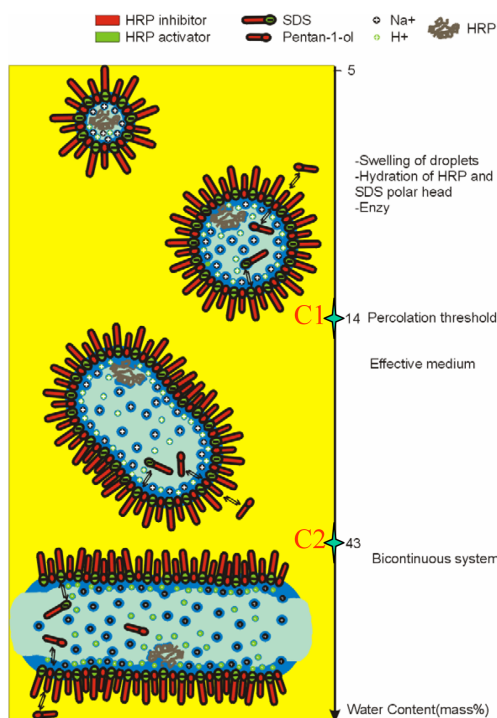


Figure 8 b

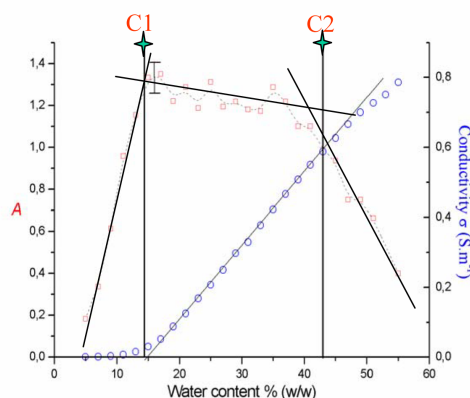


Figure 8 c

Figure 8.8: HRP enzymatic activity in the citrate buffer / SDS / 1-pentanol / n-dodecane system. A tentative explanation between the correlation of enzymatic activities and electric conductivity data. (a) Pseudoternary diagram of the citrate buffer solution ($c = 0.025\text{M}$)/SDS/1-pentanol/n-dodecane ($K_M = 1/6.54$, $T = 25^\circ\text{C}$), (b) evolution of the microstructure through the addition of citric buffer (water content) along the experimental path, (c) HRP enzymatic activities (in red) and conductivity (in blue) as a function of the buffer content (water content) along the experimental path. C1 and C2 appearing along the experimental path represent respectively the percolation threshold (14% buffer or water content) and the borderline between the effective medium and the bicontinuous system (43%).

substrate towards the enzyme thus yielding the maximum activity, the molecularly distributed SO_4^{2-} ions could not have an effect similar to that observed with SDS.

The SDS/1-hexanol/dodecane/buffer/system

The initial enzymatic activity increase and the plateau after the maximum can be interpreted in a way similar to the 1-pentanol system. The enzymatic activity increase goes in parallel with the initial increase in electrical conductivity, between 5% and 12% bc, see Figs. 8.3 and 8.7. In this composition range the hydration of SDS and 1-hexanol increases up to a maximum. As already discussed in the preceding subsection, the high A_{max} value of 1.6 in the 1-hexanol system is due to the low solubility of 1-hexanol in water, see Table 8.2.1. It is known that 1-hexanol yields a more rigid film than the shorter alcohols do and obviously the 1-hexanol molecules are so strongly incorporated in the film that their inhibition effect is negligible in the range of buffer contents where the plateau activity is detected. At bc around 40% the structural change, discussed in section Results, leads to a dilution of enzyme and substrate in a quasi-bulk water solution and hence to a stronger decrease in activity. Probably, the enzyme is also more exposed to the film and therefore to the alcohol.

The SDS/1-heptanol/dodecane/buffer/system

As in the 1-hexanol system the first enzymatic activity increase occurs in the same range as the initial increase in conductivity, i.e. 5-11% bc, c.f. Fig.3. The maximum activity can again be linked to the completed hydration of the enzyme after the initial hydration of SDS and 1-heptanol. However, the maximum enzymatic activity is smaller ($A_{max} = 1.4$) than in the case of 1-hexanol. The explanation for this reduced maximum activity is as follows: After the final addition of the HRP buffer solution in the experimental process (c.f. section Materials and Methods: Preparation of the reaction mixtures), the enzyme is exposed to the denaturing dodecane phase during a certain time. Because of the rigidity of the interfacial film, the penetration of the HRP into the buffer droplets becomes more difficult. As the SDS is not soluble in dodecane (e.g. in contrast to AOT), the added HRP buffer droplets are not immediately stabilized by the surfactant. It takes a certain time until the microemulsion is formed. This time is the longer the longer is the alcohol chain and the more rigid is the interfacial film [30, 61]. In addition, the long-chain alcohols are highly soluble in dodecane so that the enzyme is initially also exposed to the inhibiting alcohol before the protecting reverse buffer droplets are formed. Note that in contrast to SDS systems the high solubility of AOT in dodecane leads to a rapid formation of micellar systems so that in AOT no enzyme degradation due to a long contact with dodecane should be found. For bc higher than 11% no plateau is detected for the enzymatic activities, but only a linear decrease. This behaviour is in agreement with the conductivity, which indicates no structural transition beyond 11% bc. As discussed in section Discussion: Conductivity measurements, the rigid

interfacial film prevents any change to reverse bicontinuous structures between 11 and 42% bc. The micelles simply swell so that the system is progressively diluted and the enzymatic activity slowly decreases. Note that along the experimental paths chosen in this paper, the slight increase of viscosity with the buffer content [21] should not influence the enzymatic activity because the enzyme conformation is affected only little by such viscosity changes [86].

The SDS/1-octanol/dodecane/buffer/system

It is not possible to measure precisely the enzymatic activity in the 1-octanol system during the first four minutes. It takes too long a time to bring the system into thermodynamic equilibrium, especially at higher buffer contents. The reasons are the same as those discussed in the case of the 1-heptanol system, but they are more pronounced for the 1-octanol system. The film is even more rigid, thus preventing the HRP from a rapid incorporation into the protecting buffer droplets. This was observed visually: after the addition of the substrates and the enzyme (see Section 8.2 Materials and Methods Preparation of the reaction mixtures) the microemulsion needed several minutes to form. Although the initial slope of the enzymatic activity cannot be determined spectroscopically, it is possible to follow the activity over a certain time range and to compare the final absorbance to those measured for the 1-heptanol system. It can be concluded from these measurements that the enzymatic activity is always lower than in the case of the 1-heptanol, a result which is also in agreement with the denaturing facts discussed in section Discussion: The SDS/1-heptanol/dodecane/buffer/system. Note that for the 1-decanol system the denaturation of the enzyme is so important that no activity could be detected in this system.

8.5 Conclusion

In this study it was shown that HRP can be used as a structural probe of the microstructure of microemulsions in a quaternary system containing an anionic surfactant (SDS). The following points deserve note:

- A maximum enzymatic activity is obtained when the hydration of the enzyme molecules is sufficient. This appears for all 1-alcohols systems once all ions in the solution including Na^+ and DS^- are completely hydrated, i.e. at around 20 water molecules per SDS pairs. In the case of the 1-pentanol system this corresponds to the percolation threshold.
- The discovered superactivity can, at least partially, be ascribed to the presence of locally high concentrations of dodecylsulphate ions.
- When more water is added, the decreasing enzymatic activity can be explained by the increase of the 1-alcohols inhibitor concentration around the enzyme:

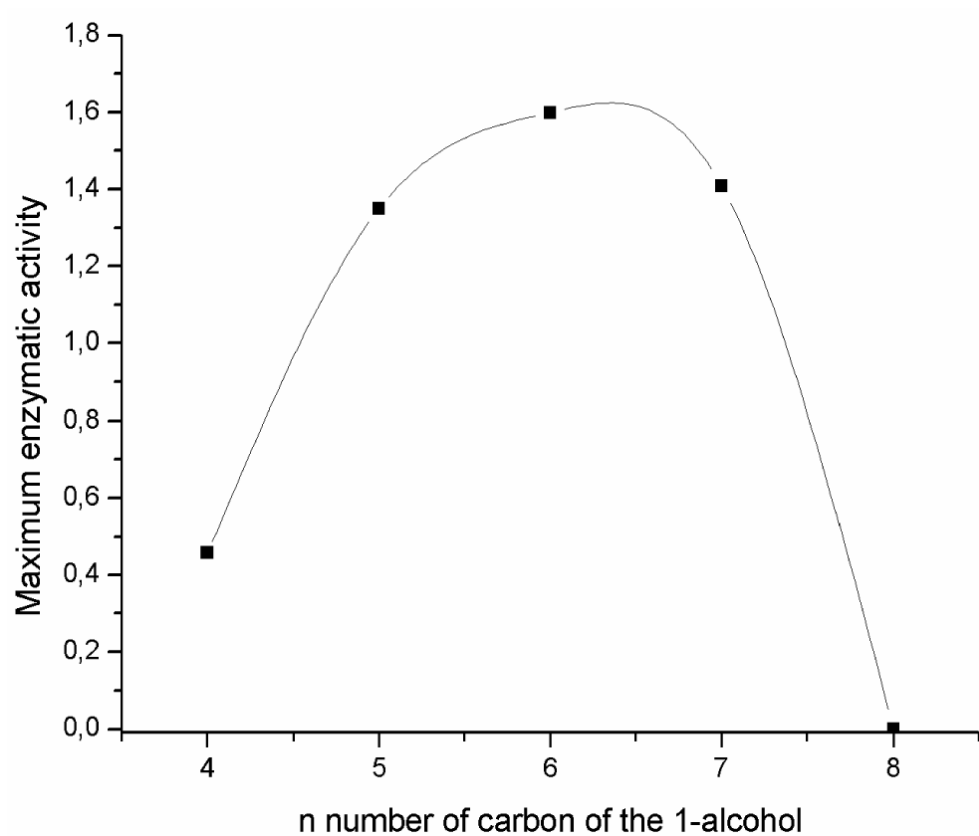


Figure 8.9: Maximum enzymatic activity observed in microemulsion vs. n , the number of carbon atom of the 1-alcohol as co-surfactant.

The probable reason is an increase of the alcohol mole fraction in the interface at the expense of the oil phase.

- The inhibiting influence of the alcohols depends both on the solubility of the alcohols in the buffer (thermodynamic reason) and the incorporation velocity of the alcohols in the interfacial film (kinetic reason). Thus the maximum enzymatic activity achieved for all 1-alcohol systems as a function of the length of the 1-alcohol is a bell-shaped curve, see Fig. 8.9. The lowest enzymatic activity observed for 1-butanol and 1-pentanol on the one hand and for 1-heptanol and 1-octanol on the other hand is explained respectively by the partial alcohol solubility in the buffer and by a kinetic limiting factor. Indeed if the thermodynamic equilibrium of the microemulsion is not achieved within a short time, the enzyme is exposed to the denaturing dodecane and also to the alcohol molecules dissolved in the oil phase. This is the consequence of a highly rigid film, caused by long-chain alcohols and of the way we prepare the solutions. As a result, the enzymatic activity in the final microemulsion state is lower than in systems where the equilibrium is immediately reached, as in the case where the more hydrophobic AOT is used as surfactant.

Bibliography

- [1] Jonathan S. Dordick. *Biocatalysts for Industry*. Plenum, New York, 1991.
- [2] A. Schmid, J. S. Dordick, B. Hauer, A. Kiener, M. Wubbolts, and B. Witholt. Industrial biocatalysis today and tomorrow. *Nature*, 409:258–68., 2001.
- [3] F. van der Velde, F. van Rantwijk, and R. A. Sheldon. Improving the catalytic performance of peroxidases in organic synthesis. *Trends in Biotechnology*, 19:73–80, 2001.
- [4] Joseph A. Laszlo and David L. Compton. Comparison of peroxidase activities of hemin, cytochrome c and microperoxidase-11 in molecular solvents and imidazolium-based ionic liquids. *Journal of Molecular Catalysis B: Enzymatic*, 18:109–120, 2002.
- [5] Kevyn Smith, Nathan J. Silvernail, Kenton R. Rodgers, Timothy E. Elgren, Mauro Castro, and Robert M. Parker. Sol-gel encapsulated horseradish peroxidase: A catalytic material for peroxidation. *Journal of the American Chemical Society*, 124:4247–4252, 2002.
- [6] Ekaterina N. Kadnikova and Nenad M. Kostic. Oxidation of abts by hydrogen peroxide catalyzed by horseradish peroxidase encapsulated into sol-gel glass. effects of glass matrix on reactivity. *Journal of Molecular Catalysis B: Enzymatic*, 18:39–48, 2002.
- [7] J.A. Akkara, D.L. Kaplan, and M. Ayyagari. Control of the molecular weight and polydispersity of substituted polyphenols and polyaromatic amines by enzymatic synthesis in organic solvents, microemulsions, and biphasic systems for use in film, uv stabilizers and photoresists. *U.S. Pat. Appl. Publ. US 20010002417 A1 20010531*, page 19 pp., 2001.
- [8] J.A. Akkara, D.L. Kaplan, and M. Ayyagari. Process to control the molecular weight and polydispersity of substituted polyphenols and polyaromatic amines by enzymatic synthesis in organic solvents, microemulsions, and biphasic systems. *U.S. Pat. Appl. Publ. US 6096859 A20000801*, page 17 pp., 2000.
- [9] Alexander M. Klibanov. Improving enzymes by using them in organic solvents. *Nature (London)*, 409:241–246, 2001.

- [10] S. M. S. Chauhan and B. B. Sahoo. Biomimetic oxidation of ibuprofen with hydrogen peroxide catalysed by horseradish peroxidase (hrp) and 5,10,15,20-tetrakis-(2',6'-dichloro-3'-sulphonatophenyl)porphyrinatoiron(iii) and manganese(iii) hydrates in aot reverse micelles. *Bioorganic & Medicinal Chemistry*, 7:2629–2634, 1999.
- [11] Lidia Gebicka and Jaroslaw. Pawlak. Kinetic investigations of horseradish peroxidase in aot/n-heptane reverse micelles. *Journal of Molecular Catalysis B: Enzymatic*, 2:185–192, 1997.
- [12] L. Setti, P. Fevereiro, E. P. Melo, P. G. Pifferi, J. M. S. Cabral, and M. R. Aires-Barros. Superactivity of peroxidase solubilized in reversed micellar systems. *Applied Biochemistry and Biotechnology*, 55:207–18, 1995.
- [13] Sanghamitra Parida, Gyan Ranjan Parida, and Amar Nath. Maitra. Studies on the catalytic activity of horseradish peroxidase hosted in aerosol ot reverse micelles containing cholesterol. *Colloids and Surfaces*, 55:223–9, 1991.
- [14] A. N. Eremin and D. I. Metelitsa. Regulation of the catalytic activity of peroxidase in surfactant mixed reversed micelles. *Biokhimiya*, 50:102–8, 1985.
- [15] N. L. Klyachko, A. V. Levashov, and Karel. Martinek. Catalysis by enzymes entrapped into reversed micelles of surfactants in organic solvents. peroxidase in the aerosol ot-water-octane system. *Molekulyarnaya Biologiya (Moscow)*, 18:1019–31, 1984.
- [16] Karel Martinek, A. V. Levashov, Yu. L. Khmel'nitskii, N. L. Klyachko, and I. V. Berezin. Colloidal solution of water in organic solvents: a microheterogeneous medium for enzymic reactions. *Science (Washington, DC, United States)*, 218:889–91, 1982.
- [17] Keungarp Ryu and Sunwook. Kim. Peroxidase-catalyzed polymerization of p-cresol in supercritical co2. *Korean Journal of Chemical Engineering*, 13:415–418, 1996.
- [18] Bhanu Kalra and R. A. Gross. Hrp-mediated polymerizations of acrylamide and sodium acrylate. *Polymer Preprints (American Chemical Society, Division of Polymer Chemistry)*, 41:1828–1829, 2000.
- [19] Noriho Kamiya, Masahito Inoue, Masahiro Goto, Nobuhumi Nakamura, and Yoshinori. Naruta. Catalytic and structural properties of surfactant-horseradish peroxidase complex in organic media. *Biotechnology Progress*, 16:52–58, 2000.
- [20] Boiko Cohen, Dan Huppert, Kyril M. Solntsev, Yossi Tsfadia, Esther Nachliel, and Menachem. Gutman. Excited state proton transfer in reverse micelles. *Journal of the American Chemical Society*, 124:7539–7547, 2002.

- [21] Marc Clausse, L. Nicolas-Morgantini, A. Zradba, and D.. Touraud. *Water-ionic surfactant-alkanol-hydrocarbon systems: influence of certain constitution and composition parameters upon the realms-of-existence and transport properties of microemulsion-type media.*, volume 24 of *Science Surfactant Series*, chapter 1, pages 15–62. Marcel Dekker, New York, 1987.
- [22] P. G. De Gennes and C.. Taupin. Microemulsions and the flexibility of oil/water interfaces. *Journal of Physical Chemistry*, 86:2294–304, 1982.
- [23] M. P. Savelli, C. Solans, R. Pons, M. Clausse, and P. Erra. Keratin cystine reactivity in microemulsion media: influence of cosurfactant chain length. *Colloids and Surfaces, A: Physicochemical and Engineering Aspects*, 119:155–162, 1996.
- [24] M. P. Savelli, C. Solans, E. Rodenas, R. Pons, M. Clausse, and P. Erra. Kinetic study of keratin cystine reduction in w/o microemulsion media. *Colloids and Surfaces, A: Physicochemical and Engineering Aspects*, 143:103–110, 1998.
- [25] D. Touraud, C. Solans, N. Azemar, P. Erra, J. L. Parra, and M.. Clausse. Reactivity of cystine of keratin materials in microemulsion media. *Analysis*, 18:9–18, 1990.
- [26] Christopher K. Njue and James F. Rusling. Controlling catalytic activity of a polyion scaffold on an electrode via microemulsion composition. *Journal of the American Chemical Society*, 122:6459–6463, 2000.
- [27] De-Ling Zhou, Christopher K. Njue, and James F. Rusling. Covalently linked scaffold of cobalt corrins on graphite for electrochemical catalysis in microemulsions. *Journal of the American Chemical Society*, 121:2909–2914, 1999.
- [28] Jean-Marie Aubry and Sabine. Bouttemy. Preparative oxidation of organic compounds in microemulsions with singlet oxygen generated chemically by the sodium molybdate/hydrogen peroxide system. *Journal of the American Chemical Society*, 119:5286–5294, 1997.
- [29] F. M. Menger and A. R. Elrington. Rapid deactivation of mustard via microemulsion technology. *Journal of the American Chemical Society*, 112:8201–3, 1990.
- [30] John C. Russell and David G.. Whitten. Photochemical reactivity in organized assemblies. 24. solute partitioning in aqueous surfactant assemblies: comparison of hydrophobic-hydrophilic interactions in micelles, alcohol-swollen micelles, microemulsions, and synthetic vesicles. *Journal of the American Chemical Society*, 104:5937–42, 1982.
- [31] Michael C.. Hovey. Micellar photochemistry. photooxidation with intramolecular-generated singlet oxygen. *Journal of the American Chemical Society*, 104:4196–202, 1982.

- [32] Mats Almgren, Franz Grieser, and J. K. Thomas. Photochemical and photo-physical studies of organized assemblies. interaction of oils, long-chain alcohols, and surfactants forming microemulsions. *Journal of the American Chemical Society*, 102:3188–93, 1980.
- [33] Chr. Schirmer, Y. Liu, D. Touraud, A. Meziani, S. Pulvin, and W. Kunz. Horse liver alcohol dehydrogenase as a probe for nanostructuring effects of alcohols in water/nonionic surfactant systems. *Journal of Physical Chemistry B*, 106:7414–7421, 2002.
- [34] A. Meziani, D. Touraud, A. Zradba, S. Pulvin, I. Pezron, M. Clausse, and W. Kunz. Comparison of enzymic activity and nanostructures in water/ethanol/brij 35 and water/1-pentanol/brij 35 systems. *Journal of Physical Chemistry B*, 101:3620–3625, 1997.
- [35] Francesco Lopez, Giuseppe Cinelli, Luigi Ambrosone, Giuseppe Colafemmina, Andrea Ceglie, and Gerardo. Palazzo. Role of the cosurfactant in water-in-oil microemulsion: interfacial properties tune the enzymatic activity of lipase. *Colloids and Surfaces, A: Physicochemical and Engineering Aspects*, 237:49–59, 2004.
- [36] Lili Zheng and John D.. Brennan. Measurement of intrinsic fluorescence to probe the conformational flexibility and thermodynamic stability of a single tryptophan protein entrapped in a sol-gel derived glass matrix. *Analyst (Cambridge, United Kingdom)*, 123:1735–1744, 1998.
- [37] Atherton. Seidell. *Solubilities of Inorganic and Organic Compounds. 2nd Ed. revised and enlarged.* D. Van Nostrand Co. Inc., 1928.
- [38] H. Stephen and T. Stephen. *Solubilities of Inorganic and Organic Compounds, Vol. 1: Binary Systems, Part II.* 1963.
- [39] P. M. Ginnings and Rhoda. Baum. Aqueous solubilities of the isomeric pentanols. *Journal of the American Chemical Society*, 59:1111–13, 1937.
- [40] Ibert. Mellan. *Industrial Solvents Handbook. 2nd Ed.* Noyes Data Corporation, Park Ridge, N.J., 1977.
- [41] Magdalena Dominguez, Santiago Rodriguez, M. Carmen Lopez, Felix M. Royo, and Jose S. Urieta. Densities and viscosities of the ternary mixtures 1-butanol + 1-chlorobutane + 1-butylamine and 2-methyl-1-propanol + 1-chlorobutane + 1-butylamine at 298.15 k. *Journal of Chemical and Engineering Data*, 41:37–42, 1996.
- [42] Carlos Franjo, Eulogio Jimenez, Teresa P. Iglesias, Jose Luis Legido, and Maria I. Paz Andrade. Viscosities and densities of hexane + butan-1-ol, + hexan-1-ol, and + octan-1-ol at 298.15 k. *Journal of Chemical and Engineering Data*, 40:68–70, 1995.

- [43] Zhengjun Shan and Abdul-Fattah A. Asfour. Viscosities and densities of nine binary 1-alkanol systems at 293.15 k and 298.15 k. *Journal of Chemical and Engineering Data*, 44:118–123, 1999.
- [44] Mohamed M. El-Banna. Densities and viscosities for mixtures of pentyl acetate and hexyl acetate with normal alkanols at 298.15 k. *Journal of Chemical and Engineering Data*, 42:31–34, 1997.
- [45] Tejraj M. Aminabhavi and Kamalika. Banerjee. Density, viscosity, refractive index, and speed of sound in binary mixtures of 2-chloroethanol with alkanols (c1-c6) at 298.15, 303.15, and 308.15 k. *Journal of Chemical and Engineering Data*, 43:509–513, 1998.
- [46] Lorenzo De Lorenzi, Maurizio Fermeglia, and Giovanni. Torriano. Densities and viscosities of 1,1,1-trichloroethane with 13 different solvents at 298.15 k. *Journal of Chemical and Engineering Data*, 40:1172–7, 1995.
- [47] D. Touraud, C. Mazzoco, S. Darnet, A. Meziani, and M. Clausse. In *2nd World Surfactants Congress, ASPA, Paris, p. 192*, 1988.
- [48] M.P. Savelli-Bou Khaled. PhD thesis, Université de Technologie de compiègne, Compiègne, France,, 1992.
- [49] P. Bauduin, F. Nohmie, D. Touraud, R. Neueder, and W. Kunz. *Journal of Molecular Liquids (Accepted)*, 2005.
- [50] Eric W. Kaler, Karl E. Bennett, H. Ted Davis, and L. E. Scriven. Toward understanding microemulsion microstructure: a small-angle x-ray scattering study. *Journal of Chemical Physics*, 79:5673–84, 1983.
- [51] B. Lagourette, J. Peyrelasse, C. Boned, and M. Clausse. *Nature*, 281:60, 1979.
- [52] M. Clausse. *Encyclopedia of Emulsion Technology*. Marcel Dekker, New York, 1983.
- [53] M. Clausse, J. Peyrelasse, J. Heil, C. Boned, and B.. Lagourette. Bicontinuous structure zones in microemulsions. *Nature*, 293:636–8, 1981.
- [54] Ruth E. Riter, Erik P. Undiks, and Nancy E.. Levinger. Impact of counterion on water motion in aerosol ot reverse micelles. *Journal of the American Chemical Society*, 120:6062–6067, 1998.
- [55] Ruth E. Riter, Dale M. Willard, and Nancy E.. Levinger. Water immobilization at surfactant interfaces in reverse micelles. *Journal of Physical Chemistry B*, 102:2705–2714, 1998.
- [56] Debi Pant, Ruth E. Riter, and Nancy E.. Levinger. Influence of restricted environment and ionic interactions on water solvation dynamics. *Journal of Chemical Physics*, 109:9995–10003, 1998.

- [57] P. Fernandez. PhD thesis, University of Regensburg, Germany, 2002.
- [58] Jihu Yao and Laurence S.. Romsted. Arenediazonium salts: New probes of the interfacial compositions of association colloids. 3. distributions of butanol, hexanol, and water in four-component cationic microemulsions. *Journal of the American Chemical Society*, 116:11779–86, 1994.
- [59] David Andelman, M. E. Cates, D. Roux, and S. A. Safran. Structure and phase equilibria of microemulsions. *Journal of Chemical Physics*, 87:7229–41, 1987.
- [60] M. E. Cates, D. Andelman, S. A. Safran, and D.. Roux. Theory of microemulsions: comparison with experimental behavior. *Langmuir*, 4:802–6, 1988.
- [61] W. K. Kegel and H. N. W.. Lekkerkerker. Phase behavior of an ionic microemulsion system as a function of the cosurfactant chain length. *Colloids and Surfaces, A: Physicochemical and Engineering Aspects*, 76:241–8, 1993.
- [62] M. V. Rodionova, A. B. Belova, V. V. Mozhaev, K. Martinek, and I. V. Berezin. Mechanism of denaturation of enzymes by organic solvents. *Doklady Akademii Nauk SSSR*, 292:913–17, 1987.
- [63] Gonul Velicelebi and Julian M.. Sturtevant. Thermodynamics of the denaturation of lysozyme in alcohol-water mixtures. *Biochemistry*, 18:1180–6, 1979.
- [64] Seishi Shimizu and Kentaro. Shimizu. Alcohol denaturation: Thermodynamic theory of peptide unit solvation. *Journal of the American Chemical Society*, 121:2387–2394, 1999.
- [65] V. V. Mozhaev, Yu. L. Khmel’nitskii, M. V. Sergeeva, A. B. Belova, N. L. Klyachko, A. V. Levashov, and Karel. Martinek. Catalytic activity and denaturation of enzymes in water/organic cosolvent mixtures. a-chymotrypsin and laccase in mixed water/alcohol, water/glycol and water/formamide solvents. *European Journal of Biochemistry*, 184:597–602, 1989.
- [66] S. Cinelli, G. Onori, and A. Santucci. Effect of 1-alcohols on micelle formation and protein folding. *Colloids and Surfaces, A: Physicochemical and Engineering Aspects*, 160:3–8, 1999.
- [67] Douglas S. Clark and James E.. Bailey. Deactivation of a-chymotrypsin and a-chymotrypsin-cyanogen bromide-sepharose 4b conjugates in aliphatic alcohols. *Biochimica et Biophysica Acta*, 788:181–8, 1984.
- [68] Jian-bo Chen, Chun-gu Xia, Shu-ben Li, and Chi-li. Yu. Study on the catalysis of horseradish peroxidase in the reverse micelles. *Fenzi Cuihua*, 13:453–456, 1999.

- [69] Shusheng Zhang, Kui Jiao, Manxia Wang, and Pengxue. Yu. Micellar solubilization and synergistic effect of surfactants in determination of hrp with voltammetric enzyme-linked immunoassay. *Qingdao Huagong Xueyuan Xuebao*, 19:110–115, 1998.
- [70] Shuyun Niu and Kui. Jiao. Micellar solubilization and sensitization of surfactants in determination of horseradish peroxidase (hrp) with coupling reaction voltammetric enzyme-linked immunoassay based on benzidine-h₂o₂-hrp system. *Qingdao Huagong Xueyuan Xuebao*, 18:201–205, 1997.
- [71] J. Kulys and R. Vidziunaite. The role of micelles in mediator-assisted peroxidase catalysis. *Progress in Colloid & Polymer Science*, 116:137–142, 2000.
- [72] Lidia. Gebicka. Kinetic approach to the interaction of sodium n-dodecyl sulfate with heme enzymes. *International Journal of Biological Macromolecules*, 24:69–74, 1999.
- [73] N. N. Ugarova and E. V. Vorob'eva. Peroxidase activity of hemin in aqueous and micellar solutions. *Vestnik Moskovskogo Universiteta, Seriya 2: Khimiya*, 28:391–6, 1987.
- [74] Alexander D. Ryabov and Vasily N.. Goral. Steady-state kinetics, micellar effects, and the mechanism of peroxidase-catalyzed oxidation of n-alkylferrocenes by hydrogen peroxide. *Journal of Biological Inorganic Chemistry*, 2:182–190, 1997.
- [75] P. Bauduin, A. Renoncourt, D. Touraud, B.W. Ninham, and W. Kunz. *Current Opinion in Colloid and Interface Science*, 9:43, 2004.
- [76] G. Cassin, S. Illy, and M. P. Pileni. Chemically modified proteins solubilized in aot reverse micelles. influence of proteins charges on intermicellar interactions. *Chemical Physics Letters*, 221:205–12, 1994.
- [77] J. P. Huruguen and M. P. Pileni. Drastic change of reverse micellar structure by protein or enzyme addition. *European Biophysics Journal*, 19:103–7, 1991.
- [78] Patrick Fernandez, Simon Schroedle, Richard Buchner, and Werner. Kunz. Micelle and solvent relaxation in aqueous sodium dodecylsulfate solutions. *ChemPhysChem*, 4:1065–1072, 2003.
- [79] Samuel Schacher, Eric Holtzman, and Donald C.. Hood. Synaptic activity of frog retinal photoreceptors. a peroxidase uptake study. *Journal of Cell Biology*, 70:178–92, 1976.
- [80] M. Deschenes, P. Landry, and A. Labelle. The comparative effectiveness of the "brown and blue reactions" for tracing neuronal processes of cells injected intracellularly with horseradish peroxidase. *Neuroscience letters*, 12:9–15., 1979.

Bibliography

- [81] P. Buma and E. W.. Roubos. Calcium dynamics, exocytosis, and membrane turnover in the ovulation hormone-releasing caudodorsal cells of *lymnaea stagnalis*. *Cell & Tissue Research*, 233:143–59, 1983.
- [82] R. Zana. Aqueous surfactant-alcohol systems: a review. *Advances in Colloid and Interface Science*, 57:1–64, 1995.
- [83] Eli Ruckenstein and Prakash. Karpe. On the enzymic superactivity in ionic reverse micelles. *Journal of Colloid and Interface Science*, 139:408–36, 1990.
- [84] Prakash Karpe and Eli. Ruckenstein. Effect of hydration ratio on the degree of counterion binding and ph distribution in reverse micelles with aqueous core. *Journal of Colloid and Interface Science*, 137:408–24, 1990.
- [85] Prakash Karpe and Eli. Ruckenstein. The enzymic superactivity in reverse micelles: role of the dielectric constant. *Journal of Colloid and Interface Science*, 141:534–52, 1991.
- [86] Anjum Ansari, Colleen M. Jones, Eric R. Henry, James Hofrichter, and William A. Eaton. The role of solvent viscosity in the dynamics of protein conformational changes. *Science*, 256:1796–8, 1992.

Conclusion

In this thesis a relatively new class of amphiphilic molecules designated C_nPO_m s ($n = 1, 3$ or 4 ; $m = 1-3$) were characterized mainly by comparing their hydrophilic / lipophilic behaviors to that of n-alcohols and C_nEO_m s². In water this was done by determining their temperature dependent phase diagrams (Chapter 2). A first, surprising, observation emerged from this work: an increase in the number of propylene glycol groups, i.e. m , leads to a decrease in the hydrophilic behavior; that is to a decrease in the lower critical solution temperature (LCST) or in the aqueous solubility. By contrast an increase in the number of ethylene glycol groups is well known to have the opposite effect.

In Chapter 3, the LCSTs of C_3PO_m /water mixtures were measured through salt addition. The usual salting-in and -out effects of salts were observed i.e. salting-in and -out salts lead respectively to increase and to decrease of the LCST. As in the case of protein precipitation, the LCSTs had only a weak specific cation dependence, and a strong anion dependence. The anion specificity was found to follow precisely the standard Hofmeister series for anions whatever the nature of the cation. This study embraced both ionic specificity and the effect of salt addition on the phase behavior of C_3PO_m /water mixtures. What emerged from that study is that a measurement of LCST changes to C_3PO_m /water systems via salt addition is a precise and simple way to characterize the salting-in or -out behavior of salts.

The ability of C_nPO_m s to solubilize hydrophobic compounds, i.e. in this case a hydrophobic dye, in water³ was evaluated and compared to classical hydrotrope and co-solvent molecules (Chapter 4). The solubilization of hydrophobic compounds in water is of great interest in various industrial fields such as in the formulation of detergents, cosmetics or pharmaceuticals. C_nPO_m s were found to be very efficient in the aqueous solubilization of sparingly water soluble compounds. In addition to the characterization of C_nPO_m s as solubilizing agents, a new unified concept of water solubilization by hydrotropes or co-solvents emerged. This new concept is based on the evaluation of the hydrophobic part volume of the hydrotrope or co-solvent molecules which was found to be the major factor influencing the hydrotropic efficiency.

A general conclusion could be drawn: the hydrophilic/lipophilic behaviors of C_nPO_m s, C_nEO_m s and n-alcohols correlate well not only with their efficiency in dissolving hydrophobic compounds in water (Chapter 4), but also with surface tension measurements⁴ and the lowering of CMCs of classical surfactants in water (Chapter 5). It can be noted that in these three cases a water / hydrophobe interface is present i.e. water/micellar (Chapter 5), water/hydrophobic dye (Chapter 4) and water/air interfaces. In other words the affinity of these molecules for a water / hydrophobe interface is, in these three cases, highlighted. By contrast the hydrophilic/lipophilic

² C_nPO_m and C_nEO_m molecules can be considered as the combination of short alcohols (propanol, butanol) with a certain number of propylene glycol groups or ethylene glycol groups (m from 1 to 3).

³This property is also called co-solvency or hydrotropy.

⁴Sokolowski et al. *Tenside Detergents*, 19:282-6, **1982** and *Journal of Colloid and Interface Science*, 94:369-79, **1983**.

behaviors of these molecules according to their aqueous solubilities or LCST values, which represent only the affinity for water of these molecules, are as expected different (Chapter 2).

The most interesting property of C_nPO_m s which arose from the different studies in this thesis is certainly their co-surfactant property in the formation of microemulsions (Chapter 6). Such microemulsion systems present indeed several advantages: low surfactant levels, low toxicity and a temperature dependence which can be finely tuned and used advantageously for example in the recovery of reaction products or in extraction processes.

In this context enzymatic reactions were investigated in microemulsion systems. As reaction media for enzymatic reactions, microemulsions present several advantages (see Chapters 6 and 8). At first the model enzymatic reaction of oxidation of ABTS by hydrogen peroxide and catalyzed by the *horseradish peroxidase* (HRP) was studied in buffer with different salts and at different pHs (Chapter 7). The resulting catalytic efficiency $V_{maxABTS} / K_{mABTS}$ was found to follow the usual Hofmeister series for anions with opposite deviations from the pure pH effect for salting-in and salting-out ions. In microemulsions the microstructure changes, as inferred by the conductivity measurements, were found to correlate remarkably well with the changes in the enzymatic activities. Consequently, it was concluded that enzymatic activity measurements are a valuable tool to study confined systems such as microemulsions and that enzymatic activities can be finely tuned by small changes in microemulsion structures, probably in a predictive way. Enzymatic activities with the same enzymatic system were studied elsewhere in other microstructured liquids, i.e. in catanionic microemulsions⁵ and in micellar and vesicular systems⁶ and were analyzed in the same way.

⁵Mahiuddin, S., Renoncourt, A.; Bauduin, P.; Touraud, D.; Kunz W. Horseradish Peroxidase activity in a reverse catanionic microemulsion. *Langmuir* (Accepted) **2005**

⁶Audrey Renoncourt Ph.D Thesis **2005** University of Regensburg

List of Figures

1.1	Formula of glycol ethers from the ethylene and propylene glycol series (E and P series).	10
1.2	Metabolisms of ethylene and propylene glycol ethers (C_nEO_m and C_nPO_m).	13
1.3	Formula of glycol ethers.	15
1.4	Synthesis of C_3PO_1 and C_3PO_2 .	15
1.5	Composition of an industrial C_3PO_2 determined with gas chromatography/mass spectroscopy analysis. The mass % of each isomers was determined by the pic area obtained from gas chromatography (column Stabiwax-DA).	16
1.6	δ_P vs. δ_H plot showing the location of various common solvents and of some C_nPO_m s. The glycols are ethylene glycol (E) and propylene glycol (P). The alcohols include methanol (M), ethanol (E), 1-butanol (B) and 1-octanol (O). The amides include dimethylformamide (F) and dimethyl acetamide (D). The nitriles are acetonitrile (A) and butyronitrile (B). The esters are ethyl acetate (E) and n-butyl acetate (B). The amines are ethyl amine (E) and propyl amine (P). The phenols are phenol (P) and m-cresol (C). The ethers are symbolized by diethyl ether.	18
1.7	Wetting and non-wetting of a water droplet on plan surfaces, θ represents the contact angle of the water droplet.	22
1.8	Cleaning of a metal plate (see text).	23
1.9	Contact angle θ of a water droplet on aluminium plates as a function of time: plate without treatment (■), clean plate (●) and plate after acetone treatment (▲).	23
1.10	Contact angle θ of a water droplet on aluminium plates as a function of time: plate without treatment (■), clean plate (●), plates after treatment with: C_3PO_2 (▲), C_3PO_1 (▼), $CH_3PO_2CH_3$ (▷), CH_3PO_1Ac (◁) and with Isopar G (□).	25
1.11	Contact angle θ of a water droplet on copper plates as a function of time: plate without treatment (■), clean plate (●), plates after treatment with: acetone (▲), C_3PO_1 (▼), $CH_3PO_2CH_3$ (▷) and with CH_3PO_1Ac (◁).	26

2.1	Cloud point versus the C_3PO_m mass fraction for: C_3PO_1 (\blacktriangle), C_3PO_2 (\bullet) and C_3PO_3 (\blacksquare) /water systems.	36
2.2	Cloud point versus the C_nPO_m mass fraction for: C_4PO_1 (\blacktriangle), C_4PO_2 (\bullet), C_4PO_3 (\blacksquare) and iso- C_4PO_1 (\blacktriangledown) /water systems.	37
2.3	Surface tension σ (\blacktriangle , mN/m), measured at 25°C, versus C_3PO_1 mass fraction for the C_3PO_1 /water system.	39
3.1	Phase diagrams of C_3PO_1 (\blacksquare) and C_3PO_2 (\blacktriangle) mixtures with pure water as a function of temperature.	49
3.2	The shifts of the LCST of the C_3PO_2 /water mixture upon the addition of salts. Positive shifts indicate a salting-in effect of the ions whereas negative shifts can be interpreted as the manifestation of a salting-out effect. The sequence of the curves follows exactly the Hofmeister series for anions. The slope of the linear parts of all curves is described by Eqn. (3.1) and indicated in Table 3.1.	51
3.3	Representation of the a coefficients obtained with different 1:1 salts according to Eqn. (3.1) in °C per mmols of salt added to a mixture of C_3PO_2 and water with a total liquid amount of 1 mole. The accuracy of the a coefficient is better than 0.2 °C/mmols.	53
3.4	The phase diagrams of the pure binary C_3PO_2 /water mixture (\blacksquare) is compared to the corresponding diagrams made from an aqueous solution containing an electrolyte at a fixed concentration of 0.041 M: Na_2SO_4 (\circ), which is a typical salting-out salt, and of $NaSCN$ (\square), which is salting-in. The insert in the Figure shows the differences between the curves, ΔCP , i.e. the difference in the cloud points of the system with and without salt, in absolute values.	54
4.1	The optical density (O.D.), proportional to the amount of dissolved dye, versus the molar concentrations of hydrotropes (or co-solvents) in water: SXS (∇), 1-propanol (Δ), C_3PO_1 (\square), C_3EO_1 (\circ) and acetone (\diamond).	68
4.2	The optical density (O.D.), proportional to the amount of dissolved dye, versus the molar concentrations of SDS (\triangleleft) in water. This curve is compared to the ones obtained with SXS (∇) and C_3EO_1 (\circ). . .	69
4.3	The optical density (O.D.) as a function of (a) molar concentrations of hydrotropes (or co-solvents) in water, (b) molar concentrations of hydrotropes (or co-solvents) in water multiplied by the evaluated molar volume of the hydrophobic part of the respective hydrotrope (or co-solvent) molecules; SXS (∇), 1-propanol (Δ), C_3PO_1 (\square), C_3EO_1 and acetone (\diamond).	70

4.4	The optical density (O.D.) as a function of (a) molal concentrations of hydrotropes (or co-solvents) in water, (b) molal concentrations of hydrotropes (or co-solvents) in water multiplied by the evaluated molar volume of the hydrophobic part of the respective hydrotrope (or co-solvent) molecules; C ₃ PO ₂ (●), t-C ₄ PO ₁ (▲), C ₃ PO ₁ (□), C ₁ PO ₃ (■), C ₃ EO ₁ (○), 1-propanol (Δ) and C ₁ PO ₁ (◆).	73
4.5	Representations of the electron density in hydrotrope and co-solvent molecules, green/blue and yellow/red areas represent respectively the low and high electron density parts in the molecules: SXS (a), acetone (b), 1-propanol (c), C ₃ EO ₁ (d) and C ₃ PO ₁ (e).	74
5.1	-ln(CMC) values, for some of the studied amphiphiles, as a function of the amphiphile content Y _a , amphiphile mole fraction: (■) 1-butanol, (●) 1-hexanol, (▲) C ₃ PO ₂ , (◆) C ₃ PO ₃ and (►) C ₄ PO ₁	85
5.2	ln(-dlnCMC/dY _a) values obtained for n-alcohols as a function of the carbon number of the alcohol: (■) from the present work and (▲) data from <i>Hayase et al.</i> [2].	87
5.3	ln(-dlnCMC/dY _a) values obtained C ₄ PO _{<i>m</i>} (●) and C ₃ PO _{<i>m</i>} (■) as a function of the number of propylene glycol units, <i>m</i>	88
5.4	ln(-dlnCMC/dY _a) values obtained C ₄ EO _{<i>m</i>} and C ₃ EO _{<i>m</i>} as a function of the number of ethylene glycol units, <i>m</i>	89
5.5	ln(-dlnCMC/dY _a) values of some short amphiphiles derived from ethylene and propylene glycol ethers and of n-alcohols (●) versus the corresponding alcohol carbon number.	91
5.6	water/SDS/co-surfactant ternary phase diagrams, the co-surfactants being: 1-butanol, 1-pentanol, 1-hexanol and C ₄ PO ₃ . The black areas represent monophasic isotropic solutions being typically micellar solutions or microemulsions. L1 and L2 stand respectively for direct and reverse microemulsions i.e. oil in water and water in oil. The white areas represent polyphasic systems, i.e. liquid/liquid or solid/liquid systems, or ordered surfactant phases such as hexagonal or lamellar.	92
6.1	(a) Tetrahedral representation of quaternary systems composed of water / SDS / dodecane / co-surfactant, the grey triangle represents pseudo-ternary systems having a constant SDS/co-surfactant mass ratio (K _M), (b-d) pseudo-ternary phase diagrams of water / SDS / dodecane / C _{<i>n</i>} PO _{<i>m</i>} systems obtained for C ₃ PO ₁ (b), C ₄ PO ₂ (c) and C ₄ PO ₃ (d) at SDS/C _{<i>n</i>} PO _{<i>m</i>} mass ratio K _M of 1/2 (b), 1/2(c) and 1/3.33 (d). The dark areas represent the realms of existence of monophasic and isotropic phases. The diagrams were determined at 25°C.	101

- 6.2 (a) Tetrahedral representation of the quaternary systems composed of water / SDS / dodecane / co-surfactant. The cut included in this tetrahedron represents the pseudo-ternary phase diagram of systems composed of water / co-surfactant / (SDS/dodecane) at a constant SDS/dodecane mass ratio of 1/3, (b) representation of the dodecane/SDS/co-surfactant ternary phase diagram, the dark line represents the projection of the studied pseudo-ternary phase diagram. (c-e) phase diagrams of water / SDS / dodecane / co-surfactant systems, with C_4PO_3 (c), 1-butanol (d) and 1-pentanol (e) as co-surfactants and at a constant SDS/dodecane mass ratio of 1/3. The dark areas represent the realms of existence of the monophasic and isotropic phases. The diagrams were determined at 25°C. 104
- 6.3 Binary representation of the monophasic areas shown in Figs. 6.2(c-e) with C_4PO_3 (\blacktriangle), 1-butanol (\blacksquare) and 1-pentanol (\bullet) as co-surfactant; the abscissa and the ordinate represent respectively x , the number of mole of co-surfactant per 1g of SDS/dodecane mixture and the water solubility in wt%. 105
- 6.4 Cloud point of water/ C_nPO_m mixtures (mass ratio 1/1) as a function of SDS content in wt%: C_3PO_2 (\triangle), C_3PO_3 (\circ), C_4PO_2 (\diamond) and C_4PO_3 (\square). The dashed and dotted lines represent the water/n-alcohol (mass ratio 1/1) solubilization lines obtained with 1-butanol and 1-pentanol, respectively. 106
- 6.5 Representation of the realms of existence of the three phase region (Winsor III) of systems composed of brine (water+NaCl) / dodecane / SDS / co-surfactant (for the exact compositions see *Experimental Section*), obtained with C_3PO_2 (\bullet), 1-butanol (\blacksquare) and 1-pentanol (\blacktriangle) as co-surfactant at 13°C (a) and 69°C (b). 109
- 6.6 (a) Cloud points versus the C_4PO_3 mass fraction in the water / C_4PO_3 binary system, (b) cloud points of water / C_4PO_3 mixtures (mass ratio 1/1) as a function of SDS content in wt%, (c) pseudo-ternary phase diagram of the water / SDS / dodecane / C_4PO_3 system at SDS / C_4PO_3 mass ratio K_M of 1/6.26 and at 21°C. The dark area represents the realm of existence of the monophasic and isotropic phases. (d) Cloud points versus the pseudo-component (SDS+ C_4PO_3) content, at a SDS/ C_4PO_3 mass ratio of 1/6.26, in the (SDS+ C_4PO_3) / water system. This composition line corresponds to the left side of the pseudo-ternary phase diagram shown in (c). (e) Cloud points versus the water content along the white experimental path shown in (c). The cross and the asterisk marked in the diagrams represent similar compositions and temperatures. 110
- 7.1 pH vs. ionic strength of a citrate buffer solution ($c = 0.025M$) containing different sodium salts: SO_4^{2-} (\square), Cl^- (\triangle), NO_3^- (\circ) and Br^- (∇). 124

7.2	$V_{maxABTS}$ and K_{mABTS} vs. pH of a citrate buffer ($c = 0.025\text{M}$), the measured pH was adjusted by the addition of small amounts of NaOH or HCl.	125
7.3	K_{mABTS} vs. ionic strength of a citrate buffer solution ($c = 0.025\text{M}$) containing different sodium salts: SO_4^{2-} (\square), Cl^- (\triangle), NO_3^- (\circ) and Br^- (∇).	126
7.4	$V_{maxABTS}$ vs. ionic strength of a citrate buffer solution ($c = 0.025\text{M}$) containing different sodium salts: SO_4^{2-} (\square), Cl^- (\triangle), NO_3^- (\circ) and Br^- (∇).	127
7.5	Catalytic efficiency $V_{maxABTS} / K_{mABTS}$ vs. ionic strength (and vs. salt molar concentration in the insert figure) of a citrate buffer solution ($c = 0.025\text{M}$) containing different sodium salts: SO_4^{2-} (\square), Cl^- (\triangle), NO_3^- (\circ) and Br^- (∇).	129
7.6	Catalytic efficiency $V_{maxABTS} / K_{mABTS}$ vs. pH of a citrate buffer solution ($c = 0.025\text{M}$) without additional salts (solid line) and containing different sodium salts (dotted lines): SO_4^{2-} (\square), Cl^- (\triangle), NO_3^- (\circ) and Br^- (∇).	130
8.1	The phase diagrams of pseudo-ternary water/SDS/dodecane/n-alcohol systems (S stands for SDS/n-alcohols, W for water, and O for dodecane) taken from [21], (a) 1-butanol, (b) 1-pentanol, (c) 1-hexanol, (d) 1-heptanol and (e) 1-octanol. In every case the molar ratio K_M between surfactant and alcohol of 1/6.54. The full lines indicate the chosen compositions of the reaction media.	139
8.2	Pseudoternary diagram of the citrate buffer solution ($c = 0.025\text{M}$) / SDS / 1-pentanol / n-dodecane ($K_M = 1/6.54$, $T = 25^\circ\text{C}$) in comparison with the water system indicated by the dashed line.	143
8.3	Variations of citrate buffer/SDS/n-alcohols/n-dodecane microemulsion conductivity (expressed in Sm^{-1} , $T = 25^\circ\text{C}$) with the citrate buffer content in mass percent, along the composition paths, for different n-alcohols: 1-butanol (\blacktriangle), 1-pentanol (\bullet), 1-hexanol (\blacklozenge), 1-heptanol (\blacksquare) and 1-octanol (\blacktriangledown). Also given is the ratio of water to surfactant molecules for the 1-butanol system (\square) and the other alcohol systems (\circ), see Fig. 8.1 and the discussion of the phase diagrams.	144
8.4	Variations of conductivity along the experimental path in the system: citrate buffer solution ($c = 0.025\text{M}$)/SDS/1-pentanol/n-dodecane (\bullet) ($K_M = 1/6.54$, $T = 25^\circ\text{C}$) in comparison with the water system (\circ), and the 1-butanol system with buffer solution (\blacksquare).	145
8.5	Enzymatic activities of HRP in citrate buffer solutions ($c = 0.025\text{M}$, $\text{pH} = 5$) saturated with different n-alcohols from 1-butanol to 1-octanol where n_a is the number of carbon atoms in the alcohol. The corresponding measured pH values are also given.	146

8.6	Enzymatic activities of HRP versus SDS concentration (mass percent) in citrate buffer ($c = 0.025\text{M}$, initial buffer $\text{pH} = 5$).	147
8.7	Enzymatic activities in microemulsions (citrate buffer solution / SDS / dodecane / n-alcohol ($K_M = 1/6.54$)) as a function of the buffer content. 1-butanol (\blacktriangle), 1-pentanol (\square), 1-hexanol (\circ) and 1-heptanol (\blacktriangledown). Typical error bars are also included.	149
8.8	HRP enzymatic activity in the citrate buffer / SDS / 1-pentanol / n-dodecane system. A tentative explanation between the correlation of enzymatic activities and electric conductivity data. (a) Pseudoternary diagram of the citrate buffer solution ($c = 0.025\text{M}$)/SDS/1-pentanol/n-dodecane ($K_M = 1/6.54$, $T = 25^\circ\text{C}$), (b) evolution of the microstructure through the addition of citric buffer (water content) along the experimental path, (c) HRP enzymatic activities (in red) and conductivity (in blue) as a function of the buffer content (water content) along the experimental path. C1 and C2 appearing along the experimental path represent respectively the percolation threshold (14% buffer or water content) and the borderline between the effective medium and the bicontinuous system (43%).	155
8.9	Maximum enzymatic activity observed in microemulsion vs. n , the number of carbon atom of the 1-alcohol as co-surfactant.	158

List of Tables

1.1	Trade names for glycol ether solvents.	11
1.2	From the discovery of ethylene glycol ether toxicity to the beginning of their phase-out from formulated products and from industrial processes.	12
1.3	Flash point ($^{\circ}\text{C}$), evaporation rate ($n_{\text{ButylAcetate}} = 1$) and LD50 (Lethal Dose 50% in g/Kg, rat ingestion) of some industrial solvents.	19
1.4	Deinking power obtained with PVC and PU cables (see text), Flash point ($^{\circ}\text{C}$), evaporation rate ($n_{\text{ButylAcetate}} = 1$) and LD50 (Lethal Dose 50% in g/Kg, rat ingestion) of some industrial solvents.	20
2.1	Chemical name, abbreviation, purity grade, solubility of organic compound in water at 25°C (mass %) (S_o) and water solubility in organic compound at 25°C (mass %) (S_w) of the studied propylene glycol alkyl ether (C_nPO_m) and of some classical n-alcohols.	35
2.2	LCST values of the studied C_nPO_m s and of their corresponding C_nEO_m isomers.	41
3.1	a coefficients for different sodium salts according to Eqn. (3.1) in $^{\circ}\text{C}$ per mmols of salt added to a mixture of C_nPO_m and water with a total liquid amount of 1 mole. The liquid mixtures have a molar ratio of 1/8 C_nPO_m /water. The accuracy of the a coefficient is better than $0.2^{\circ}\text{C}/\text{mmols}$	52
3.2	a coefficients for different 1:1 salts according to Eqn. (3.1) in $^{\circ}\text{C}$ per mmols of salt added to a mixture of C_3PO_2 and water with a total liquid amount of 1 mole. The accuracy of the a coefficient is better than $0.2^{\circ}\text{C}/\text{mmols}$	53
5.1	$\ln(-\text{dlnCMC}/\text{dYa})$ values obtained for all the studied amphiphiles and their calculated n_{eq} (see text).	87
8.1	Used alcohols	141

List of Publications

Published:

1- Bauduin, P.; Wattebled, L.; Schrodle, S.; Touraud, D.; Kunz, W. Temperature dependence of industrial propylene glycol alkyl ether/water mixtures. *Journal of Molecular Liquids* **2004** 115(1), 23-28.

2- Renoncourt, A.; Bauduin, P.; Touraud, D.; Kunz, W.; Azemar, N.; Solans, C. Transition from mixed micelles to vesicles in a cat-anionic system of surfactants applied in cosmetics. *Comunicaciones presentadas a las Jornadas del Comité Espanol de la Detergencia* **2004** 34, 273-283.

3- Bauduin, P.; Wattebled, L.; Touraud, D.; Kunz, W. Hofmeister ion effects on the phase diagrams of water-propylene glycol propyl ethers. *Zeitschrift fuer Physikalische Chemie* (Muenchen, Germany) **2004** 218(6), 631-641.

4- Bauduin, P.; Renoncourt, A.; Touraud, D.; Kunz, W.; Ninham, B. W. Hofmeister effect on enzymatic catalysis and colloidal structures. *Current Opinion in Colloid and Interface Science* **2004** 9(1,2), 43-47.

Accepted:

5- Mahiuddin, S., Renoncourt, A.; Bauduin, P.; Touraud, D.; Kunz, W. Horseradish Peroxidase activity in a reverse catanionic microemulsion. *Langmuir* **2005**

6- Renoncourt, A.; Bauduin, P.; Touraud, D.; Azemar, N.; Solans, C.; Kunz, W. Effect of temperature on the realms of existence of vesicles in several catanionic systems. *Colloids and Surfaces A* **2004**

7- Bauduin, P.; Basse, A.; Touraud, D.; Kunz, W. Effect of short non-ionic amphiphiles derived from ethylene and propylene glycol alkyl ethers on the CMC of SDS. *Colloids and Surfaces A* **2004**

8- Bauduin, P.; Nohmie, F.; Touraud, D.; Neueder, R.; Kunz, W.; Ninham, B.W. Hofmeister Specific-Ion Effects on Enzyme Activity and buffer pH: Horseradish Peroxidase in citrate buffer. *Journal of Molecular Liquids* **2005**

Submitted:

9- Bauduin, P.; Touraud, D.; Kunz, W.; Ninham, B.W. The influence of structure and composition of a reverse SDS microemulsion on enzymatic activities. *Journal of Colloid Interface Science* **2005**

10- Bauduin, P.; Renoncourt, A.; Kopf, A.; Touraud, D.; Kunz, W. Unified concept of solubilization in water by hydrotropes and co-solvents. *Langmuir* **2005**

11- Bauduin, P.; Touraud, D., Kunz, W. Design of low-toxic anionic temperature sensitive microemulsions using short propyleneglycol alkylethers as co-surfactants. *Langmuir* **2005**

In preparation:

12- Pinna, M.C.; Bauduin, P.; Touraud, D.; Monduzzi, M.; Ninham, B.W.; Kunz, W. Effect of choline addition on the salt-induced superactivity of Horseradish peroxidase and its implication for salt resistance of plant(s).

13- Bauduin, P.; Voinescu, A.; Pinna, M.C.; Touraud, D.; Kunz, W.; Ninham, B. From buffers to proteins, electrostatic and Hofmeister specific-ion effects: determining factors in protein conformation.

List of Poster Presentations in Congress

02/2004 **Workshop on short range interactions in soft condensed matter**, Regensburg:

- Bauduin, P.; Wattebled, L.; Schrodle, S.; Touraud, D.; Kunz, W. Hofmeister specific ion effects on the phase diagrams of water-propylene glycol propyl ethers.
- Bauduin, P.; Nohmie, F.; Touraud, D.; Neueder, R.; Kunz, W.; Ninham, B.W. Hofmeister specific ion effects on pH and on the activity of Horseradish peroxidase.
- Renoncourt, A.; Bauduin, P.; Touraud, D.; Kunz, W. Hofmeister specific ion effects on vesicle formation in aqueous SDS/DTAB mixtures.

03/2004 **Jornadas del comite Espanol de la Detergencia** in Barcelona (Spain):

- Renoncourt, A.; Bauduin, P.; Touraud, D.; Kunz, W.; Azemar, N.; Solans, C. Transition from mixed micelles to vesicles in a cat-anionic system of surfactants applied in cosmetics.

09/2004 **European Colloids and Interface Society (ECIS)** in Almèria (Spain):

- Bauduin, P.; Basse, A.; Touraud, D.; Kunz, W. Effect of short non-ionic amphiphiles derived from ethylene and propylene glycol alkyl ethers on the CMC of SDS.
- Bauduin, P.; Touraud, D.; Kunz, W.; Ninham, B.W. The use of Horseradish peroxidase as a probe of microemulsion structures.
- Renoncourt, A.; Bauduin, P.; Touraud, D.; Azemar, N.; Solans, C.; Kunz, W. Effect of temperature on the realms of existence of vesicles in several catanionic systems.